

Copyright Warning & Restrictions

The copyright law of the United States (Title 17, United States Code) governs the making of photocopies or other reproductions of copyrighted material.

Under certain conditions specified in the law, libraries and archives are authorized to furnish a photocopy or other reproduction. One of these specified conditions is that the photocopy or reproduction is not to be “used for any purpose other than private study, scholarship, or research.” If a user makes a request for, or later uses, a photocopy or reproduction for purposes in excess of “fair use” that user may be liable for copyright infringement,

This institution reserves the right to refuse to accept a copying order if, in its judgment, fulfillment of the order would involve violation of copyright law.

Please Note: The author retains the copyright while the New Jersey Institute of Technology reserves the right to distribute this thesis or dissertation

Printing note: If you do not wish to print this page, then select “Pages from: first page # to: last page #” on the print dialog screen

The Van Houten library has removed some of the personal information and all signatures from the approval page and biographical sketches of theses and dissertations in order to protect the identity of NJIT graduates and faculty.

ABSTRACT

SIGNAL PROCESSING TECHNIQUES IN HEART RATE AND SYSTOLIC ARTERIAL BLOOD PRESSURE VARIABILITY STUDIES

**by
Christopher O'Bara**

Power spectral analysis of heart rate and systolic arterial blood pressure variability provides a window to the activity of the autonomic nervous system. To derive power spectra from raw blood pressure and electrocardiogram signals, many steps of signal processing must be performed. Most popular methods of spectral analysis require evenly spaced samples; therefore interpolation and resampling techniques must be used.

The results of the present study indicate that different interpolation techniques result in spectral distortions that vary depending upon the interpolation methods used as well as physiological parameters such as heart and respiration rate. Different interpolation methods applied to heart rate and systolic blood pressure data are compared and evaluated in an attempt to determine optimal interpolation methods for each type of data. Algorithms designed to derive systolic arterial pressure variability spectra from raw blood pressure data based on these results are also presented.

These algorithms were used to perform analysis of blood pressure signals. The resulting systolic arterial pressure variability spectra were then compared to respiratory data as well as spectra of heart rate variability. A method was developed that provides a means of explaining the interaction of the parasympathetic and sympathetic influence on heart rate in terms of systolic arterial blood pressure and heart rate variability spectra.

**SIGNAL PROCESSING TECHNIQUES IN HEART RATE AND SYSTOLIC
ARTERIAL BLOOD PRESSURE VARIABILITY STUDIES**

by
Christopher O'Bara

**A Thesis
Submitted to the Faculty of
New Jersey Institute of Technology
in Partial Fulfillment of the Requirements for the Degree of
Master of Science in Biomedical Engineering**

Biomedical Engineering Committee

January 1996

APPROVAL PAGE

SIGNAL PROCESSING TECHNIQUES IN HEART RATE AND SYSTOLIC ARTERIAL BLOOD PRESSURE VARIABILITY STUDIES

Christopher O'Bara

Dr. Stanley S. Reisman, Thesis Advisor
Professor of Electrical Engineering and Associate
Chairperson for Graduate Studies, NJIT

Date

Dr. David Kristol, Committee Member
Professor of Chemistry and Director of Biomedical
Engineering Program, NJIT

Date

Dr. Thomas W. Findley, Committee Member
Associate Professor of Medicine, UMDNJ
Director of Research, Kessler Institute for
Rehabilitation

Date

BIOGRAPHICAL SKETCH

Author: Christopher O'Bara

Degree: Master of Science in Biomedical Engineering

Date: January 1996

Undergraduate and Graduate Education:

- Master of Science in Biomedical Engineering
New Jersey Institute of Technology, Newark, New Jersey, 1996
- Bachelor of Science in Electrical Engineering
New Jersey Institute of Technology, Newark, New Jersey, 1994

Major: Biomedical Engineering

This thesis is dedicated to my family as well as
all those who have encouraged me to excel

ACKNOWLEDGMENT

The author would like to thank his advisor Dr. Stanley Reisman for his valuable advice and suggestions in directing this research.

Thanks also to Dr. David Kristol and Dr. Thomas W. Findley for serving as members of my thesis committee.

Special thanks to John F. Andrews at Kessler Institute for Rehabilitation for providing the much needed help in providing the computer resources required by this research.

Last but not least, special thanks to fellow graduate student and good friend David Caggiano for his support and friendship throughout the Master's program at NJIT. The author appreciates his help in times where new ideas were needed.

TABLE OF CONTENTS

Chapter	Page
1 PHYSIOLOGICAL BACKGROUND	1
1.1 Introduction.....	1
1.2 The Cardiovascular System.....	1
1.2.1 The Heart and Cardiac Cycle.....	1
1.2.2 The Electrocardiogram.....	6
1.2.3 Systemic Circulation	8
1.2.4 Blood Pressure.....	10
1.3 Respiration	13
1.4 Neural Control Systems	15
1.4.1 The Autonomic Nervous System.....	15
1.4.2 Autonomic Control of the Heart.....	17
1.4.3 Autonomic Regulation of Blood Pressure.....	18
1.5 Heart Rate Variability	20
1.6 Systolic Arterial Pressure Variability	22
1.7 Statement of Objective.....	25
2 DATA ACQUISITION	27
2.1 Introduction.....	27
2.2 Laboratory Setup.....	27
2.3 Experimental Protocol	31

TABLE OF CONTENTS (continued)

Chapter	Page
3 SIGNAL PROCESSING TECHNIQUES	33
3.1 Introduction.....	33
3.2 Interpolation Methods	33
3.2.1 Overview of Interpolation Methods.....	34
3.2.2 Comparison of Interpolation Methods	38
3.2.3 Spectral Analysis without Resampling	39
3.2.4 Experiments Involving Interpolation.....	42
3.2.5 Conclusion.....	54
3.3 Normalized Units.....	54
3.4 Analysis of Blood Pressure	57
3.4.1 Peak Detection.....	58
3.4.2 Correction of Misdetections	63
3.4.3 Calculating Spectra	66
4 RATE AND VOLUME CONTROLLED RESPIRATION STUDY	73
4.1 Introduction.....	73
4.2 Methods	73
4.3 Results	77
4.3.1 Relationships with Tidal Volume.....	77
4.3.2 Measurement of Sympathetic Activity	83
4.4 Conclusions	92

TABLE OF CONTENTS (continued)

Chapter	Page
5 CONCLUSIONS.....	94
5.1 Introduction.....	94
5.2 Summary of Results.....	94
5.3 Future Work.....	97
APPENDIX A HEART RATE VARIABILITY ANALYSIS STEPS	98
APPENDIX B HEART RATE VARIABILITY ANALYSIS PROGRAMS.....	100
APPENDIX C DATA USED IN NORMALIZED UNITS EXPERIMENT	106
APPENDIX D BLOOD PRESSURE VARIABILITY ANALYSIS STEPS.....	107
APPENDIX E BLOOD PRESSURE ANALYSIS PROGRAMS	108
APPENDIX F RESULTS OF DATA ANALYSIS	119
REFERENCES	129

LIST OF TABLES

Table	Page
1.1 Relative Cross-Sectional Areas of Blood Vessels	10
3.1 Results of Spectral Analysis of Simulated IBI Data	44
3.2 Results of Comparison of Interpolation Methods on Real IBI Data	46
3.3 Results of Comparison of Interpolation Methods on SAP Data	49
3.4 Comparison of LF Areas of Blood Pressure and SAP Spectra	51
3.5 Comparison of HF Areas of Blood Pressure and SAP Spectra.....	51
3.6 Results of Comparison of Absolute and Normalized Units	56
4.1 Ranges Used to Calculated LF and HF Areas.....	74
4.2 Correlations Between HF SAP and Volume.....	78
4.3 Correlations Between HF BP in Absolute Units and Volume.....	80
4.4 Correlations Between Vagal Tone and Volume.....	81
4.5 Correlations Between HR and HF SAP in Absolute Units	82
4.6 Correlations Between HR and LF SAP in Absolute Units.....	84
4.7 Correlations Between HR and Vagal Tone.....	84
4.8 Possible Combinations of Correlations	85
4.9 Classification of Pairs of Correlation Coefficients.....	87
4.10 Correlations Between HR and LF BP in Absolute Units	88
4.11 Classification of Pairs of Correlation Coefficients.....	88
4.12 Correlations Between HR and LF SAP in Normalized Units.....	89
4.13 Correlations Between HR and Vagal Tone in Normalized Units	89
4.14 Classification of Pairs of Correlation Coefficients.....	90

LIST OF TABLES
(continued)

Table	Page
4.15 Data for Subject 2 at 2/3 Normal Respiration Rate.....	91
C.1 Data Used in Normalized Units Experiment	106
F.1 Results for Subject 1	119
F.2 Results for Subject 2	121
F.3 Results for Subject 3	123
F.4 Results for Subject 4	125
F.5 Results for Subject 5	127

LIST OF FIGURES

Figure	Page
1.1 The Structure of the Heart.....	2
1.2 The Conducting System of the Heart	5
1.3 Bipolar Limb Lead Configuration	7
1.4 A Typical Electrocardiogram	8
1.5 Blood Pressure Wave	12
1.6 Organization of the Respiratory System	14
1.7 Heart Rate Variability Power Spectrum	21
3.1 Forward Step Interpolation of Blood Pressure	35
3.2 Cubic Spline Interpolation of Blood Pressure	36
3.3 Backward Step Interpolation of the IBI	37
3.4 Straight Line Fits for Individual Respiration Rates	52
3.5 Straight Line Fit for All Respiration Rates Combined	52
3.6 Results for Subject 5 at 2/3 Normal Respiration Rate.....	53
3.7 Flowchart of Blood Pressure Analysis Steps	59
3.8 Peak Detection Algorithm Used in Presap.m.....	62
3.9 Flowchart of Undet.m.....	65
3.10 Flowchart of Mdet.m.....	67
3.11 Flowchart of Sapspec.m.....	70
3.12 Flowchart of Rspect.m.....	72
4.1 HF SAP vs. Volume for Subject 1 at 3/2 Normal Rate	78
4.2 HF SAP vs. Volume for Subject 5 at Normal Rate	79

LIST OF FIGURES (continued)

Figure	Page
4.3 Volume vs. Vagal Tone for Subject 1 at 3/2 Normal Respiration Rate.....	81
4.4 Volume vs. Vagal Tone for Subject 2 at 2/3 Normal Respiration Rate.....	82
4.5 Volume vs. Vagal Tone for Subject 4 at 2/3 Normal Respiration Rate.....	82
4.6 Plot of HF SAP vs. HR for Subject 3	83

CHAPTER 1

PHYSIOLOGICAL BACKGROUND

1.1 Introduction

The purpose of this chapter is to provide an overview of the physiological systems that are relevant to the research in this thesis. The understanding of these physiological systems is essential to the interpretation of the experimental results and to further expand upon this research.

1.2 The Cardiovascular System

The purpose of the circulatory system is to provide the body's tissues with necessary nutrients such as oxygen as well as to carry waste products such as carbon dioxide away to be expelled from the body [1]. The primary components of the circulatory system are the blood, the blood vessels, and the heart, which is responsible for pumping the blood through the vasculature. The lungs and kidneys also play an important role in the circulatory system. The lungs are the site of the blood's gas exchanges and the kidneys are responsible for the filtration of substances in the blood that are not utilized by the body.

1.2.1 The Heart and Cardiac Cycle

As stated before, the heart is the pumping mechanism for the circulatory system and is the primary focus of the research presented in this thesis. The heart is really composed of two separate pumping mechanisms, the right heart which is responsible for pumping blood

though the lungs and the left heart which is responsible for pumping blood through the rest of the body.

As seen in figure 1.1, each side of the heart is divided into an upper compartment called the atrium and a lower part called the ventricle [1]. The right atrium is fed by the superior and inferior vena cava veins which return the blood from the body's tissues. From here, the blood flows into the right atrium, through the right AV valve, or tricuspid valve, into the right ventricle. The blood is then passed through the pulmonary valve into the pulmonary artery, where it travels to the lungs to exchange gases. The blood is then returned to the left atrium of the heart through the pulmonary vein. From here it passes through the left AV valve, or mitral valve, into the left ventricle. The blood is then released through the aortic valve into the aorta, which provides blood to the systemic circulatory system.

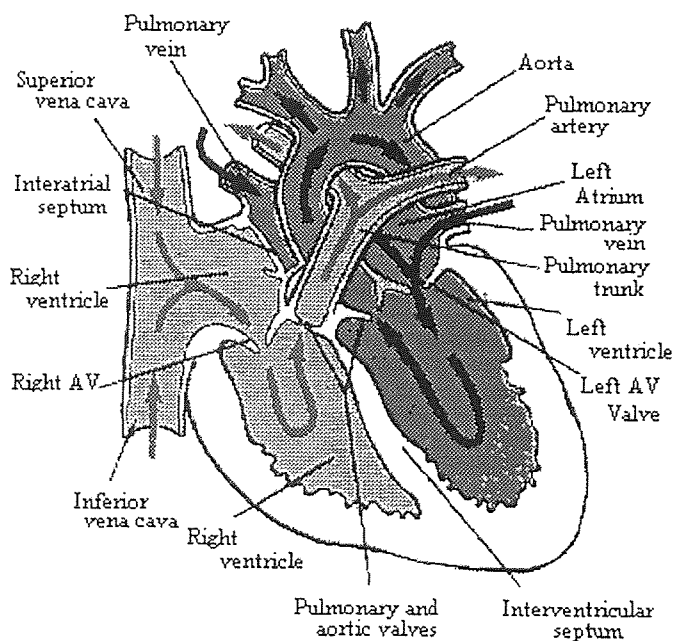


Figure 1.1 The Structure of the Heart (From A. J. Vander et al., *Human Physiology: The Mechanisms of Body Function*, McGraw Hill, 1990).

The pumping action of the heart is a result of a complex sequence of electrical events throughout the heart. Proper coordination of these electrical events is vital to the effective pumping of blood through the circulatory system. The fundamental unit of these electrical events is called the action potential and is responsible for the contraction of the cardiac muscle.

All cells under resting conditions have a potential difference across their plasma membranes due to the relative concentrations of ions inside and outside of the cell [1]. The ions in the highest concentrations in the body are sodium and potassium, and therefore are mainly responsible for the resting membrane potential, which is approximately -90 mV (measured with reference to the interstitial fluid.) A cell maintains this constant potential using the plasma membrane active transport system. This system uses channels in the membrane to cause ions to flow in or out of the cell as necessary to maintain the resting membrane potential.

Action potentials are transient changes in the membrane potential of nerve and muscle cells that travel along the cell to transmit information to and from surrounding cells [1]. They are rapid depolarizations of the membrane to a positive voltage and then quickly back to the resting membrane potential. During the depolarization stage, the membrane suddenly becomes very permeable to sodium ions, causing a large number of them to flow into the cell. This causes the membrane potential to increase by approximately 100 mV. The sodium channels then close and the potassium channels open, allowing potassium ions to rush out of the cell, which allows the membrane to repolarize to its resting value. This entire series of events takes approximately 0.3 seconds to occur in ventricular muscle.

A heart beat is initiated in a small group of cells located in the right atrium called the sinoatrial (SA) node [1]. An SA node cell is different from typical cells in that it automatically depolarizes, causing action potentials to occur periodically without any external influence. This depolarization is known as a pacemaker potential and is responsible for the automaticity of the heart beat. Without any external influence, the SA node depolarizes at a rate of approximately 100 depolarizations per minute.

The action potentials initiated in the SA node are then conducted through gap junctions between the cells of the myocardium (cardiac muscle) from the right atrium to the left atrium. The spread of the action potentials through the atria is rapid enough to cause both of the atria to contract at the same time. This atrial excitation ends in another group of cells located in the lower right atrium called the atrioventricular (AV) node. The AV node conduction is slower than the rest of the cardiac cells and is on the order of a tenth of a second [2]. This allows a small delay between atrial and ventricular contraction so that more blood may be pumped by the atria into the ventricles before ventricular contraction occurs.

The electrical impulses at the AV node then pass through conducting fibers called the bundle of His into the interventricular septum (the wall between the ventricles) and then divide into the right and left bundle branches which travel down the septum to the bottom of the heart [1]. These then divide into smaller conducting fibers called Purkinje fibers that spread throughout the walls of the ventricles. These fibers reside about a third of the way into the walls of the ventricles. The conduction of an impulse from the AV node throughout the ventricles to the terminal Purkinje fibers takes approximately three

hundredths of a second which results in the rapid simultaneous contraction of the entire ventricles. Figure 1.2 shows the structure of the conducting system of the heart.

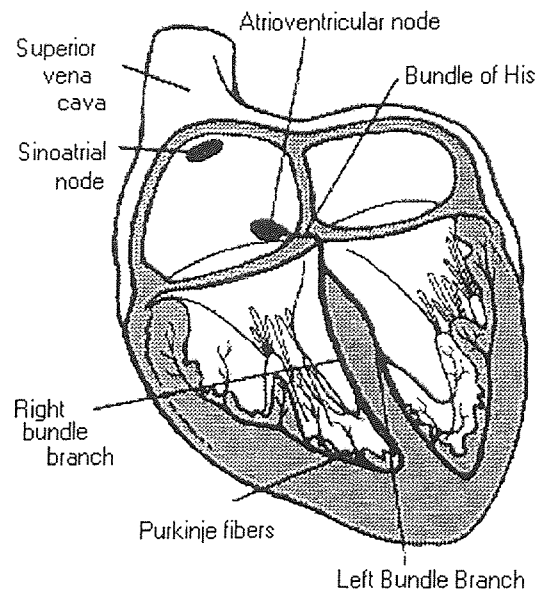


Figure 1.2 The Conducting System of the Heart (From A. J. Vander et al., *Human Physiology: The Mechanisms of Body Function*, McGraw Hill, 1990).

The periodic repetition of the sequence of events in the heart's conducting system results in the cardiac cycle [1]. The cycle is divided into two major parts: systole, which is the period of ventricular contraction and blood pumping, and diastole, which is the period of ventricular filling. Systole begins with a period called isometric ventricular contraction. This occurs when the AV, aortic, and pulmonary valves are closed and the ventricles just begin to contract. During this stage, since the ventricle is completely closed, the blood is compressed, causing the ventricular pressures to increase. When the pressures in the ventricles exceed the pressures in the aorta and pulmonary vein, the aortic and pulmonary valves are pushed open and ventricular ejection occurs. It is during this phase of the cardiac cycle that the ventricles pump blood to the lungs and systemic circulatory system.

Diastole begins with the aortic and pulmonary valves closing and the ventricles relaxing. This phase is called isovolumetric ventricular relaxation because all the ventricles' valves are closed. As the pressures in the ventricles decrease, the AV valves open and ventricular filling occurs. At the very end of diastole, the atria contract forcing still more blood into the ventricles before the AV valves close. This occurs during the last twenty percent of diastole.

1.2.2 The Electrocardiogram

As electrical impulses travel through the heart, some of the electrical activity travels through the surrounding tissue to the skin. By placing electrodes on the skin near the heart, this electrical activity can be amplified, measured, and recorded. The electrical activity of the heart recorded through the skin is known as an electrocardiogram or EKG.

The basic method for recording EKG that is used in many studies is through what is commonly referred to as the standard bipolar limb lead configuration [2]. Figure 1.3 shows the basic electrode positioning for recording the standard bipolar limb leads. Lead I can be considered as the placement of a voltmeter across the chest with the positive lead on the left arm and the negative lead on the right arm. The resulting time varying voltage recording is referred to as the Lead I EKG. Lead II is measured with the positive lead on the left leg and the negative lead on the right arm. Lead III is measured with the positive lead on the left leg and the negative lead on the left arm.

Along with these three basic leads, various other standard leads can be measured totaling twelve different leads. Twelve leads of EKG are commonly used by cardiologists

to provide a more complete picture of the electrical activity of the heart, but are not necessary for the studies presented in this thesis.

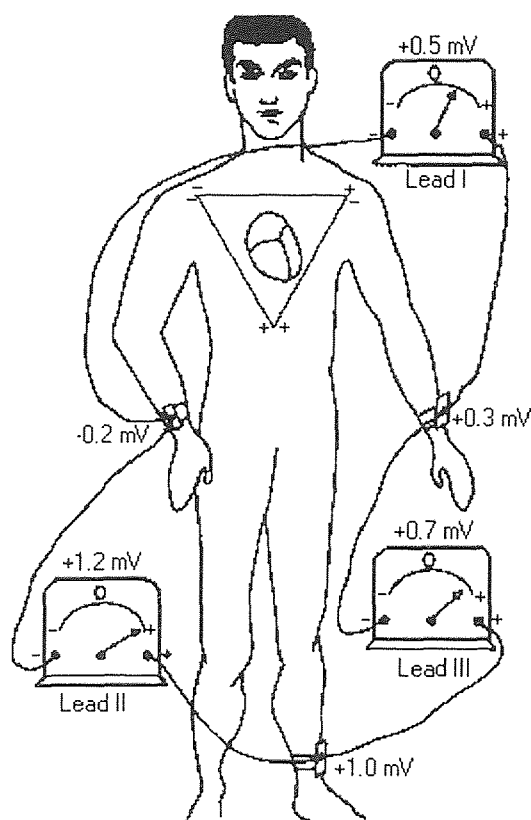


Figure 1.3 Bipolar Limb Lead Configuration (From A. C. Guyton, *Textbook of Medical Physiology*, W. B. Saunders Company, 1986).

Figure 1.4 shows an example of one cycle of a typical Lead I EKG. From the figure, it can be seen that all of the various features of an EKG are given names: the P, Q, R, S, and T waves. Each of these segments of the EKG correspond to a particular electrical event in the cardiac cycle. By observing abnormalities in these various components of the EKG, many different diseases of the heart may be diagnosed. For instance, changes in the relative amplitudes or frequencies of the different components may indicate various heart conditions such as the death of cardiac muscle or a blocked conduction system component.

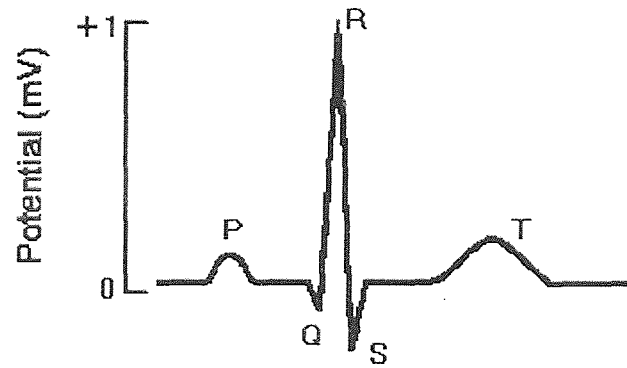


Figure 1.4 A Typical Electrocardiogram (From A. J. Vander et al., *Human Physiology: The Mechanisms of Body Function*, McGraw Hill, 1990).

The first deflection of the EKG, the P wave, is a result of the depolarization of the atria prior to ventricular contraction [1]. The next events in the EKG, the Q, R, and S waves, are commonly referred to together as the QRS complex. The QRS complex corresponds to ventricular depolarization, which occurs approximately 0.15 seconds after the occurrence of a P wave. Between 0.25 and 0.35 seconds after the QRS complex occurs, the ventricles repolarize, which results in the T wave. Atrial repolarization is not seen in the EKG due to the fact that it occurs during ventricular depolarization and is therefore hidden by the QRS complex.

1.2.3 Systemic Circulation

The function of the vascular system is to provide a means for nutrient carrying blood to reach the body's tissues. The vascular system is divided into two major parts: the systemic circulation and pulmonary circulation. The pulmonary circulation is responsible for carrying blood to the lungs for gas exchange while the systemic circulation supplies blood to the rest of the body.

The systemic circulatory system is composed of several types of blood vessels which are subdivided according to structure and function [2]. Leaving the aorta, the first type of blood vessels are the arteries which transport blood under high pressures to the rest of the systemic circulation. Due to the high pressures, the arteries have extremely thick walls and carry blood at high velocities.

The arterioles are the final subdivisions of the arteries before the capillaries and serve the function of controlling the amount of blood released into the capillaries. This is because the arterioles have strong muscular walls which allow the vessel to drastically change diameter, or close completely.

The capillaries are the smallest blood vessels in the circulatory system but perform the ultimate goal of the circulatory system: supplying the tissues with oxygen and removing waste products. The capillaries have extremely thin walls which are permeable to small molecular substances. While being the smallest diameter vessels, they are the most abundant and therefore have the highest combined cross-sectional area of all the different types of vessels.

The next component of the systemic circulation is the venules, which are responsible for collecting the blood from the capillary networks, as well as small amounts of exchange of materials between the blood and interstitial fluid (the fluid surrounding cells.)

The veins are the final component of the systemic circulatory system which return the blood to the heart. Since the pressure of blood returning to the heart is low, the walls of the veins are thin. They are also muscular which allows them to expand or contract which allows for the storage of blood until it is needed by the body. The veins coalesce

into two large veins called the superior and inferior vena cavae, which return blood from the upper and lower portions of the body, respectively.

The relative cross-sectional areas of the various types of blood vessels are shown in table 1.1. As mentioned before, the fact that the capillaries contribute the greatest cross-sectional area to the vascular system can be seen from this table. Also evident in this table is the fact that veins have a larger cross-sectional area than the arteries, which explains why most blood storage occurs in the veins compared to the arteries.

Table 1.1 Relative Cross-Sectional Areas of Blood Vessels (From A. C. Guyton, *Textbook of Medical Physiology*, W. B. Saunders Company, 1986.)

Blood Vessel	Cross-Sectional Area (sq. cm.)
Aorta	2.5
Small Arteries	20
Arterioles	40
Capillaries	2500
Venules	250
Small Veins	80
Venae Cavae	8

1.2.4 Blood Pressure

In order to adequately describe blood pressure, certain concepts regarding hydrostatic pressure (the pressure exerted by a fluid) must first be explained. The first of these concepts is that of flow. A difference in pressure between two points will cause fluid to flow from the region of higher pressure to the region of lower pressure [1]. A factor in the determination of flow is the amount of resistance in the path of the fluid. A linear approximation to fluid flow is as follows:

$$F = \frac{\Delta P}{R} \quad (1.1)$$

where ΔP is the difference in pressure between two points in the fluid, R is the resistance of the path in which the fluid flows, and F is the rate of flow.

Relating equation (1.1) to blood flow in vessels, ΔP is the difference in pressures on the ends of the vessel [1]. The resistance in blood vessels is varied by altering the radius of the blood vessels which will be discussed later. The following equation relates the radius of the vessel to its resistance to flow:

$$R = \frac{8 \eta L}{\pi r^4} \quad (1.2)$$

where η is the fluid viscosity, L is the length of the vessel, and r is the radius of the vessel. From this equation, it can be seen that the resistance from blood vessels is highly dependent on its radius. For example, doubling the radius corresponds to a decrease of resistance by a factor of 16. This demonstrates the effectiveness of varying blood vessel diameter in the regulation of blood pressure.

From equation (1.1), the relationship between flow, pressures, and resistance can be used to determine an equation for the mean systemic arterial pressure (MAP) [1]. This equation is as follows:

$$MAP = CO \times TPR \quad (1.3)$$

where CO is the cardiac output (the volume of blood pumped by the heart per unit time) and TPR is the total peripheral resistance, which is defined as the sum of the resistance to flow offered by of all the systemic blood vessels. This equation is analogous to equation (1.1) because CO describes the flow of the system and TPR defines the resistance of the system.

The blood pressure in the body varies depending upon the location in which it is measured [1,2]. Since the aorta is the first stage in the systemic circulation, that is, it is closest to the left ventricle, the blood pressure is very high: averaging approximately 100

mm Hg. Since the resistance in arteries is small due to the large diameter, the blood pressure is still approximately 95 mm Hg at the end of the arteries. The resistance of the arterioles is the greatest of any part of the systemic circulatory system, and therefore causes the largest pressure drop. The resulting pressure of the blood is close to 30 mm Hg when the blood enters the capillaries. The pressure then drops approximately 20 mm Hg in the capillaries to 10 mm Hg. The pressure is then reduced to nearly zero at the end of the venous system..

Since the pumping of the heart is pulsatile, the blood pressure fluctuates between a maximum, called the systolic pressure, when the heart ejects blood, and a minimum, called the diastolic pressure, which occurs just before ejection. A cycle of a typical blood pressure wave appears in figure 1.5.

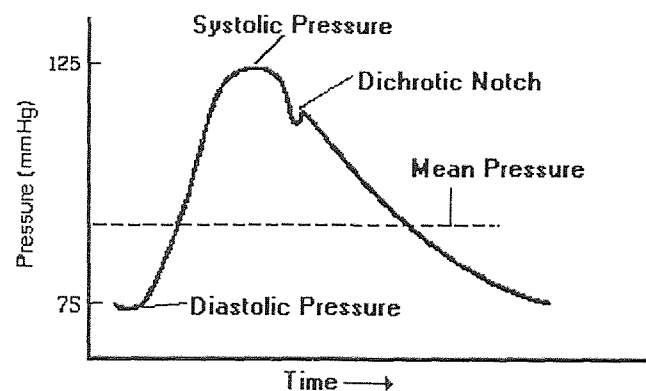


Figure 1.5 Blood Pressure Wave (From A. J. Vander et al., *Human Physiology: The Mechanisms of Body Function*, McGraw Hill, 1990).

Another important mechanism that affects blood pressure is that compliance [1]. Compliance is defined as how easily a structure can be compressed. This effect is most prominent in the arteries in which it maintains blood pressure during diastole by allowing the arterial walls to stretch during systole, storing energy which is released during diastole. The amount of blood stored in the arteries during systole is significant: only a third of the

stroke volume (the volume of blood ejected from each ventricle with each heart beat) leaves the arteries. During diastole, the arterial walls passively recoil, pushing the remainder of the blood into the arterioles.

1.3 Respiration

The function of the respiratory system is to provide the cells in the body with oxygen, which is required to perform chemical reactions from which energy is obtained. The respiratory system is also required to remove carbon dioxide, a result of these reactions, from the body. While the circulatory system is responsible for the exchange of nutrients on the cellular level, the respiratory system is responsible for obtaining oxygen from the external environment and providing it to the circulatory system, as well as removing carbon dioxide from the circulatory system and releasing it into the external environment.

Figure 1.6 shows the basic structure and components of the respiratory system. Upon inhalation, air flows into the nose and/or mouth, through the trachea and bronchi, and into the lungs. Inside the lungs, the bronchi divide into approximately 20 generations of branchings.

The alveoli is the site in the lungs that is responsible for gas exchange and are located in the final branching of the airway [1]. The alveoli are tiny hollow sacs that are separated from the capillaries of the pulmonary circulatory system by a thin layer of cells approximately 2 μm thick. The abundance of the alveoli allow the total surface area of alveoli in contact with capillaries to be approximately 75 m^2 . These two factors combined allow the rapid exchange of carbon dioxide and oxygen to occur in the pulmonary

capillaries. This oxygenated blood is then returned to the left heart to be delivered to the tissues of the body via the systemic circulatory system.

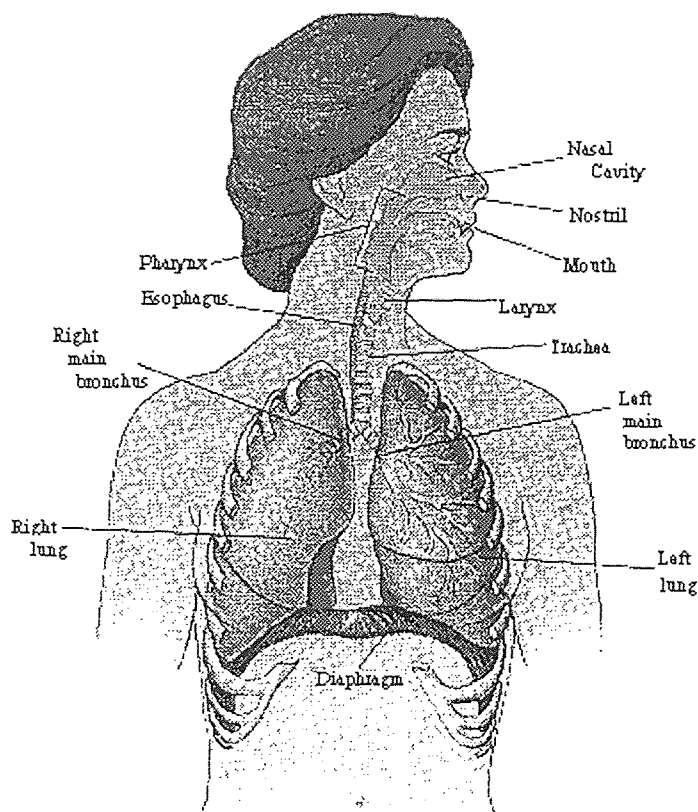


Figure 1.6 Organization of the Respiratory System (From A. J. Vander et al., *Human Physiology: The Mechanisms of Body Function*, McGraw Hill, 1990).

Air is transported to the airways of the lungs by bulk flow from a region of high pressure to a region of lower pressure [1]. Lower pressure is created in the lungs by the contraction of the diaphragm, causing it to move downward in the chest cavity, and the contraction of the intercostal muscles which cause the ribs to move upward and outward. Since the walls of the lungs are pulled downward and outward with the diaphragm and ribs, these actions cause the volume of the lungs to increase and, consequently, the pressure in the lungs to drop below atmospheric pressure. This difference in pressure causes air to flow into the lungs.

Exhalation is achieved by the relaxation of the diaphragm and intercostal muscles. This results in the lungs returning to their normal volume due to their elasticity, forcing the inhaled air out of the lungs. One inhalation combined with an exhalation comprise one respiratory cycle, or one breath. The volume of air inhaled and exhaled is referred to as the tidal volume.

1.4 Neural Control Systems

The purpose of the nervous system is to provide the body with a means of communication between the brain and the rest of the body. It is divided into two major parts: the central nervous system and the peripheral nervous system. The central nervous system is composed of the brain and the spinal cord and the peripheral nervous system consists of the nerves connecting the brain and spinal cord to the rest of the body.

The peripheral nervous system is further divided into two major divisions: the somatic nervous system and the autonomic nervous system. The somatic nervous system is composed of all the nerves connecting the central nervous system to skeletal muscle cells, and is usually under voluntary control. The autonomic nervous system is composed of the nerves connecting the central nervous system with tissue other than skeletal muscle. The structure and function of the autonomic nervous system is discussed in the following subsection.

1.4.1 The Autonomic Nervous System

The autonomic nervous system is divided into two subdivisions called the sympathetic and parasympathetic divisions. The two divisions differ in the type of neurotransmitter used to

convey information to the different locations in the body, and therefore cause the receptor site to behave differently.

The sympathetic nervous system is usually associated with a response to stress or a “fight or flight” situation [1]. For example, some of the effects of a sympathetic response would be increased heart rate, contracted salivary glands, and increased blood pressure. The parasympathetic nervous system has opposite effects on the body. Parasympathetic activity results from relaxation and allows the body to perform “housekeeping” functions such as increased digestive system activity. These two divisions of the autonomic nervous system behaving in opposite ways allow the autonomic nervous system to exert precise control over bodily function. This type of control may be compared to the combined use of a brake and accelerator pedal in a car: releasing pressure on the accelerator pedal will slow the car, but use of the brake in conjunction with this allows decreased response time and increased accuracy.

This type of precise control over bodily function allows the body to maintain homeostasis, which is defined as the maintenance of relatively constant internal conditions by the body [1]. When changes occur within the body, the regulatory systems of the body quickly compensate for these changes to return the body to normal conditions. An example of a normal response of this type is the autonomic nervous system’s increasing respiration rate and volume by increasing output to the muscles responsible for breathing when a lowered concentration of oxygen is detected in the blood. The mechanisms for autonomic regulation of heart rate and blood pressure are discussed in the following subsections.

1.4.2 Autonomic Control of the Heart

The autonomic nervous system has a strong control over heart rate as a large number of sympathetic and parasympathetic nerve fibers terminate in the SA node of the heart [1]. As mentioned before, the SA node spontaneously depolarizes at approximately 100 beats per minute without nervous system input. The nerve fibers acting on the SA node control the depolarization rate of the SA node by altering the slope of the pacemaker potential. The sympathetic nerves increase the slope of the pacemaker potentials, causing the SA node cells to reach the threshold potential more rapidly, increasing the heart rate. Similarly, the parasympathetic nerves decrease the slope of the pacemaker potentials, thereby decreasing the heart rate.

The autonomic nervous system also controls heart rate by affecting the conducting system of the heart [2]. Parasympathetic outflow slows the conduction of the action potentials throughout the entire conducting system of the heart, while sympathetic outflow speeds the conduction. The combined effect of these influences on heart rate can cause the heart rate to vary from 20 to 30 beats per minute under maximum parasympathetic stimulation up to approximately 250 beats per minute under maximum sympathetic stimulation.

Sympathetic and parasympathetic nerve fibers controlling the heart also affect the contractile force of the heart [1]. An increased contractile force caused by increased sympathetic stimulation of the heart combined with an increase in end diastolic volume causes an increased stroke volume. Parasympathetic nerves reduce the contractility of the heart but have a smaller influence than sympathetic nerves.

The combination of autonomic control of heart rate and contractility, which affects stroke volume, cause changes in cardiac output [1]. Cardiac output is defined as the volume of blood pumped by the heart per unit time (usually measured in liters/minute.) It is calculated from the following equation:

$$CO \text{ (L/min.)} = HR \text{ (beats/min.)} \times SV \text{ (L)} \quad (1.4)$$

where CO is the cardiac output, HR is the heart rate, and SV is the stroke volume. From this equation, it can be seen that increased sympathetic influence on the heart causes increases in heart rate and contractility, and consequently stroke volume, increasing the cardiac output. Conversely, parasympathetic stimulation on the heart reduces cardiac output.

1.4.3 Autonomic Regulation of Blood Pressure

The autonomic nervous system also plays a role in the regulation of blood pressure due to the sympathetic innervation of all of the vasculature except the capillaries [2]. While some of these nerve fibers cause vasodilation, most cause vasoconstriction. Varying the diameter of the blood vessels alters the resistance and therefore the rate of blood flow through the system. The parasympathetic division of the autonomic nervous system does not play a role in altering the resistance of the vasculature but does affect blood pressure as discussed in the following paragraph.

As mentioned previously, the MAP is given as the product of the TPR and CO. From this equation, it can be seen that since a sympathetic response increases the CO and constricts blood vessels, causing the TPR to increase, the result is an increase in MAP. Conversely, a decrease in sympathetic activity and an increase in parasympathetic activity

causes the blood vessels to relax, decreasing the TPR, and the CO to decrease, resulting in a decrease in MAP.

It can be seen that blood pressure is regulated by the a complex interaction between the sympathetic and parasympathetic innervation of the heart and the sympathetic innervation of the vasculature [1]. These interactions can be viewed as a control system utilizing negative feedback to maintain stability. The sensors for this control system that detect changes in blood pressure are called baroreceptors. Baroreceptors are located near the branching of the two carotid arteries, which supply the brain with blood, and in the aortic arch. These baroreceptors constitute the arterial baroreceptors. Baroreceptors sense the degree of stretching in the arterial walls which is directly proportional to the amount of pressure exerted by the blood on the arterial wall. Nerve fibers then relay this pressure information to the cardiovascular control centers of the brain.

Under steady state conditions, the baroreceptors discharge action potentials at a steady rate [1]. Changes in pressure sensed by the baroreceptors are relayed to the brain by a change in this frequency of discharge. If the MAP increases, the baroreceptors increase their rate of discharge; conversely, a decrease in MAP slows the frequency of baroreceptor firing.

When a change in the firing rate of baroreceptors is sensed by the brain, the brain responds by performing the necessary autonomic response to return the MAP to its previous value [2]. For example increased baroreceptor firing frequency caused by increased MAP causes the inhibition of vasoconstriction by reducing sympathetic activity, causing decreased TPR, and a decrease in heart rate and contractility by increasing

parasympathetic activity. Decreased MAP sensed by the baroreceptors causes the opposite autonomic response required to increase the MAP to its normal value.

It should be noted that baroreceptors regulate only short term fluctuations in blood pressure [1,2]. They respond rapidly to changes in the MAP but will adapt to changes occurring over the course of a few hours to a few days and not cause an autonomic response. Long term blood pressure is mediated mostly by the renal-body fluid-pressure mechanism which affects the blood volume by varying the amount of fluid excreted by the kidneys.

1.5 Heart Rate Variability

The autonomic regulation of heart rate causes short term fluctuations in the instantaneous heart rate [3]. Studies of these short term fluctuations are collectively referred to as heart rate variability (HRV) studies. HRV studies are performed by extracting heart rate information from the EKG by measuring the time between each R wave, referred to as the interbeat interval (IBI), and converting these IBI values into the frequency domain. This results in what is referred to as an IBI or HRV spectrum. A typical HRV spectrum appears in figure 1.7.

Three peaks usually exist in an HRV spectrum: a very low frequency peak (VLF), a low frequency peak (LF), and a high frequency peak (HF). The VLF peak is between 0.02 and 0.05 Hz., the LF peak is between 0.05 and 0.15 Hz., and the HF peak is usually between 0.15 and 0.4 Hz. but may move outside these limits and will be discussed later [4]. HRV studies are concerned with the identification and study of the physiological mechanisms that affect the power in these frequency bands.

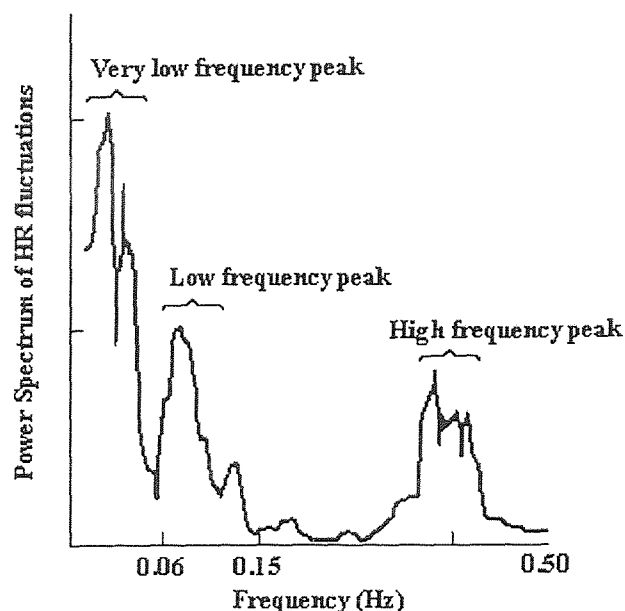


Figure 1.7 Heart Rate Variability Power Spectrum (From M. Kamath et al., *Human Physiology: The Mechanisms of Body Function*, McGraw Hill, 1990.

The HF peak power of the HRV spectrum is commonly accepted by researchers to be a marker of parasympathetic modulation of heart rate [5,6]. This was shown by administering drugs that block parasympathetic activity, such as atropine, then observing the fact that the HF peak was abolished from the HRV spectrum. The significance of the LF component is not as clear cut, however. Parasympathetic blockade significantly reduced the LF component, but not completely. Further administration of sympathetic blocking drugs removed the residual LF power [4]. It can therefore be concluded that the LF peak of the HRV spectrum is a marker of both sympathetic and parasympathetic activity.

The HF component of the HRV spectrum has been attributed to respiratory sinus arrhythmia (RSA) which is the modulation of the heart rate coincident with the frequency of respiration. The HF peak therefore may reside below 0.15 Hz. for respiratory rates below 9 breaths per minute or above 0.4 Hz. for rates above 24 breaths per minute. In the

case of the higher respiration rate, the upper frequency limit for assessing the HF power must be increased from the usual 0.4 Hz. to include the peak. In the case of the respiration rates below 9 breaths per minute, the HF peak begins to move into the LF region. Assessment of LF and HF powers is not as straightforward in this case, as the two peaks begin to merge into one peak at these low respiration rates. This is due to a phenomenon called entrainment which occurs when two coupled nonlinear oscillators approach the same frequency, and one or both oscillators shift in frequency and begin to oscillate at the same frequency. To date, there are no known methods of separating this combined peak into separate LF and HF powers.

Another useful quantity derived from power spectral analysis of HRV is the ratio of the LF to HF power. This number is commonly used as an indicator of the balance between parasympathetic to sympathetic activity and is referred to as the sympathovagal balance [5].

It can be concluded that power spectral analysis of HRV provides a noninvasive tool with which to monitor the activity of the autonomic nervous system. While parasympathetic activity is clearly quantified by present techniques, new methods must be developed in order to quantify sympathetic activity.

1.6 Systolic Arterial Pressure Variability

Similar to the concept of HRV, systolic arterial pressure variability (SAPV) is used by researchers to gain insight into the activity of the autonomic nervous system. SAPV studies involve performing power spectral analysis on the sequence of systolic blood pressure values obtained from the raw blood pressure data. The resulting spectrum is

similar to the HRV spectrum in that it contains both LF and HF components. The determination of the significance of the powers of these peaks is within the scope of SAPV research.

Similar to HRV spectra, the HF peak in SAPV spectra is coincident with the frequency of respiration. This peak however is not mediated by parasympathetic influence, but is believed to be a result of other respiratory factors [2]. First, impulses from the respiratory center in the brain are believed to “spill over” into the vasomotor center, causing modulation of vasoconstriction at the frequency of respiration. Second, the decreased pressure in the thoracic cavity caused by the contraction of the diaphragm during inspiration causes the blood vessels in the cavity to expand. This results in a decreased amount of blood to be returned to the left heart and consequently lower cardiac output and lower arterial pressure. Third, the pressure changes in the thoracic cavity are believed to excite the baroreceptors which cause changes in the blood pressure. The net effects of these factors are an increased arterial pressure during the early part of expiration and a fall in pressure during the rest of the respiratory cycle. The power of the HF peak therefore does not provide information on the functioning of the autonomic nervous system.

The LF peak in the SAPV spectrum which occurs at approximately 0.1 Hz. is also a result of many different physiological parameters. These 0.1 Hz. oscillations are commonly referred to as vasomotor waves or Mayer waves [2,7]. One of the causes of these oscillations in blood pressure is the oscillation of the baroreceptor reflex [2]. That is, the frequency at which the baroreceptors detect increased pressure, inhibit the sympathetic nervous system to lower the pressure, then detect the low pressure and

stimulate the sympathetic nervous system to raise it is coincident with the frequency of the Mayer waves.

Another regulatory mechanism that occurs at this frequency is that of the chemoreceptor reflex [2]. Chemoreceptive cells lie near the carotid arteries and aorta and detect decreased blood pressure by the decreased oxygen level and increased carbon dioxide level. Upon detecting decreased blood pressure, these cells excite the vasomotor center, which causes the arterial pressure to increase. While baroreceptors have a much stronger effect on pressure control at normal blood pressures, these chemoreceptors have a much stronger effect on blood pressure at arterial pressures in the range of 40 to 80 mm Hg.

The central nervous system (CNS) ischemic response also regulates arterial pressure at these low frequencies [2]. The CNS ischemic response is caused by decreased blood flow to the vasomotor center in the brain. This is believed to be initiated by the buildup of carbon dioxide in the vasomotor center, which has an extremely strong effect in stimulating sympathetic activity. The CNS ischemic response causes severe vasoconstriction of the peripheral blood vessels as well as arterial pressure elevation of up to 270 mm Hg for up to 10 minutes. Like the chemoreceptor reflexes, this response regulates blood pressure only when it drops below 60 mm Hg, and exerts the strongest effects at blood pressures as low as 15 mm Hg.

While a sympathetic response directly elevates blood pressure by causing vasoconstriction, increased heart rate, and increased contractility of the heart, it also causes a hormonal response that increases blood pressure [2]. Norepinephrine and epinephrine are released into the blood by the brain by a sympathetic response. These

hormones excite the heart as well as cause vasoconstriction in blood vessels that are not innervated by the sympathetic nervous system, both causing blood pressure to increase. Since the release of these hormones is a direct result of a sympathetic response, they are considered a part of the sympathetic blood pressure regulatory mechanism.

Since blood pressure modulation near 0.1 Hz. is associated mainly with sympathetic regulation of blood pressure, it is commonly accepted in present research that the LF peak power in the SAPV spectrum is an indicator of purely sympathetic activity [8,9,10]. This is supported by the fact that the LF component disappears completely in neurologically complete quadriplegics, which is assumed to be due to the fact that the sympathetic pathways near the spinal cord are disrupted.

1.7 Statement of Objective

The purpose of this research was to examine systolic arterial blood pressure variability in conjunction with heart rate variability to provide a more complete picture of the activity of the autonomic nervous system. While current heart rate variability methods allow measurement of parasympathetic activity, they do not isolate sympathetic activity and therefore cannot be used to measure sympathetic activity. Current research suggests that power spectral analysis of systolic arterial blood pressure may provide an indicator of sympathetic activity and therefore complete the picture of the autonomic nervous system.

Power spectral analysis of systolic arterial blood pressure spectra from continuous blood pressure data is not straightforward: resulting spectra are highly dependent upon the methods used in deriving the spectra. In order to determine an appropriate method for

blood pressure as well as heart rate variability analysis, several different signal processing techniques were compared.

Interpolation is a digital signal processing technique required for performing spectral analysis using Fast Fourier Transform (FFT) methods. Several different interpolation methods were performed on systolic blood pressure data, interbeat interval data, as well as simulated data, and the spectra were found and compared. The changes in the spectra were determined depending upon the interpolation methods and the factors changing the spectra were quantified.

Previous studies have indicated that reproducibility in heart rate variability studies may be poor when comparing a person to himself on different days. A technique for normalizing spectral areas was evaluated to aid in this reproducibility.

Upon determining an acceptable method for analyzing systolic arterial blood pressure data, a set of algorithms were designed and implemented using MATLAB. These algorithms detect systolic peaks, interpolate these values, and perform spectral analysis on the interpolated systolic arterial pressure signal as well the raw blood pressure signal.

Finally, these algorithms were used to perform analysis of blood pressure signals. The resulting systolic arterial pressure variability spectra were then compared to respiratory data as well as spectra of heart rate variability. These data were then used to determine relationships between the spectra and various physiological parameters.

CHAPTER 2

DATA ACQUISITION

2.1 Introduction

The data acquisition and experimental protocol presented in this chapter were originally used by Leifer for the purpose of accounting for complex interactions between various physiological parameters, specifically, with respect to heart rate variability [4]. While EKG and respiratory data were utilized by Leifer, blood pressure data were not because the algorithms to analyze blood pressure were not yet developed. Since the development of these algorithms was within the scope of this research, the blood pressure data collected during these studies were utilized to expand upon Leifer's research.

This chapter describes the laboratory setup and equipment, data acquisition techniques and experimental protocol used by Leifer. While these are described in their entirety, not all of the acquired data were used in this research.

2.2 Laboratory Setup

For collection of the experimental data used in this research, several pieces of equipment were utilized. The purpose of this section is to describe the interconnection of the equipment used to collect this data as well as the connection of this equipment to the subject.

Lead I and Lead III EKG data were obtained using a Quinton Q4000 stress test monitor. Along with the two bipolar limb leads, a pulse train synchronous with the

occurrence of R waves (sync pulse) is also obtained from the Quinton Q4000. This sync pulse allows the elimination of the off line R wave detection algorithms required by HRV studies.

Respiratory rate data were obtained using impedance pneumographic methods. This allows the detection of the respiratory cycle by measuring the impedance of the subject's chest cavity which is a function of the length and area of the chest cavity. Since these parameters change as the subject inhales and exhales, the impedance of the chest cavity therefore varies during respiration. The impedance is measured by placing two electrodes on the subject: one on the right shoulder and the other on the lowest rib on the left side of the chest, then passing a small current at 50 kHz. through these electrodes. The potential difference between these electrodes is then measured and the impedance is found as the ratio of the measured potential difference to the induced current. It should be noted that by this method, the resulting respiratory signal is in arbitrary units, that is, the true value of the volume of air inspired is not obtained from this method. Relative volumes are, however, observed by the degree of change in the amplitude of the respiration signal.

Blood pressure data were collected using an Ohmeda 2300 Finapres blood pressure monitor. This device allows the continuous measurement of arterial blood pressure by a small cuff worn on the finger. The Finapres estimates arterial blood pressure as the amount of pressure required on the finger to maintain a constant volume of blood in the finger. The volume of blood in the finger is measured by photoplethysmographic methods: that is, a light is shone into the skin of the finger and the amount of light

reflected by the finger is detected. The amount of blood in the finger directly affects the amount of light reflected by the skin.

Respiratory volume was measured by collecting data from a spirometer. The spirometer requires the subject to wear a mask that contains valves that allow him to inhale room air but exhale into a tube that is connected to the spirometer. The total volume exhaled is digitally displayed by the spirometer but it also includes an output that gives a series of pulse trains, each group corresponding to an exhalation. Each pulse in a group corresponds to a 0.1 liters of air. Therefore, by counting the number of pulses in each group, the volume of air exhaled can be computed for each breath.

Finally, various respiratory data were collected using the Quinton Q-PLEX cardio-pulmonary exercise system. This device measures parameters such as the amount of carbon dioxide remaining in the pulmonary arteries following exhalation and the amount of carbon dioxide that diffuses from the blood to the alveoli. Since the Q-PLEX measures respiratory parameters, a mask is required to interface it to the patient. It was connected in series with the spirometer: air flows from the mask, through the spirometer and into the Q-PLEX.

These various pieces of equipment were connected to a KEITHLEY - Metrabyte DAS-16 board, containing a 12 bit analog to digital (A/D) converter, mounted in a IBM compatible personal computer (PC.) This board samples the data and stores it in packed binary form files for subsequent computer analysis. The equipment was connected to the A/D board on channels 0 through 5 in the following order: respiration, sync pulse, blood pressure, Lead I EKG, respiration volume (from the spirometer), and Lead III EKG. The Q-PLEX does not interface to the data acquisition computer.

Before collecting data, a program called PRIMPLOT, which was developed in our laboratory, is used to assure the presence and proper gain of each of the signals. This program displays the input signals from the equipment on the computer monitor in real time. In this manner, the connection and setup of the equipment is checked by monitoring each of the channels 0 through 5, and making sure the appropriate signals are present.

Next, data files are created using a program called MKFILE. A required input argument for this program is the size of the file in kilobytes. This is calculated as follows:

$$\text{size (kb)} = \# \text{channels} * \text{sec. of data} * \frac{2 \text{ bytes}}{\text{sample}} * \frac{\# \text{ of samples}}{\text{second}} * \frac{1 \text{ kilobyte}}{1000 \text{ bytes}} \quad (2.1)$$

For the experiment described in this chapter, the number of channels is 6, the number of seconds of data to be collected is 120 (two minutes), and the sampling rate is 200 samples per second. Using these values in equation (2.1) results in a file size of 288 kilobytes.

In order to collect data, a high speed data acquisition software package called KEITHLEY - Metrabyte Streamer is utilized. This allows the actual sampling of data to begin and writes this data to the specified file.

In sections of the experiments where pacing (maintenance of a constant rate) of respiration was required, subject used visual feedback obtained by following a series of lights mounted in a box and programmed to light in sequence at an adjustable rate. By requiring the subject to complete a full respiratory cycle upon the completion of the illumination of the series of lights, a comfortable ratio of inhalation and exhalation could be chosen depending upon the comfort of the individual. For example, given 5 seconds to complete a respiratory cycle, the subject could choose to inhale for 2 seconds and exhale for 3 seconds or adjust this depending upon comfort.

Where maintenance of a specific tidal volume was required, visual feedback using the digital display on the spirometer was used. The display showed the volume of air in liters exhaled by the subject. Since the displayed volume exhaled with each breath was additive, it was required that the display be manually reset to zero during the inhalation of the subject, for ease of monitoring volume.

2.3 Experimental Protocol

Data were collected from ten subjects, six male and four female, with ages ranging from 20 to 42 years old. The experiment was performed on three separate days on at approximately the same time of day.

On the first day of the experiment, five two minute intervals of data were collected while the subject rested in a seated position. The subject's resting respiration rate and average tidal volume were then obtained from this data prior to performing the next part of the experiment.

The second day of the experiment consisted of first collecting a two minute interval of data while the subject was at rest and breathing spontaneously. The next two minute interval was collected while the subject performed paced breathing at his normal respiration rate. The next five two minute sequences of data were collected while the subject maintained paced breathing at his normal respiration rate and maintained a tidal volume at a specified level. Five sets of volumes were used: either 0.4, 0.7, 1.0, 1.2, and 1.4 liters or 0.5, 0.8, 1.0, 1.3, and 1.5 liters. The set of volumes was chosen based on the resting tidal volume of the particular subject. If, for example, the subject's tidal volume averaged less than, 0.4 liters, the set of lower volumes was used.

On the third day of the experiment, two minutes of data were collected with subject at rest. Next, the subject duplicated two of the exercises performed on the second day of the experiment. The subject then performed paced breathing at $3/2$ his normal rate without tidal volume control for the next two minute interval of data. The next five two minute intervals of data were collected while the subject maintained paced breathing at this rate and maintained the five different tidal volumes used on day two of the experiment. The next two minute interval of data was collected while the subject paced his breathing at $2/3$ his normal rate without volume control. The next five two minute intervals of data were collected while the subject maintained this respiratory rate as well as the five different volumes used in the previous sections of the experiment.

During the controlled rate and volume controlled experiments, the subject was required to quantify the level of comfort experienced during each two minute interval on a scale of 1 to 4. Specifically, a rating of 1 was given to indicate that the exercise was comfortable, 2 indicates light difficulty, 3 indicates moderate difficulty, and 4 indicates the exercise felt very difficult for the subject.

In order to avoid ordering effects, the order of the protocol on the third day of the experiment was varied from subject to subject: that is whether the six two minute exercises performed at $3/2$ normal respiration rate was performed before or after the six two minute exercises at $2/3$ normal respiration rate. Also since some of the extreme exercises such as high respiration rate combined with low tidal volume caused extreme discomfort, some two minute intervals of data were skipped.

CHAPTER 3

SIGNAL PROCESSING TECHNIQUES

3.1 Introduction

The transformation of the electrocardiogram and blood pressure signals into heart rate variability and systolic arterial pressure variability spectra requires several intermediate steps such as peak detection, interpolation, resampling, and spectral analysis. To date, there are not standardized ways to process this data to study blood pressure and heart rate variability. This leads to varying experimental results and difficulties in the comparison of experimental results from one research facility to another.

The purpose of this chapter is to introduce various signal processing methods used in HRV and SAP analysis as well as compare them. Research and experiments were performed on these various techniques to determine the best method to utilize for subsequent SAP analysis. Upon choosing a method for analysis, a series of programs were written to perform the analysis.

3.2 Interpolation Methods

Spectral analysis is usually performed by one of three methods: the Discrete Fourier Transform (DFT), the Fast Fourier Transform (FFT), and autoregressive spectral analysis (AR). The FFT is similar to the DFT but is implemented in such a way that the computational time is greatly reduced. Due to its efficiency, the FFT is the best known and widely used of spectral analysis methods [11]. This method as well as the AR method

suffer from the drawback that the signal samples must be uniformly spaced in time before performing spectral analysis. Therefore, to apply the FFT to IBI or systolic blood pressure data, which are not evenly spaced in time, the data must be altered in such a way as to become uniformly sampled. Since all interpolation methods involve alteration of the original signal, distortion of the results occurs. The purpose of this section is to describe different interpolation techniques used by researchers and compare them in an attempt to determine which techniques are best in terms of minimization of spectral distortion as well as computational efficiency. Different techniques are also presented for correction of spectra derived using various interpolation methods.

This section first describes the mechanics and terminology of common interpolation techniques. A discussion and comparison of the different techniques and their effects on spectral analysis based on the research of other laboratories is then presented. Finally four different experiments which were designed to compare interpolation methods are described and the results compared to the those of other laboratories. These results were then used to determine a method of SAP analysis to be used for the remainder of the analysis required by this research.

3.2.1 Overview of Interpolation Methods

One method of creating a uniformly sampled signal from heart rate data is to create a tachogram which is simply a list of the IBI values evenly spaced in time. For SAPV, a list of systolic pressures is created. In both cases, the average IBI length is calculated and is assumed to be the distance between each IBI or systolic pressure data point. An FFT can then be derived from the signals, using the inverse of the mean IBI as the sampling rate.

Some resampling techniques require the insertion of intermediate values between data points, then resampling the signal at a constant sampling rate. One example of this type of interpolation is called step interpolation. Step interpolation of the systolic arterial blood pressure is achieved by detecting the systolic peaks and filling in the samples between peaks with the value of the previous peak. The resulting interpolated systolic arterial pressure signal has a step-like quality; each step's value represents one systolic peak's value. Figure 3.1 is an example of a segment of a blood pressure signal with the step interpolated systolic arterial pressure signal overlying it.

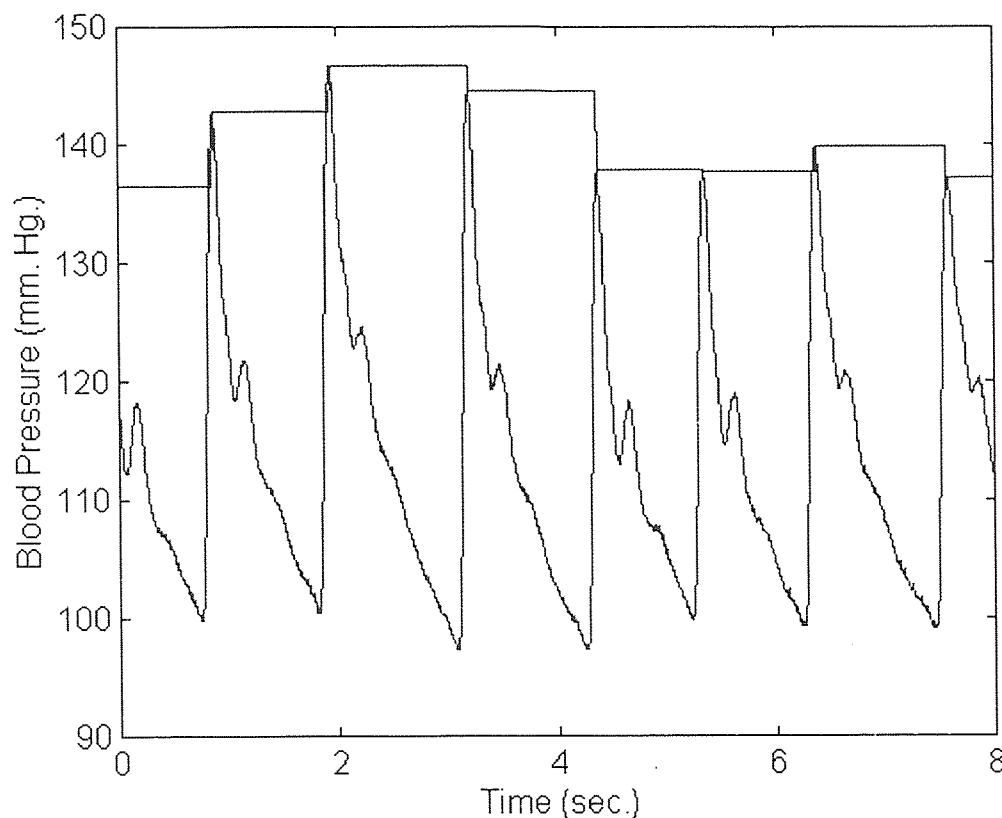


Figure 3.1 Forward Step Interpolation of Blood Pressure.

The systolic peaks may also be interpolated using a cubic spline instead of constant valued steps. This is done by first detecting the systolic peaks and filling the samples

between peaks with a cubic spline fit so that the resulting interpolated signal has the same sampling frequency as the original blood pressure signal. Figure 3.2 shows an example of a blood pressure signal with the cubic spline interpolated systolic arterial pressure signal overlying it.

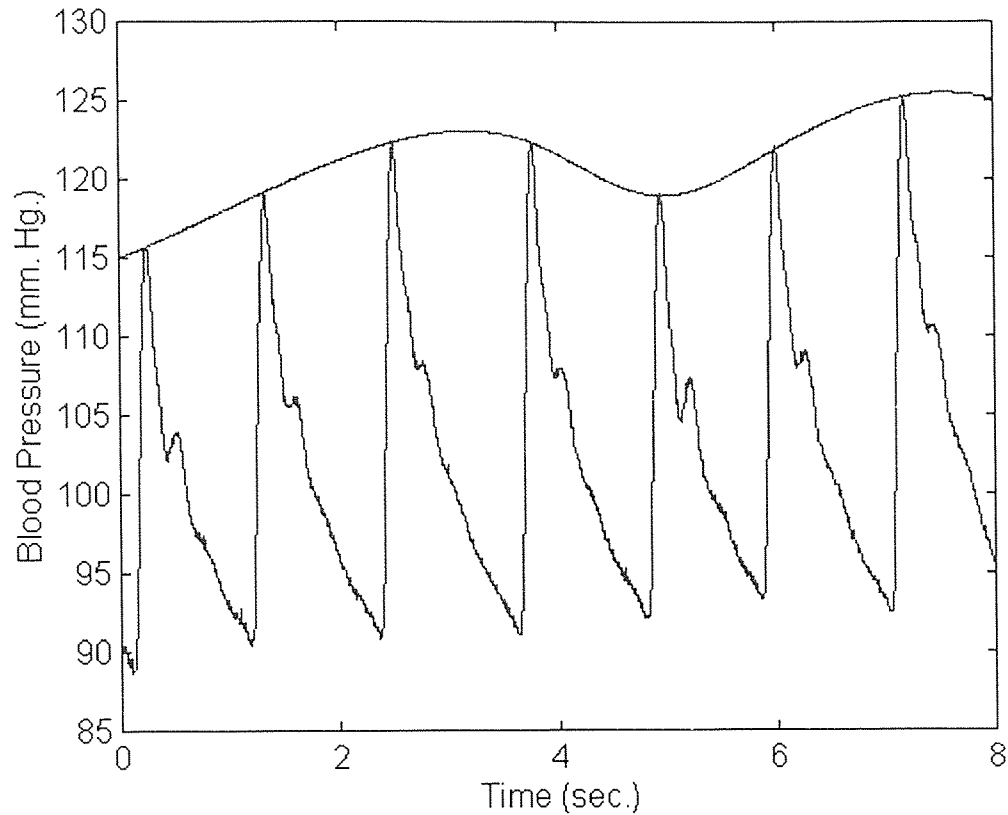


Figure 3.2 Cubic Spline Interpolation of Blood Pressure.

Interpolation of the IBIs is performed in a slightly different manner since the variability is contained in the horizontal (time) axis rather than in the amplitudes as is the case with SAPV [12]. Step interpolation of the IBIs is performed as follows: first the point process signal is derived from the EKG by detecting the R waves. The point process signal consists of an impulse at every time instant that an R wave occurs. The samples between each impulse are then filled in with a constant value corresponding to the

duration of the interval preceding that R wave. This is referred to as backward step interpolation. The samples may also be filled in with a constant equal to the inverse of the duration of the previous IBI [13]. Figure 3.3 shows the steps in deriving the backward step interpolated IBI signal.

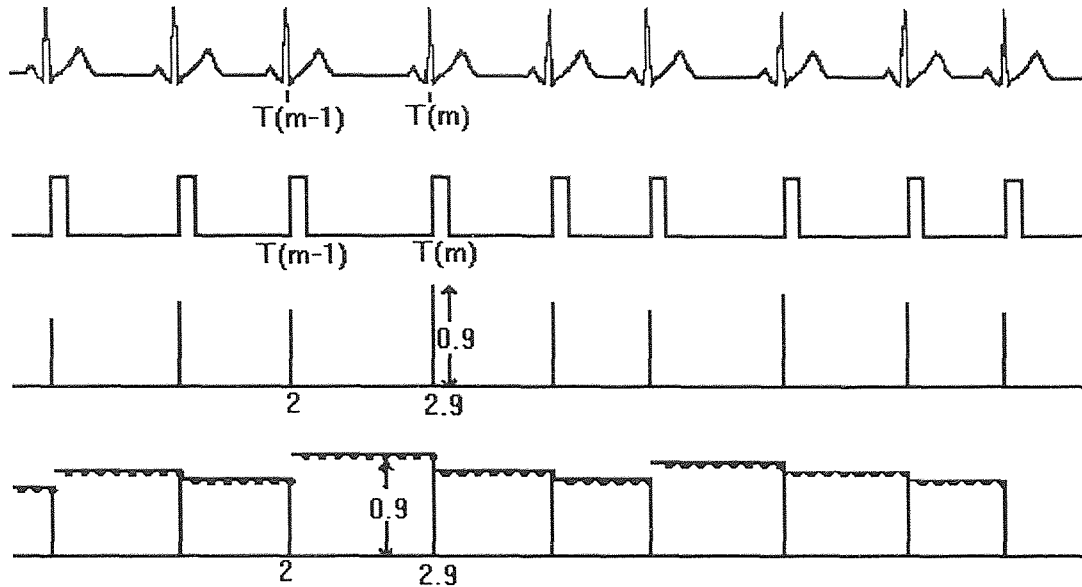


Figure 3.3 Backward Step Interpolation of the IBI (From S. Shin et al., “Assessment of Autonomic Regulation by the Method of Complex Demodulation,” IEEE Trans. Biomedical Engineering, 1989)

All of the methods mentioned thus far resulted in evenly sampled signals, lending themselves to the benefits of FFT processing. Other methods of spectral analysis do not require evenly spaced samples and therefore require other methods of spectral analysis such as the Lomb periodogram (described in detail in subsection 3.2.3) or the DFT. This allows the spectrum to be calculated directly from the systolic arterial pressure data points while retaining their original locations in time. This can also be applied to IBI data by creating a signal that contains evenly weighted impulses at the time of the occurrence of each R wave. This signal is referred to as a point process. These impulses retain their

original time locations before spectral analysis, eliminating one step of intermediate processing.

The IBI signal may also be interpolated using the cubic spline method. Once the point process is derived, each impulse's magnitude is made equal to the preceding IBIs duration. The samples between each impulse are then filled in with a cubic spline fit, resulting in a smooth interpolation of the IBI signal.

3.2.2 Comparison of Interpolation Methods

Different methods of interpolation give rise to many different results for the same EKG or blood pressure data. Much research has been devoted to the comparison of these different methods. Generally, it has been shown that most interpolation methods actually distort the spectra, introducing a low pass filtering effect on the spectra [11,13,14]. Several methods have also been presented that propose different techniques for correcting the spectral distortion and normalizing the results.

A study by Haaksma et al. [11] compares IBI spectra obtained using different interpolation techniques with spectra obtained from the DFT, which is calculated directly from the point process signal. The total power reproduced by the DFT was then verified using Parseval's theorem:

$$\int_{-\infty}^{\infty} |h(t)|^2 dt = \int_{-\infty}^{\infty} |H(f)|^2 df \quad (3.1).$$

This theorem states that the power in the time domain is equal to the power in the frequency domain. In other words, the variance of the IBI interval series is equal to the power returned by spectral analysis.

Haaksma et al. [11] performed interpolation and spectral analysis on three simulated IBI signals: each having average IBI durations of 600, 800, and 1000 milliseconds. These signals were then interpolated using linear interpolation and cubic spline interpolation. It was found that, when compared to the DFT spectrum, the linear interpolation method led to attenuations in frequencies above 0.05 Hz. In the case of the signal with the average IBI duration of 1000 milliseconds, the power was reduced to 40% of the total power at 0.4 Hz. using this method. The cubic spline method also led to attenuations but at frequencies higher than 0.2 Hz.. In both cases, the percentage of spectral power returned compared to the DFT decreases as the average IBI length increases.

This fact is consistent with the findings of the study performed by Frey et al. but it was also found that the respiration rate also affects the amount of spectral biasing [14]. In this study, the characteristic of the low pass filter introduced to spectra as a result of backward step interpolation was computed as a function of respiratory rate and mean heart rate. This allows for corrections to be made when using this method of interpolation. In this study, however, spectral biasing is quantified by comparing the interpolated signal's spectrum with the spectrum of the tachogram. This may not be an accurate method of comparison because the tachogram method can also introduce a low pass filtering effect to the spectra [13,15].

3.2.3 Spectral Analysis without Resampling

The Lomb periodogram allows spectral analysis to be performed on unevenly spaced samples and therefore eliminates the need for interpolation altogether [16]. Given a signal

that consists of a unit impulse occurring at the time of each heart beat:

$$h(i) = \sum_i \delta(t - t_i) \quad (3.2)$$

the Lomb method first calculates the mean and variance of the data. The mean is calculated as follows:

$$\bar{h} = \frac{1}{N} \sum_i^N h_i \quad (3.3)$$

where N is equal to the number of data points. The variance is then calculated as follows:

$$\sigma^2 = \frac{1}{N-1} \sum_i^N (h_i - \bar{h})^2 \quad (3.4)$$

The Lomb periodogram is then defined by:

$$P_N(\omega) = \frac{1}{2\sigma^2} \left\{ \frac{\left[\sum_j (h_j - \bar{h}) \cos \omega(t_j - \tau) \right]^2}{\sum_j \cos^2 \omega(t_j - \tau)} + \frac{\left[\sum_j (h_j - \bar{h}) \sin \omega(t_j - \tau) \right]^2}{\sum_j \cos^2 \omega(t_j - \tau)} \right\} \quad (3.5)$$

Where τ is defined by the following equation:

$$\tan(2\omega\tau) = \frac{\sum_j \sin 2\omega t_j}{\sum_j \cos 2\omega t_j} \quad (3.6)$$

These equations are identical to the results obtained by estimating the harmonic content of a signal, at a given frequency ω , by linear least-squares fitting to the following model:

$$h(t) = A \cos \omega t + B \sin \omega t \quad (3.7)$$

An important feature of the Lomb periodogram is that since the data are not evenly sampled, the Nyquist frequency is undefined [16]. Therefore when calculating the periodogram, the user must specify the maximum frequency of search. This was demonstrated [16] by calculating the Lomb periodogram for unevenly sampled data that

contained a 0.81 Hz. component. The data had an average sampling rate of 0.5 Hz., but the peak was accurately found by searching frequencies up to 1 Hz. With FFT methods, a 0.81 Hz. component in a signal sampled at 0.5 Hz. would have resulted in aliasing of the spectral peak below the Nyquist frequency of 0.25 Hz. The reason this 0.81 Hz. peak was accurately found by the Lomb method is that some of the points are closer than the average sampling rate of 0.5 Hz.

Spectral analysis without resampling is desirable due to the elimination of one step of data alteration but may not always be ideal. For example, Hyndman et al. [15] has shown that the Lomb periodogram still introduces the low pass filtering effect to spectra as do other methods as well as certain types of nonlinear distortion. Also, the computational demand for the Lomb periodogram is much greater than that of FFT or AR methods, which until recently has restricted its general use [17]. To overcome this factor, new algorithms have been designed to decrease this computational burden such as the Press-Rybicki algorithm [17].

Besides eliminating the need for interpolation, the Lomb periodogram method also provides a robust estimate of the PSD in the presence of irregularities such as ectopic beats, missed detections, or noise, all of which can severely affect PSD estimates obtained from the FFT or AR methods [17]. This allows the elimination of the additional complication of insertion of probable replacements for outliers in cases such as premature ventricular contractions.

Although Hyndman et al. find spectral biasing and nonlinear distortions resulting from the use of the Lomb periodogram compared to FFT methods, Moody considers FFT, AR, and Lomb methods to be equivalent, even though both use the same algorithm for

calculating the Lomb periodogram . This may be due to the fact that Moody compares the Lomb method to the FFT and AR methods which require interpolation. This suggests that the Lomb periodogram was compared to PSDs that already have spectral biasing due to the interpolation methods used in the study. Hyndman et al. compare the Lomb periodogram with PSDs obtained from many different interpolation schemes, some of which cause minimal spectral biasing. The biasing caused by the Lomb periodogram was therefore made evident.

Moody concludes by stating that under normal circumstances, there is no difference between the FFT, AR., and Lomb methods, but in the presence of noise or ectopy, the Lomb periodogram offers the best estimate of the PSD. He also states that this method introduces no drawbacks of its own and is the method of choice for analyzing IBI data [17].

While being appropriate in the analysis of IBI data, the Lomb periodogram may not be the best method for systolic arterial pressure data. This is because, since the time locations of the systolic peaks are retained before performing spectral analysis, the frequency contributions of HRV will be also be included in the spectra, which may complicate interpretation of the results.

3.2.4 Experiments Involving Interpolation

This section describes four different experiments performed to attempt to quantify the amount of distortion introduced by different interpolation methods and to determine the effects of these distortions on the resulting spectra. The first experiment uses simulated

IBI data, and the following experiments involve blood pressure and EKG data collected under the conditions described in chapter 2.

All processing of blood pressure signals in this research was performed by writing programs for MATLAB. MATLAB is a software package that allows for interactive data analysis and problem solving in many engineering applications. It contains many standard mathematics and graphics functions and as well a signal processing toolbox that includes many common signal processing algorithms that may be utilized as building blocks in the design of more complex algorithms.

The first experiment consists of comparing spectra derived from backward step interpolation of simulated IBI data with spectra derived using the tachogram method. The experiment was performed by creating two minute sequences of IBI data, then performing spectral analysis on the tachograms and interpolated IBI sequences and comparing the areas under the spectral components.

The four different simulated IBI series used in this experiment were designed to represent IBI data obtained from two minute sequences of EKG data having mean IBI durations of 0.6, 0.8, 1.0, and 1.2 seconds. These signals were constructed in MATLAB as follows:

$$y_1(i) = 0.6 + 0.1\sin(2\pi(0.1)(0.6)i) + 0.2\sin(2\pi(0.3)(0.6)i) \quad \text{for } i=1:200$$

$$y_2(i) = 0.8 + 0.1\sin(2\pi(0.1)(0.8)i) + 0.2\sin(2\pi(0.3)(0.8)i) \quad \text{for } i=1:150$$

$$y_3(i) = 1 + 0.1\sin(2\pi(0.1)i) + 0.2\sin(2\pi(0.3)i) \quad \text{for } i=1:120$$

$$y_4(i) = 1.2 + 0.1\sin(2\pi(0.1)(1.2)i) + 0.2\sin(2\pi(0.3)(1.2)i) \quad \text{for } i=1:100$$

These signals were chosen to result in spectral peaks at 0.1 and 0.3 Hz. and the index numbers correspond to two minutes of EKG data for each mean IBI duration.

Spectral analysis was then performed directly on the above signals which are already in tachogram form because IBI values are evenly spaced in time. Next, the tachograms were interpolated using the backward step interpolation algorithm which was coded in MATLAB (called bsinterp.m) and appears in appendix B. The interpolated IBI signals were then resampled at 20 Hz. (decimated by 10) and the spectra were calculated.

The LF (0.05 to 0.15 Hz.) and HF (0.15 to 0.4 Hz.) areas of the spectra derived using the two methods were then calculated for the four signals. Since the data lengths varied for the two methods, the spectral areas were then normalized to aid in comparing spectra. The normalized areas were calculated as follows:

$$\text{LF (n.u.)} = \frac{\text{LF}}{\text{LF} + \text{HF}} * 100 \quad (3.8)$$

$$\text{HF (n.u.)} = \frac{\text{HF}}{\text{LF} + \text{HF}} * 100 \quad (3.9)$$

where LF and HF are the areas under the LF and HF regions (respectively) of the spectra. A more detailed discussion of normalized units appears in section 3.3. The results the two methods for each IBI sequence is shown in table 3.1.

Table 3.1 Results of Spectral Analysis of Simulated IBI Data

Mean IBI (seconds)	Tachogram			Backward Step Interpolated		
	LF area	HF area	LF/HF Ratio	LF area	HF area	LF/HF Ratio
0.6	20.002	79.998	0.250	19.967	80.033	0.249
0.8	20.004	79.996	0.250	22.046	77.954	0.283
1.0	20.006	79.994	0.250	24.874	75.126	0.331
1.2	20.008	79.992	0.250	26.621	73.379	0.363

Since the amplitudes of the LF (0.1 Hz.) and HF (0.3 Hz.) sine components of the test signals in the time domain are 0.1 and 0.2 seconds, respectively, their LF/HF ratio is 0.5. In the frequency domain, since the power of a sine wave is its amplitude squared, the expected LF/HF ratio of the powers is 0.1/0.4 or 0.25. In the case of the tachogram

method, this ratio is very nearly preserved over the range of mean IBIs. A very small low pass filter effect is seen since the HF area decreases as the mean IBI increases, but the change is on the order of thousandths of a percent. In the backward step interpolated cases, however, the ratio increased by as much as 46% (for a mean IBI duration of 1.2 seconds) as the mean IBI increases. This is due to the low pass filtering effect of the interpolation attenuating the HF peak. At an average IBI duration of 0.6 seconds, the ratio is nearly 0.25 and therefore the spectral power is reproduced most accurately around this mean IBI duration.

The percent reduction of the HF peak area for each case resulting from the interpolation was then calculated for each simulation, and the correlation of these with the mean IBI duration was calculated and found to be 0.9962. This shows that there is a very strong relationship between the increase in mean IBI duration and HF peak area reduction. This is consistent with the results found by Haaksma et al. for cubic spline and linear interpolation when compared to the DFT for different mean IBI durations [11]. Using both methods, the low pass filtering introduced by the interpolation method was shown to become more pronounced as the mean IBI duration increases.

According to Frey et al., the characteristics of the low pass filtering effect introduced by backward step interpolation (when compared to the tachogram) are affected by the product of the respiratory rate (f) and the mean heart rate (I) [14]. This was verified by calculating this product for each simulation and finding the correlation between it and the percent reduction of the HF peak areas. The respiration rate was taken to be 18 breaths per minute since the HF peak was located at 0.3 Hz., and the mean heart rate was calculated as 60 divided by the mean IBI length in seconds. The correlation coefficient of

the product of these parameters and the percent reduction of HF peak power was then calculated to be -0.9798. This shows that there is a strong inverse relationship between the product of the respiratory rate and mean heart rate and the HF peak power reduction. This result is significant because Frey et al. suggest a correction for spectra derived using the backward step interpolation algorithm in which the amount of correction is dependent upon the product of the mean heart rate and respiratory rate.

The second experiment was then performed using data from selected files obtained from the experimental protocol described in section 2.3. Data collected from a variety of different situations were used: resting, paced breathing, and rate and volume controlled respiration.

First, the tachogram was derived for each data file by detecting the sync pulses generated by the Quinton Q4000. The spectrum of the tachogram was then obtained, and the LF and HF areas were calculated and normalized. The IBI data was then interpolated using the backward step interpolation algorithm, the data was resampled at 20 Hz. and the spectrum of this signal was calculated. The LF and HF areas for these spectra were then calculated and normalized. The mean IBI duration for each case was then calculated. The results of these steps appear in table 3.2.

Table 3.2 Results of Comparison of Interpolation Methods on Real IBI Data.

Data	Mean IBI (seconds)	Tachogram			Backward Step Interpolation		
		LF	HF	LF/HF Ratio	LF	HF	LF/HF Ratio
1	0.8990	16.42	83.58	0.196	18.86	81.14	0.232
2	0.7708	19.32	80.68	0.239	25.61	74.39	0.344
3	1.0968	18.28	81.72	0.224	23.83	76.17	0.313
4	1.0703	27.89	72.12	0.387	32.79	67.21	0.488
5	0.9283	18.48	81.52	0.227	26.82	73.18	0.367
6	1.1023	57.96	42.04	1.378	66.53	33.47	1.987

As with the simulated data, the correlation coefficient between the percent reduction of the HF area introduced by step interpolation and the mean IBI duration was calculated and was found to be 0.4032. This is much lower than the corresponding correlation coefficient computed for the simulated IBI signals. In the study by Haaksma et al. the reduction in power was shown to increase as the mean IBI increased when the interpolated method was compared to the DFT [11]. In this study, the step interpolated method was compared to the tachogram method, in which the amount of spectral biasing is unknown. The lower correlation may also be due to the effect of the nonstationarity of the real IBI data, whereas the simulated IBI data was perfectly stationary.

As in the first experiment, the correlation coefficient between the percent reduction of the HF area introduced by the backward step interpolation algorithm and the product of the respiratory rate and the mean heart rate was computed for each data file and found to be equal to -0.6257. This is consistent with the findings of Frey et al. and the results of the first experiment using simulated IBIs although the correlation is lower [14].

Another interesting result in this comparison can be seen from table 3.2. When utilizing the backward step interpolation method, the IBI data is coded twice in the interpolated signal: in amplitude and in time. Since, in most cases, most of the power in the IBI signal is under the HF peak, one would expect the HF areas to be larger when the signal is interpolated. This is not the case, however, presumably due to the low pass filtering introduced by the interpolation. The spectra of the interpolated signals would have to be corrected to make such a comparison. A method for correcting spectra derived from backward step interpolated IBI signals is suggested by Frey et al. [14].

The third experiment was designed to help determine the best method of interpolating SAP data. As mentioned before some methods of interpolating the SAP signal result in the inclusion of the HRV components in the SAP spectra. This is a result of the timing information between peaks being retained by the interpolation method. This is most obvious when using the step interpolation method because the timing between each step is determined by the heart rate.

This experiment was designed to determine if the HRV components of the SAP signal can be removed by either not interpolating the SAP signal or using cubic spline interpolation. It is hypothesized that both methods will reduce the HRV contribution from the spectra due to the fact that using these methods, the timing information of the occurrence of the systolic peaks is removed.

For this experiment, the blood pressures from the six sets of data used in the previous experiment were analyzed by detecting the systolic peaks (described in detail in section 3.4), performing step and cubic spline interpolation, and then performing spectral analysis on the uninterpolated SAP data as well as the interpolated data. The areas under the LF and HF peaks were then calculated and normalized using the methods described earlier. The results of this analysis are shown in table 3.3.

Since most of the HRV power is in the HF region for most of the cases (which is evident from table 3.2), it is expected that when comparing the noninterpolated SAP spectrum's HF area to that of the step interpolated case, the value would be lower in the noninterpolated case because of the removal of the HF contribution of HRV. This is not seen in any of the six cases however, and may be due to the fact that the step interpolated method introduces a low pass filter effect, attenuating the HF peaks in the step

interpolated spectra. This makes comparison of these methods impossible unless the spectra obtained from step interpolation are corrected for this low pass filtering effect.

Table 3.3 Results of Comparison of Interpolation Methods on SAP Data.

No interpolation			
<u>Data</u>	<u>LF</u>	<u>HF</u>	<u>LF/HF Ratio</u>
1	42.26	57.74	0.732
2	23.71	76.29	0.311
3	41.77	58.23	0.717
4	39.82	60.18	0.662
5	25.38	74.62	0.340
6	72.37	27.63	2.620
Step interpolation			
<u>Data</u>	<u>LF</u>	<u>HF</u>	<u>LF/HF Ratio</u>
1	43.72	56.28	0.777
2	30.54	69.46	0.440
3	44.34	55.66	0.797
4	47.12	52.88	0.891
5	36.62	63.38	0.578
6	78.77	21.23	3.710
Cubic Spline Interpolation			
<u>Data</u>	<u>LF</u>	<u>HF</u>	<u>LF/HF Ratio</u>
1	41.080	58.920	0.697
2	26.423	73.577	0.359
3	41.106	58.894	0.698
4	42.644	57.357	0.743
5	32.288	67.712	0.477
6	76.547	23.453	3.264

Upon comparing the cubic spline method to the step interpolation method, it can be seen that all of the HF areas are higher in the cubic spline interpolated case. This again is contrary to the expected results. It is expected that the cubic spline method will remove the HF contribution from HRV. This may be due to the fact that cubic spline interpolation introduces a much smaller low pass filtering effect than do most other interpolation methods [11]. Therefore, since the step method results in a greater amount of low pass filtering to the spectra, it is difficult to compare these methods to determine if the HRV contribution is indeed removed.

A fourth experiment was designed to test the hypothesis that since step interpolation of SAP results in the inclusion of HRV components in the SAP spectrum, the LF and HF areas of SAP spectra derived using this method should be comparable to the LF and HF areas of the spectrum of the entire blood pressure signal. This is expected because the blood pressure signal contains both SAP information as well as HRV information contained in the spacing of the systolic peaks as does the step interpolated signal.

The study was done by performing spectral analysis on raw blood pressure signals and step interpolated SAP signals using the programs described in section 3.4, as well as calculating the LF and HF areas of both spectra in absolute units. Data from five subjects performing the controlled respiratory rate and volume protocol described in section 2.3 were used in this experiment.

For each subject the LF and HF areas (in absolute units) of the spectra were grouped first by respiratory rate, then by all respiratory rates combined. The correlation coefficients between the LF areas of both spectra and the HF areas of both spectra were then computed for each group of data. The correlations between LF areas appear in table 3.4 and the correlations between HF areas appear in table 3.5.

From table 3.4 it is observed that while most of the correlations are high a few are near zero or negative. This suggests that the LF peaks of both spectra often contain the same information but not in all cases. The cases in which low correlations occur suggest that different information is obtained from the two spectra. It should be noted that when all the rates are combined, however, these low or negative correlations are washed out, indicating that the spectra contain similar information. By plotting the data for a particular

subject for each respiration rate with a straight line fit, the reason the correlations are still high is seen when the rates are combined. For example, the LF areas of the SAP and blood pressure spectra for subject 1 are plotted against each other in figure 3.4. The markers used in the plot are as follows: 'o' corresponds to 2/3 normal respiration rate, 'x' corresponds to normal respiration rate, and '+' corresponds to 3/2 normal respiration rate.

Table 3.4 Comparison of LF Areas of Blood Pressure and SAP Spectra.

Subject	Respiration Rate			All Rates
	2/3 Normal	Normal	3/2 Normal	Combined
1	0.9280	0.5666	0.9731	0.8087
2	0.6157	0.0220	0.9912	0.8904
3	0.9703	0.9558	0.9996	0.9701
4	0.9452	0.9990	-0.9973	0.8622
5	0.1960	0.7449		0.8056

Table 3.5 Comparison of HF Areas of Blood Pressure and SAP Spectra.

Subject	Respiration Rate			All Rates
	2/3 Normal	Normal	3/2 Normal	Combined
1	0.9440	0.7813	0.9697	0.6349
2	0.9549	0.8386	0.9668	0.8713
3	0.9939	0.7606	0.9990	0.9442
4	0.9842	0.9932	0.9840	0.7417
5	0.9673	0.9741		0.9518

From figure 3.4, it can be seen that while the correlation at 3/2 normal respiration rate is -0.9973, this has little effect on the overall correlation of all the data points combined. This is because at this respiration rate, the LF areas all reside within a small range. Therefore, when combining all the respiration rates, the effect of these data points is on the overall correlation is diminished. Figure 3.5 shows the straight line fit for all the respiration rates combined for the same data. The correlation coefficient is 0.8622 for this case. This effect is similar for all the cases in comparing the LF areas of the SAP and blood pressure spectra where one respiration rate yields a low or negative correlation coefficient but the overall correlation is high for all respiration rates combined.

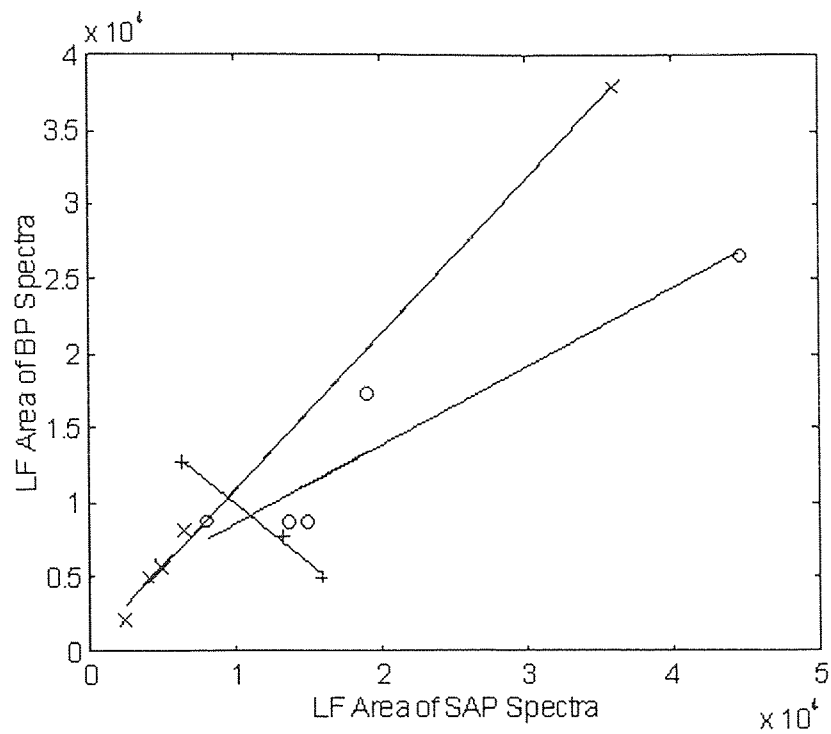


Figure 3.4 Straight Line Fits for Individual Respiration Rates

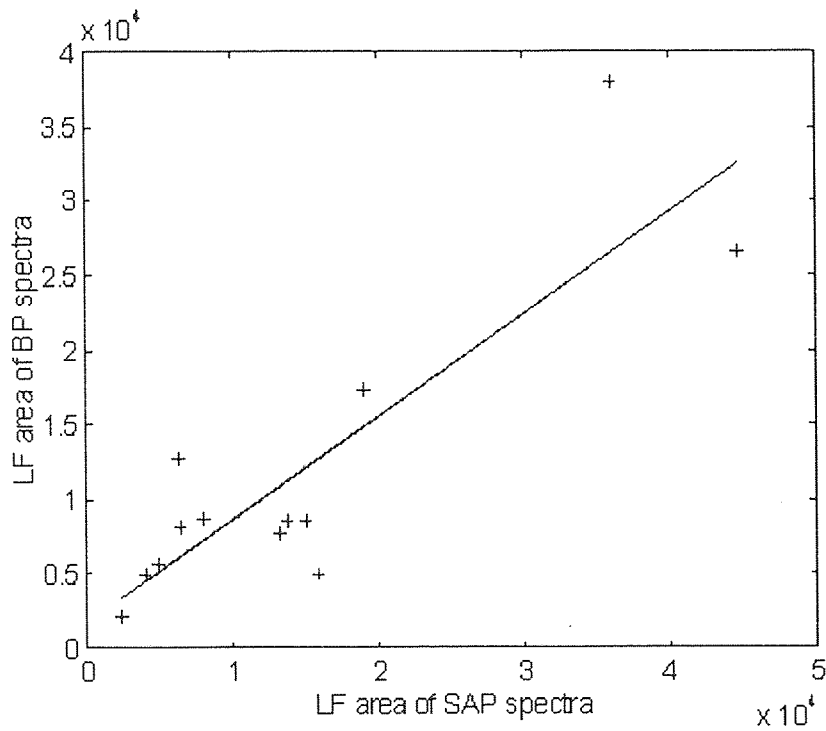


Figure 3.5 Straight Line Fit for All Respiration Rates Combined

In the case of subject 5, the correlation of 0.1960 at 2/3 normal respiration rate is explained by plotting the data. This plot appears in figure 3.6. By observing this plot, it is

seen that there is one outlier affecting the correlation coefficient. Upon removing this outlier, the correlation coefficient at this respiration rate becomes -0.5509 and the correlation coefficient for all the respiration rates combined becomes 0.8330. Again, this negative correlation coefficient has little effect on the correlation coefficient for all the respiration rates combined because at this rate, the LF area values lie within a relatively small range. All the data were plotted in this manner to assure that no other outliers were present.

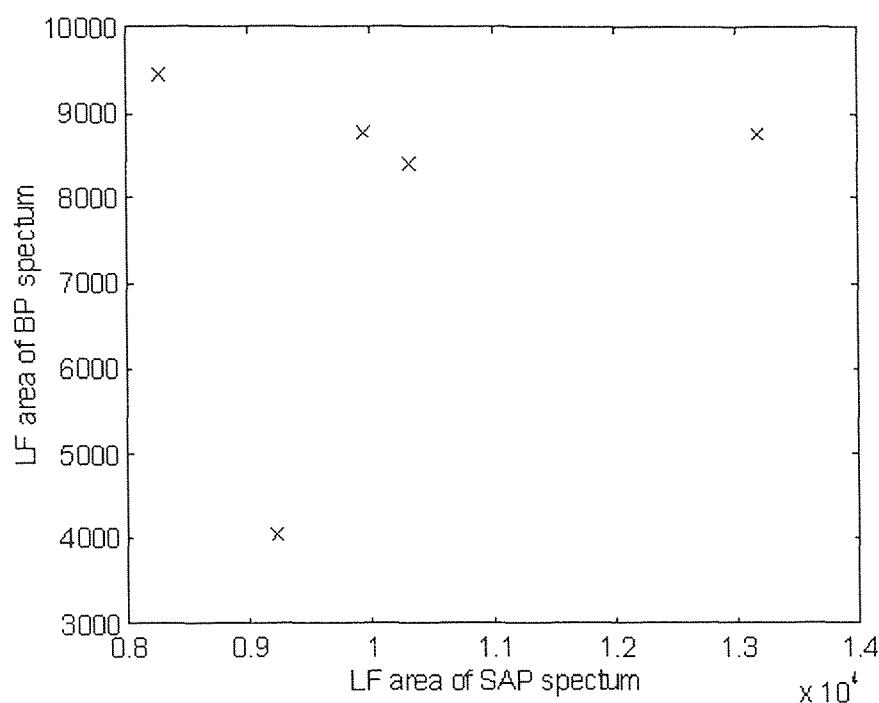


Figure 3.6 Results for Subject 5 at 2/3 Normal Respiration Rate

Table 3.5 shows that there is an even stronger relationship between the HF areas of the two spectra due to the fact that all the correlations are high. This again suggests a similarity in the information obtained from the two spectra.

3.2.5 Conclusion

These studies show that each method of processing IBI or SAP data before spectral analysis is performed introduces different degrees of change to the resulting spectra. Therefore, in studies requiring the comparison of IBI and SAP spectra, the methods for interpolating each should be chosen to be the same. Using different methods for each would make comparing the resulting spectra difficult.

Since step interpolation of the IBI was used for the current research in our laboratory, it was decided to use step interpolation to preprocess the SAP data as well. Since step interpolation of SAP data results in the inclusion of HRV contributions to the spectra, it may in the future be better to not interpolate the SAP data, and use one of the methods of correcting the step interpolated IBI spectra before comparison.

3.3 Normalized Units

Since the autonomic nervous system's activity constantly fluctuates as a result of many environmental factors, reproducibility of vagal tone studies is likely to be poor [4]. Several researchers suggest methods of normalizing spectral areas to compensate for this, as well as to aid in the comparison of different subjects performing the same protocol. The purpose of this section is to describe a common method of normalizing spectral areas and to discuss the results of an experiment performed to determine the effectiveness of normalizing areas to aid in the reproducibility of experimental results.

The most common method of normalizing spectral areas is to divide the area of the region of interest by the total power, then multiplying by 100 [5,8,9]. The total power is usually taken to be sum of the LF and HF areas. The purpose of this is to exclude the

contribution of the very LF power (below 0.05 Hz.) from the calculation because its value is highly dependent upon the data collection and analysis methods. The equations used to compute normalized powers are therefore as follows:

$$LF (n. u.) = \frac{LF}{LF + HF} * 100 \quad (3.10)$$

$$HF (n. u.) = \frac{HF}{LF + HF} * 100 \quad (3.11)$$

where LF and HF are the areas under the LF and HF regions (respectively) of the spectra.

To determine if normalizing spectral areas aids in reproducibility of results, power spectral analysis of HRV was performed in S-Plus on pairs of files containing resting data, collected between 2 days and 2 months apart, for ten subjects. The details of the analysis are presented in section 4.2. The actual analysis steps appear in appendix A and the programs used appear in appendix B. The data was obtained from the rest files collected on the second and third days of the protocol described in section 2.3.

The LF and HF areas for each file were then computed as well as the normalized LF and HF areas using equations (3.10) and (3.11), respectively. These results appear in appendix C. The percent differences between each of the four parameters obtained from the first and second day for were then calculated using the following method:

$$\text{percent difference} = \frac{|\text{value on day1} - \text{value on day 2}|}{\text{value on day1}} * 100\% \quad (3.12)$$

The mean day to day percent difference for each of the four parameters was then calculated over all ten subjects. The results appear in table 3.6.

From this table, it is seen that normalizing both the LF and HF areas results in the reduction of the mean percent differences in both the LF and HF cases. The mean day to

day percent difference in the LF area is reduced from 43% to 26.4% and from 98% to 17.7% in the case of the HF area.

Table 3.6 Results of Comparison of Absolute and Normalized Units.

	LF Area (absolute)	LF Area (normalized)	HF Area (absolute)	HF Area (normalized)
Subject	Percent Difference	Percent Difference	Percent Difference	Percent Difference
1	50.5%	49.8%	48.3%	50.2%
2	8.8%	16.0%	34.3%	3.6%
3	30.7%	13.1%	61.3%	7.3%
4	8.5%	12.5%	20.5%	17.6%
5	8.6%	10.0%	29.1%	7.0%
6	162.4%	48.1%	647.1%	47.7%
7	66.2%	5.1%	68.0%	0.6%
8	7.7%	22.1%	30.1%	7.5%
9	0.0%	12.7%	12.6%	1.4%
10	86.6%	74.7%	29.2%	33.7%
Mean:	43.0%	26.4%	98.0%	17.7%

While the percent differences are greater in some subjects after normalizing the areas, it can be seen that the increases in percent differences in most cases are small compared to the decreases in percent differences in other cases. For example subjects 6 and 7 show drastic improvements in reduction of day to day percent differences by normalizing areas. This results in an overall reduction of the mean percent differences for both LF and HF areas, indicating that reproducibility of results in heart rate variability studies is improved by normalizing the LF and HF areas.

It has also been suggested that normalizing spectral areas also aids in comparison of experimental results across different laboratories, where analysis methods may vary greatly [3]. This fact is supported by the experiments described in section 3.2.4 where different analysis methods were used on the same data which resulted in spectral areas that were not comparable across different methods. Particularly, the first experiment performed on simulated IBI data in section 3.2.4 involved comparing spectra derived from tachogram data which is on the order of 150 points and the corresponding interpolated IBI

signal which is on the order of 2500 points. The spectra derived from the interpolated data resulted in peaks that were approximately 10 times greater in magnitude due to the greater number of data points. Table 3.1 shows that after normalizing the spectral areas for both methods, the LF and HF areas were made comparable. This is because normalizing the spectral areas allows the relative areas of the spectral peaks to be evaluated regardless of the absolute values of the peaks.

Normalized units may also result in a more reproducible measure of the complex interaction of autonomic regulation of HRV and SAPV [3]. An example of this is the fact that muscarinic blockade in dogs reduces the total HRV by approximately three orders of magnitude, causing the absolute powers of both the LF and HF components to be drastically reduced. Normalization of the areas allows the interaction of the LF and HF components to be better quantified. This suggests that normalization should be used in cases where interplay between the LF and HF components are of concern but not when overall variability is concerned.

3.4 Analysis of Blood Pressure

To perform spectral analysis on systolic arterial pressure and raw blood pressure data, several algorithms were designed and implemented by programming in MATLAB. All the programs were written to analyze blood pressure data sampled at 200 Hz. and in ASCII format. Since raw blood pressure data is usually stored in files utilizing packed binary format, the data must first be unpacked, which converts it into ASCII format. The ASCII blood pressure data can then be loaded directly into MATLAB for analysis.

The steps that are taken to derive blood pressure and systolic arterial pressure spectra are shown in the flowchart in figure 3.7. Shown in this flowchart are also the names of the main programs used in the analysis, while some of the required intermediate programs were omitted for clarity. The actual commands in the proper syntax required to perform the analysis are listed in appendix D. The listings of the programs appear in appendix E. The programs are described in detail in the next section.

3.4.1 Peak Detection

The first step in spectral analysis of systolic arterial blood pressure requires the detection of the systolic peaks in the blood pressure signal. To accomplish this, a program called `getsap.m` was written. This program calls another program called `presap.m` which detects the systolic peaks as well as performs forward step interpolation as each peak is detected. `Getsap.m` then calls a program called `compare.m` that allows the accuracy of the detections to be checked.

`Getsap.m` accepts three input arguments: the blood pressure signal, an estimate of the heart rate for the data sequence and a threshold value which is discussed in detail below. The estimate of the heart rate serves as the basis for a horizontal window to discriminate against false detections, while the threshold determines a vertical window below which to ignore peaks. These three input arguments are passed on to the `presap.m` program.

The peak detection in `presap.m` is initialized by preallocating a vector called the `prsp` vector with zeros which will become the systolic arterial pressure signal. Then the maximum value of the blood pressure in the first 400 samples is found and named `bpmax`

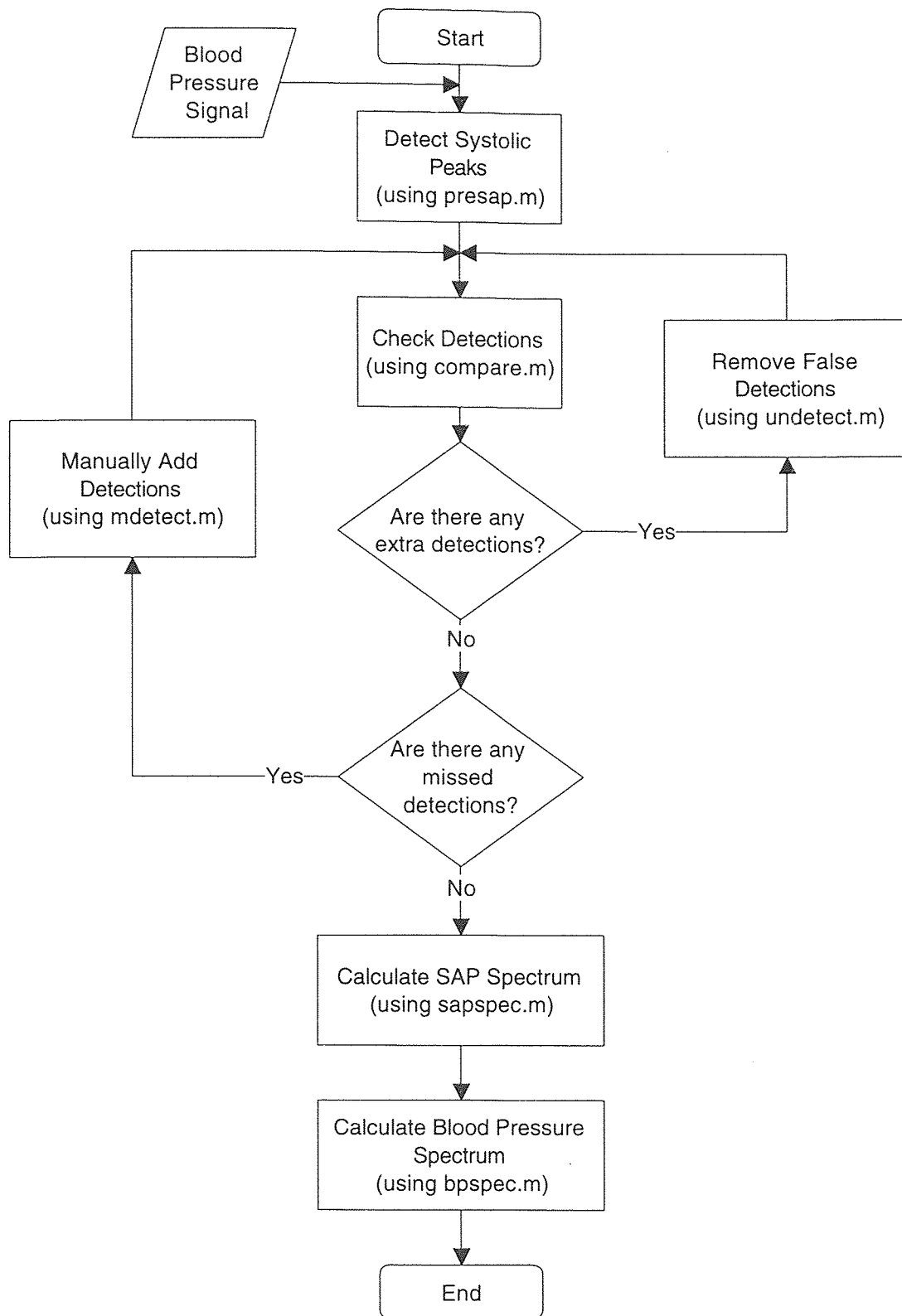


Figure 3.7 Flowchart of Blood Pressure Analysis Steps.

to serve as an estimate of the amplitudes of the first few peaks in the blood pressure signal. The program then creates a vector called `bpdiff` which contains the differences in amplitudes for each adjacent pair of samples of the blood pressure signal. This vector contains a negative number where a descending slope occurs and a positive number corresponding to an ascending slope for each pair of adjacent samples.

The basis of the peak detection algorithm is to sequentially check the values in the `bpdiff` vector until a change in sign from positive to negative occurs, corresponding to a change in the slope of the blood pressure signal from positive to negative, meaning that a peak has occurred. This is accomplished by defining a parameter called `flag` which is set to zero if the previous `bpdiff` value was negative or one if it was positive. From these values, a peak is detected by the combination of `bpdiff` being negative and `flag` being one. This corresponds to the point in which the signal stops increasing and begins decreasing.

Using the algorithm thus far, many false detections occurred due to noisy blood pressure signals as well as the presence of dichrotic notches. Therefore, when a potential peak is found by a changing slope, the vertical and horizontal window requirements must be checked before changes in the `prsp` vector are made.

First the amplitude of the potential peak is checked to make sure that it is above `bpmax` minus the threshold amount. If this condition is met, the peak location is checked to make sure that it has not occurred too soon after a previous peak. This check is made based on the assumption of the maximum heart rate in the input arguments of the `getsap` program. When both of these conditions are met, it is assumed that a valid systolic peak has been detected.

Beginning at the time of the occurrence of a peak, the prsp vector's value is changed from its previous value to the value of the amplitude of this peak and is held fixed at this value until another peak is detected. This results in the forward step interpolation of the systolic arterial pressure signal being performed during peak detection. Since the prsp vector was initialized with zeros, the prsp vector contains zeros until the time of the occurrence of the first peak in the blood pressure sequence. These leading zeros are later removed which results in the completed forward step interpolated systolic arterial pressure signal. Also, upon detection of a systolic peak, the value of bpmax is changed to the value of the amplitude of this peak, which results in a variable vertical window that is dependent upon the amplitude of the previous peak. The flowchart of the peak detection algorithm used in presap.m appears in figure 3.8.

After the detection is completed, getsap.m allows the user to check the accuracy of the peak detection by calling the compare.m program. This program plots the prsp signal and the original blood pressure signal on the same plot 1000 points at a time (five seconds of data for a sampling rate of 200 Hz.) The next 1000 samples of both signals are then shown by pressing the return key. This is done until the entire prsp signal has been checked for detection accuracy. Correct detections appear as a horizontal line extending from every systolic peak until the next peak is reached. An example of correctly detected peaks using these programs can be seen in figure 3.1.

If any peaks are missed by the program or there are false detections, the user has a choice of how to correct them. The first method is to check the characteristic of the false detections to determine if there is a pattern. If there is a pattern, the detections may be corrected by changing one of the window parameters in the input arguments of the getsap.m

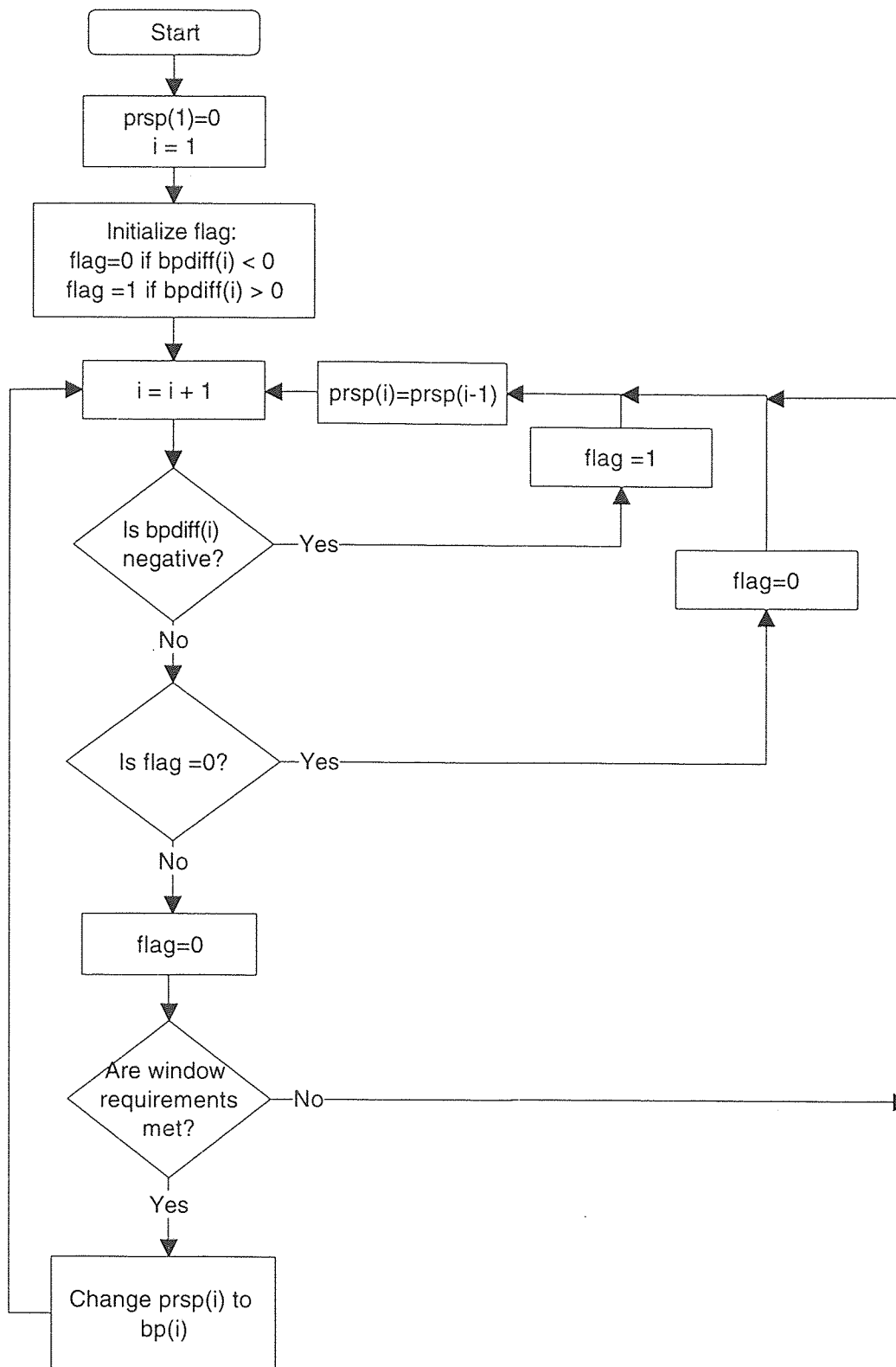


Figure 3.8 Peak Detection Algorithm Used in Presap.m.

program, and running the program again. For example, if it is noticed that many of the dichrotic notches in the blood pressure wave are detected, the thr parameter can be lowered to cause the presap.m program to discriminate against the peaks that are only slightly lower in amplitude than the systolic peaks. The hr parameter may be also be changed if, for example, detections occur too soon or peaks are missed but are within the threshold range. The values that work well for most cases are $hr = 70$ and $thr = 20$.

The second method of error correction is to manually remove false detections and manually insert detections where peaks are missed. This method is appropriate in situations where the peak detection algorithm fails due to noisy blood pressure signals or sections of signals that have unusually high variability. These methods of manual error correction are described in the next section.

3.4.2 Correction of Misdetections

If false detections occur, they may be manually removed by running the program called undetect.m. This program is similar to the compare.m program, in that the prsp signal and blood pressure signal are plotted together 1000 samples at a time, except that for each plot, the cursor becomes a crosshair, awaiting user input. If there are not any false detections in the displayed section of data, the plot may be advanced to the next 1000 samples by pressing the return key. If there are false detections, they may be removed by using the mouse to click on both sides of the incorrect detections, and pressing the return key. This causes the program called undet.m to be called. The detections specified are then removed by undet.m, the appropriate changes are made to the prsp signal, and the

updated prsp signal is replotted on the blood pressure signal. These steps are repeated until all the false detections are removed from the entire prsp signal.

The undetect.m program handles the basic plotting functions and is similar to compare.m. The main difference is that for each 1000 samples plotted, the program awaits user input from the mouse before plotting the next 1000 samples. When the locations of the false detections are input using the mouse and the return key is pressed, the x coordinates of these mouse clicks along with the prsp and blood pressure signals are used as input arguments to call the program undet.m. This program handles the actual translation of the mouse clicks into the corresponding index numbers and the correction of the prsp signal between those mouse clicks.

When the undet.m program is called, it first finds the index number of the next detection to occur after the mouse click made on the right side of the false detection. The prsp signal is then changed so that it remains the value at the left mouse click until the next correct detection (after the right mouse click.) This method may also be used to remove several incorrect detections in a row by simply clicking on both sides of the whole section where there are false detections. A flowchart of undet.m appears in Figure 3.9.

When the detections for a 1000 sample segment are corrected by undet.m, control is returned to the undetect.m program. The program then plots the corrected segment of the prsp signal along with the corresponding segment of blood pressure for verification of the detection removal. When the return key is pressed, the next 1000 samples of both signals are plotted, awaiting user input. This cycle repeats itself until the end of the prsp and blood pressure signals are reached.

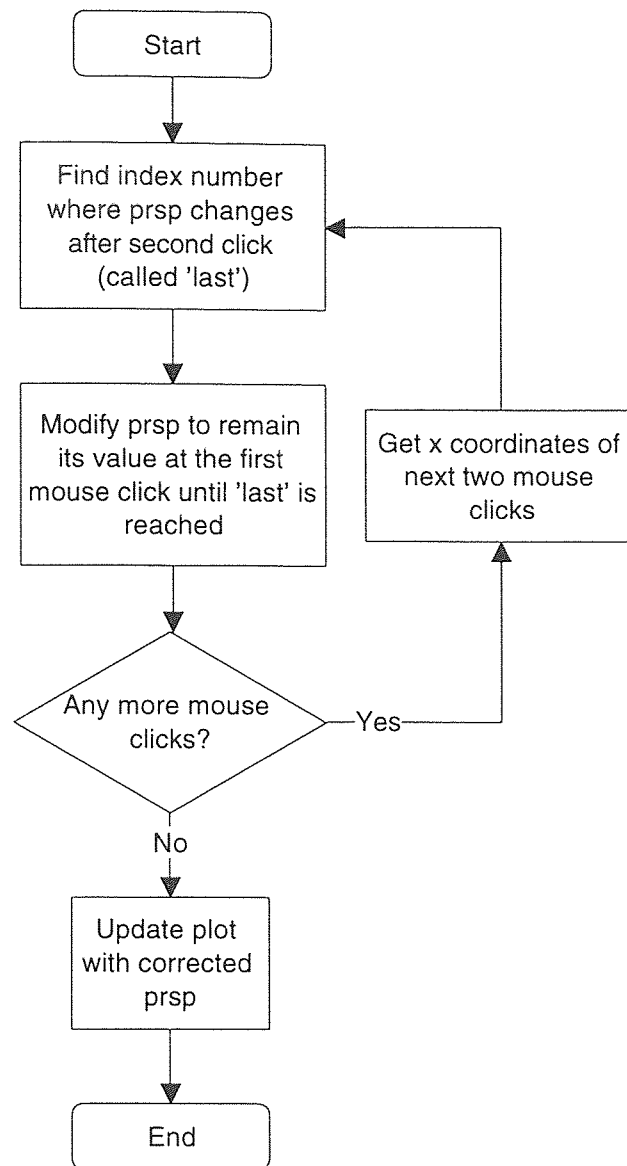


Figure 3.9 Flowchart of Undet.m

If while checking detection accuracy, it is found that some peaks have not been detected, it becomes necessary to run the `mdetect.m` program. Similar to `undetect.m`, the program plots the prsp and blood pressure signals together 1000 samples at a time and then waits for user input. If there are no missed detections on the current plot, the return key is pressed, advancing the plot to the next 1000 samples. When a missed detection is found however, the user clicks the mouse on both sides of a peak that has not been

detected, and presses the return key. The x coordinates of these mouse clicks along with the prsp and blood pressure signals are then passed on to a program called mdet.m. This program handles the actual locating of the peaks and modification of the prsp signal for each 1000 sample segment it is called upon to correct.

When mdet.m is called, the program first finds the location and amplitude of the maximum value of the blood pressure signal between the two mouse clicks. The location (index number) of the peak is called locmax and the amplitude of the blood pressure signal at this point is called bpmax. Next, the program locates the index number of the prsp signal change after the click to the right of the missed detection and calls it last. Next, the prsp signal is modified so that at the index locmax it becomes the value bpmax and remains at this value until the index number last. After these steps are completed for each pair of mouse clicks, control is returned to the mdetect.m program.. A flowchart of mdet.m appears in figure 3.10.

After adding the specified detections to the 1000 sample segment of the prsp signal by the mdet.m program, mdetect.m replots the corrected prsp segment along with the corresponding segment of the original blood pressure signal. Upon pressing the return key, the next 1000 samples of the signals are plotted together, awaiting user input. These steps are then repeated until the end of the blood pressure and prsp signals are reached.

3.4.3 Calculating Spectra

In order to calculate the systolic arterial pressure power spectral density from the prsp signal, the program sapspec.m is used. The first step in this program is to remove the zeros at the beginning of the prsp signal that correspond to the time before the occurrence

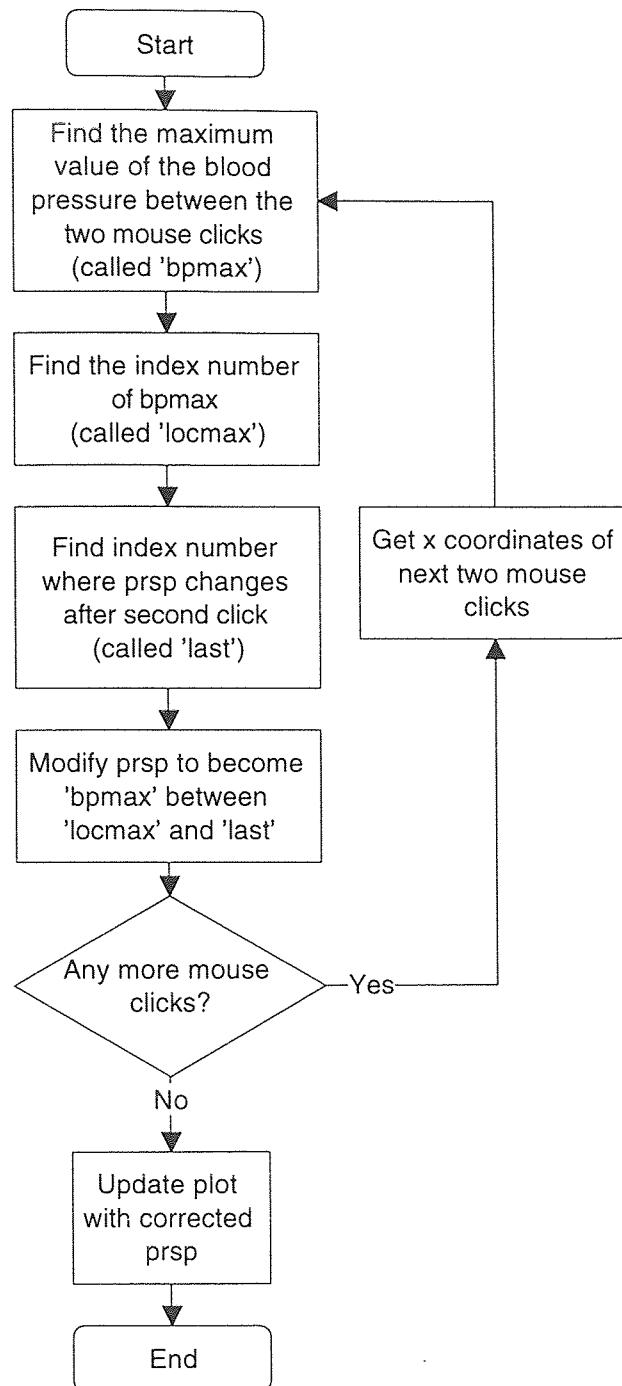


Figure 3.10 Flowchart of Mdet.m

of the first systolic peak in the corresponding blood pressure signal. After removing the zeros, the resulting signal is the forward step interpolated systolic arterial blood pressure signal, called isap. After this is done, the mean systolic blood pressure is calculated in the

program `mnsap.m` by finding the mean of the amplitudes of all the plateaus in the `isap` signal (each plateau corresponds to the systolic arterial pressure for that particular beat.)

The `isap` signal is then decimated by a factor of 10 using `decimate.m`, a program included in MATLAB's signal processing toolbox. The signal is decimated because the components of the spectra that are of interest are all at very low frequencies (frequencies lower than one hundredth of the Nyquist frequency.) Before decimation, the effective spectra run from 0 to 100 Hz. for signals sampled at 200 Hz. After decimating these signals by a factor of 10, the resulting sampling frequency is 20 Hz., so the effective spectra now run from 0 to 10 Hz. For a fixed FFT length, this allows for greater frequency resolution at the frequencies of interest which are between 0.05 and approximately 0.6 Hz.

The `decimate.m` program first filters the data to prevent aliasing using an eighth order Chebyshev type I lowpass filter with a cutoff frequency calculated from the following equation:

$$f_c = 0.8 \left(\frac{F_s}{2R} \right) \quad (3.13)$$

where F_s is the sampling frequency of the signal before decimation and R is the factor by which the signal is decimated. For an original sampling rate of 200 Hz. and a decimation factor of 10, the resulting filter cutoff frequency is 8 Hz. In theory, an ideal filter with a cutoff frequency of 10 Hz. would be used. Since the filter is not ideal, the slightly lowered cutoff frequency of the filter is presumably chosen by the author of the program to allow a margin to prevent frequencies above 10 Hz. to be attenuated sufficiently to prevent

aliasing. After filtering, the signal is resampled at one tenth of the original sampling rate, resulting in a signal sampled at 20 Hz.

The power spectral density of the decimated isap signal is then calculated by calling the program `rspect.m` which is a modification of MATLAB's `spectrum.m` program that is included in the signal processing toolbox. The details of `rspect.m` are described in detail later in this section.

After calculating the power spectral density, the areas within the ranges specified in the input arguments of `sapspec.m` are calculated. The usual ranges for areas are 0.05 to 0.15 Hz. for the LF area and 0.15 to 0.4 Hz. for the HF area. The limits of these areas may be modified depending upon the respiration frequency since the HF peak may move outside of these limits for respiration rates above 24 breaths per minute or below 9 breaths per minute. The areas are calculated by the program `area.m` by first converting the frequency range values into the corresponding index numbers, and summing the power spectral density's values over all the index number within the specified range. From the low and HF areas, the LF and HF areas in normalized units are calculated using equations (3.4) and (3.5). Finally, the ratio of the LF area to HF area is calculated.

The program then plots the systolic arterial pressure power spectral density from 0.05 to 0.6 Hz. The rest of the `sapspec.m` program concerns the appearance of the plot such as axis labels and the printing of the values for the areas and mean systolic arterial pressure. A flowchart of this program appears in figure 3.11.

Power spectral analysis of the raw blood pressure signal is calculated in nearly the same manner using the `bpspec.m` program. The signal is first decimated by a factor of 10 and the spectrum is calculated using `rspect.m`. The LF and HF areas are then calculated

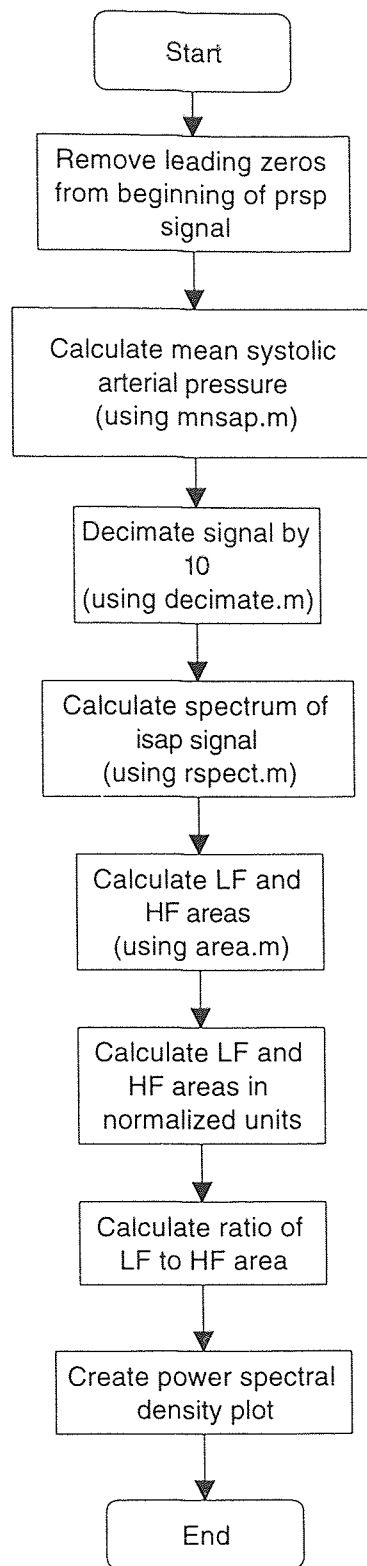


Figure 3.11 Flowchart of Sapspec.m.

using `area.m`. Normalized units and the LF to HF ratio are also calculated, and all these numbers are displayed on the plot of the blood pressure power spectral density.

The basis for the power spectral density calculation is the program `rspect.m`. This program is called by both `sapspec.m` and `bpspec.m` and requires the following input arguments: the input signal, the size of the FFT, the number of overlapping points for each window of data, the window type and size, and the sampling rate. In both cases of spectral analysis, an 8192 point FFT is used, the number of overlapping points is zero, the window is a Hanning window the length of the input signal, and the sampling rate is 20 Hz.

The spectrum is calculated by first windowing the entire data sequence with the Hanning window specified in the input argument. This is accomplished by multiplying the data sequence by the Hanning window element by element. Next, an 8192 point FFT is calculated of the windowed sequence. The magnitude of the FFT is then squared, resulting in the power spectral density vector. Finally `rspect.m` creates the corresponding frequency vector as follows:

$$f = F_s * \frac{0:nfft/2}{nfft} \quad (3.14)$$

where F_s is the sampling frequency and $nfft$ is the length of the FFT. This results in a frequency vector running from 0 to 10 Hz. for a sampling frequency of 20 Hz. and an 8192 point FFT. The power spectral density and frequency vectors are then returned by `rspect.m` to the calling program. A flowchart of this program is shown in figure 3.12.

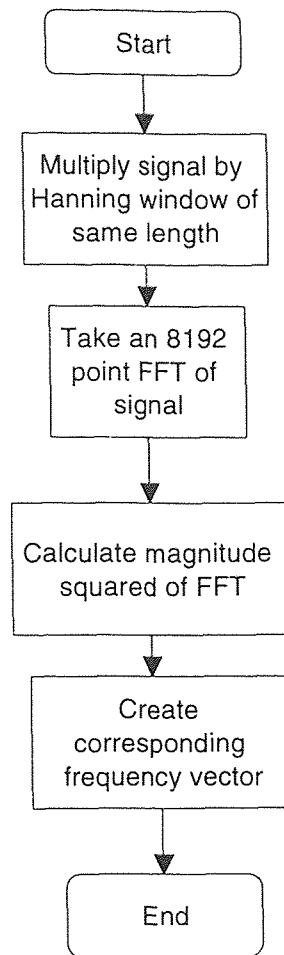


Figure 3.12 Flowchart of Rspect.m.

CHAPTER 4

RATE AND VOLUME CONTROLLED RESPIRATION STUDY

4.1 Introduction

In this chapter, the results of analysis of the data described in chapter 2 are presented. The results include heart rate variability and blood pressure variability parameters. Heart rate variability analysis was performed in S-Plus and is described in the following section. Analysis of blood pressure was performed in MATLAB using the algorithms presented in section 3.4. The purpose of this analysis is to extend the work of Leifer in determining relationships between various blood pressure, respiratory and cardiac parameters.

4.2 Methods

All heart rate variability analysis was performed in S-Plus using the programs listed in appendix B. These programs use the sync pulse signal from the Quinton Q4000 stress test monitor to compute a series of interbeat intervals, interpolate them, and perform spectral analysis on the interpolated IBI signal. The steps required in performing the analysis are presented in appendix A.

The first program used in heart rate variability analysis, pslws, first calls a program called grep, which detects the occurrences of pulses in the sync pulse signal. The program lsbp is then called by pslws which performs backward step interpolation of the IBIs as described in section 3.2.1. The interpolated IBI signal is then decimated by 10 resulting in a sampling rate of 20 Hz. since the data was initially sampled at 200 Hz. Spectral analysis

is then performed on this signal in the program spect by first windowing it with a split bell cosine window, then taking an 8192 point FFT. The magnitude squared of the FFT is then computed and the resulting spectrum is smoothed twice using a modified rectangular smoothing algorithm included with S-Plus.

After performing the analysis, stdgraf is used to plot the data and results to determine if there are outliers present. On the plot of IBIs, the presence of a low outlier indicates a false detection may have occurred. A high outlier usually indicates an R wave was not detected. If any outliers are present, the data is plotted to determine if either a detection was missed, there is false detection, or the outlier is a valid data point. If a peak was not detected, mqr5 was used to plot the EKG and the detections, then manually insert an R wave detection where appropriate. If there is an erroneous detection, dqrs is used in a similar manner to remove it. The data file is then reanalyzed using fwork to recompute the spectrum of the corrected IBI data.

Low and high frequency areas are then computed from the spectrum using spect1. The frequency limits used in computing the areas are chosen depending upon the respiration rate because the HF peak lies at the frequency of respiration. The frequency limits are chosen as shown in table 4.1.

Table 4.1 Ranges Used to Calculated LF and HF Areas

Respiration Rate (breaths per minute)	LF Area Limits (Hz.)	HF Area Limits (Hz.)
< 9.1	0.05 to 0.1	0.1 to 0.4
9.1 to 22	0.05 to 0.15	0.15 to 0.4
> 22	0.05 to 0.15	0.15 to 0.6

The average heart rate for each two minute data file was computed using the following equation:

$$\text{HR (beats / minute)} = \frac{F_s}{60 * \text{Mean IBI}} \quad (4.1)$$

Where F_s denotes the sampling rate (200 Hz.), and the Mean IBI is the average number of samples between the occurrence of each R wave.

Average respiratory rate and volume were calculated from data obtained from the spirometer. As mentioned before, the spirometer outputs a series of pulses for each exhalation, each pulse corresponding to 0.1 liters of air exhaled. The average respiration rate is therefore obtained by determining the number of clusters of pulses for the two minute file and then dividing the number by 2. This results in the average number of breaths per minute. The average tidal volume is calculated by first computing the tidal volume for each breath by counting the number of pulses in each cluster. The number of pulses for each breath is then multiplied by 0.1 to obtain the tidal volume in liters. The average of all these tidal volumes for the two minute file is then computed. While the experimental protocol required maintaining a particular respiration rate and volume, the respiration rate and volumes computed by these methods are used for subsequent analysis because the subjects were usually not able to maintain the target respiration rates and volumes exactly.

Along with HRV analysis, analysis of blood pressure signals collected during the experiments was also performed. The analysis was performed in MATLAB using the algorithms described in section 3.4. The required steps used in the analysis are presented in appendix D. This analysis results in spectra of systolic arterial pressure (SAP) and of the raw blood pressure (BP) data. The LF and HF areas under these two spectra were then computed using the same limits used for HRV analysis of the corresponding file.

Next, the areas under the three spectra were computed in normalized units using equations 3.10 and 3.11. The ratio of LF to HF area was then computed for each file by dividing the LF area by the HF area. The area used in calculating this ratio may be in either absolute or normalized units: both yield the same result because the denominators of the equations used to normalize the areas cancel each other out.

Finally, the mean systolic blood pressure was computed during blood pressure analysis using `mnsap.m`. This program finds the mean of all the systolic blood pressure peaks for a given blood pressure signal.

The results of all the analysis steps discussed in this section performed on five subjects along with the indicated comfort level felt during each exercise appear in tables F.1 through F.5 in appendix F. As mentioned before, if certain exercises were too difficult for a particular subject, the exercise was skipped. Therefore not all subjects have results for all 15 intervals of data (3 rates / 5 volumes at each rate.)

In order to determine whether linear relationships exist between the various parameters calculated for this experiment, matrices of correlation coefficients were computed using a MATLAB program called `corrcoef.m`. First, correlations were computed for each subject over all 15 two minute intervals of data. Correlations between the following parameters were found: comfort, average respiration rate, average tidal volume, mean heart rate, mean systolic arterial pressure, and the LF and HF areas in absolute and normalized units as well as the LF/HF ratios for HRV, SAP, and BP spectra.

Next, the data for each subject was broken up by respiration rate and new correlation matrices were computed for each respiration rate. That is, each group of data contains only one target respiration rate, but all five tidal volumes. This results in three

more correlation matrices for each subject. Missing correlation coefficients correspond to exercises where less than three out of five different volumes were performed for a particular respiratory rate.

Finally, plots were constructed for all the data for which correlation coefficients were computed. The purpose of this was to observe the possible cause of a low correlation, such as an outlier. Also, since correlation coefficients determine the strength of linear relationships only, a low correlation does not prove that there is not any relationship between two parameters. For example, an exponential relationship between two variables would result in a low correlation coefficient, but checking the corresponding plot would prevent the relationship from being discounted.

4.3 Results

This section describes relationships found by observing the correlation matrices and plots of the data for each subject. The purpose of this section is to relate physiological parameters to the various parameters obtained from spectral analysis of systolic arterial blood pressure as well as raw blood pressure data.

4.3.1 Relationships with Tidal Volume

As mentioned in section 1.6, the HF peak in the SAP spectrum (HF SAP) occurs at the frequency of respiration and is a mechanical consequence of respiration. Since the effects of respiration on this peak are believed to be due mainly to pressure changes in the thoracic cavity, it is hypothesized that HF SAP (in absolute units) is directly proportional

to the average tidal volume. To test this hypothesis, the correlation coefficients between these two parameters are shown in table 4.2.

The correlations shown in this table indicate that there is a strong linear relationship between HF SAP and tidal volume when the data is grouped by respiration rate. By observing the figure 4.1, it can be seen that the lower correlation in the case of subject 1 at 3/2 normal respiration rate is due to an outlier. By removing this outlier, the correlation at 3/2 normal respiration rate becomes 0.9730 and 0.4763 for all rates combined.

Table 4.2 Correlations Between HF SAP and Volume

Subject	Respiration Rate			All Rates
	2/3 Normal	Normal	3/2 Normal	Combined
1	0.9672	0.9561	0.5084	0.3748
2	0.9778	0.8159	0.9371	0.8002
3	0.9629	0.9050	0.8163	0.6202
4	0.9249	0.9491	0.9998	0.7124
5	0.9454	0.5701		0.6235

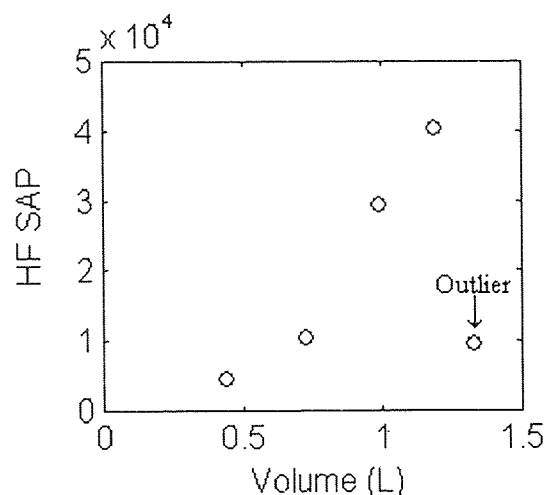


Figure 4.1 HF SAP vs. Volume for Subject 1 at 3/2 Normal Rate

The data for subject 5 at normal respiration rate is shown in figure 4.2 in an attempt to explain the correlation of 0.5701 which is much lower than the others. From this plot it can be seen that there are no obvious outliers causing this reduced correlation.

Since the correlation is greater than 0.5 the trend that the other data sets follow is still observed, so this is acceptable as showing a direct relationship.

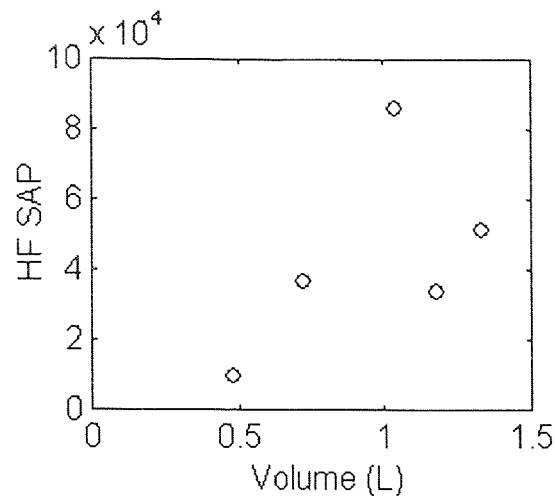


Figure 4.2 HF SAP vs. Volume for Subject 5 at Normal Rate

These results show that most of the correlations are high (above 0.75) when the data is grouped by respiration rate, but the correlations are lower when all the respiration rates are combined. This difference is shown throughout all the results presented in this section: relationships are stronger when data is broken up into the three separate respiration rates. The fact that the correlations are low with all rates combined suggests that there are other factors affecting the data besides the two parameters used in calculating the correlation coefficients.

Since all the correlations between HF SAP and volume except one are greater than 0.8 when the data is grouped by respiration rate, the hypothesis that HF SAP is strongly correlated with the average tidal volume is supported. This shows that the amount of variability of the systolic arterial blood pressure at the frequency of respiration is directly proportional to the amount of pressure changes in the thoracic cavity which is related to tidal volume.

In section 3.2.4, it was shown that performing step interpolation of the systolic arterial pressures before performing spectral analysis results in a spectrum that is similar in LF and HF peak content to the spectrum of the raw blood pressure signal. Since the spectra are similar, it is hypothesized that there is also a relationship between the HF peak area of the BP spectrum (HF BP) in absolute units and the average tidal volume. The correlations between these parameters appear in table 4.3.

Table 4.3 Correlations Between HF BP in Absolute Units and Volume

Subject	Respiration Rate			All Rates
	2/3 Normal	Normal	3/2 Normal	Combined
1	0.9559	0.8366	0.9193	0.5783
2	0.9715	0.9321	0.9788	0.9034
3	0.9845	0.9200	0.8417	0.7626
4	0.9637	0.9403	0.9877	0.5025
5	0.9764	0.6670		0.6462

Similar to the above discussion comparing HF SAP with tidal volume, it is seen that a strong linear relationship exists between HF BP and average tidal volume when the data is grouped by respiratory rate. It should be noted that the same outlier previously removed for subject 1 at 3/2 normal respiration rate was removed before computing this correlation. By comparing this table to table 4.2, it can be seen that the correlations are all similar in value. This reinforces the conclusion made in section 3.2.4 that the present methods of spectral analysis of SAP result in SAP spectra that are nearly identical in content to BP spectra.

For completeness, the correlations between average tidal volume and the HF peak power (in absolute units) of the IBI spectrum (vagal tone) were also observed. These correlations appear in table 4.4. As shown by Leifer, there is a weak relationship between vagal tone and tidal volume [4]. This is demonstrated by the fact that some of the correlation coefficients are negative but very high in magnitude, while others show very

low correlation magnitudes, indicating no relationship. This suggests that there may be an inverse linear relationship between vagal tone and tidal volume but there may be other physiological parameters affecting the relationship. Also evident from table 4.4, is the fact that when all three respiratory rates are combined for each subject, there appears to be no relationship between vagal tone and volume.

Table 4.4 Correlations Between Vagal Tone and Volume

Subject	Respiration Rate			All Rates
	2/3 Normal	Normal	3/2 Normal	Combined
1	-0.7201	-0.9181	-0.5463	-0.5015
2	0.4494	0.2388	-0.6291	0.0933
3	-0.2784	-0.9884	-0.9732	-0.2033
4	-0.2314	-0.9513	-0.9790	-0.0535
5	-0.9382	-0.9720		-0.1924

By plotting the data in which there are low correlations, a parabolic relationship between vagal tone and volume appears in three cases. The plots of vagal tone vs. tidal volume for subject 1 at 3/2 normal respiration rate, subject 2 at 2/3 normal rate, and subject 4 at 2/3 normal rate appear in figures 4.3, 4.4, and 4.5 respectively. It can be seen that while the data appears parabolic, the parabola is inverted in the case of figure 4.4 and is therefore not consistent. These parabolic relationships suggest that there may be a more complicated relationship between volume and vagal tone than is immediately apparent.

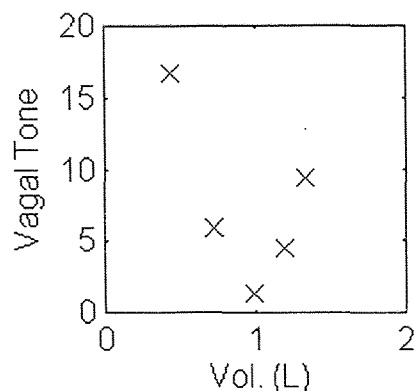


Figure 4.3 Volume vs. Vagal Tone for Subject 1 at 3/2 Normal Respiration Rate

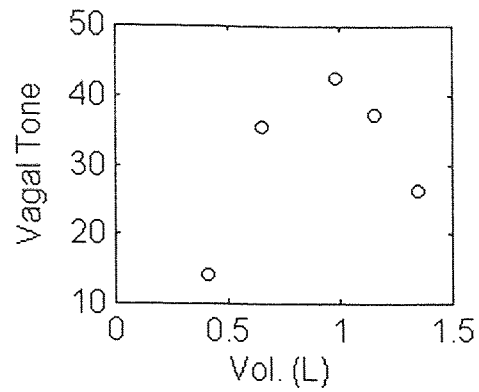


Figure 4.4 Volume vs. Vagal Tone for Subject 2 at 2/3 Normal Respiration Rate

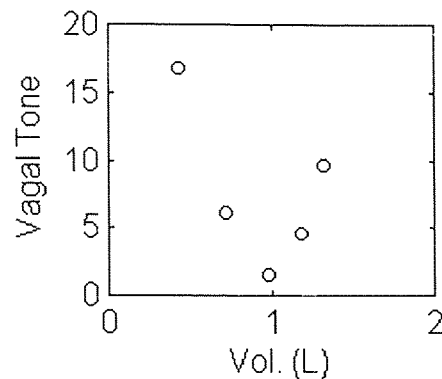


Figure 4.5 Volume vs. Vagal Tone for Subject 4 at 2/3 Normal Respiration Rate

Since heart rate (HR) was shown by Leifer to be strongly correlated to tidal volume, the correlations between HF SAP in absolute units and HR were also expected to be high. These correlations are shown in table 4.5.

Table 4.5 Correlations Between HR and HF SAP in Absolute Units

Subject	Respiration Rate			All Rates
	2/3 Normal	Normal	3/2 Normal	Combined
1	0.0946	0.9166	0.8147	-0.0243
2	0.9808	-0.8342	0.9857	0.317
3	0.9322	0.9812	0.7786	0.2558
4	0.9554	0.9019	0.9867	0.5272
5	0.912	0.6379		0.1404

From this table it is seen that in most cases, there is a strong linear relationship between HF SAP and HR. The plots of the data for subject 1 at 2/3 normal respiration

rate and subject 2 at normal rate were checked and it was found that there were not any outliers affecting the correlations.

Upon plotting straight line fits for each respiration rate for the data, another relationship is found. For example, the data for subject 3 is shown in figure 4.6. From this plot it can be seen that the order of the lines, in order of increasing slope is as follows: normal respiration rate, $3/2$ normal respiration rate, and $2/3$ normal respiration rate. This order is the same when constructing similar plots for subjects 4 and 5. This suggests that respiration rate plays a role in determining the amount that respiration volume affects heart rate since respiration volume is strongly correlated with HF SAP.

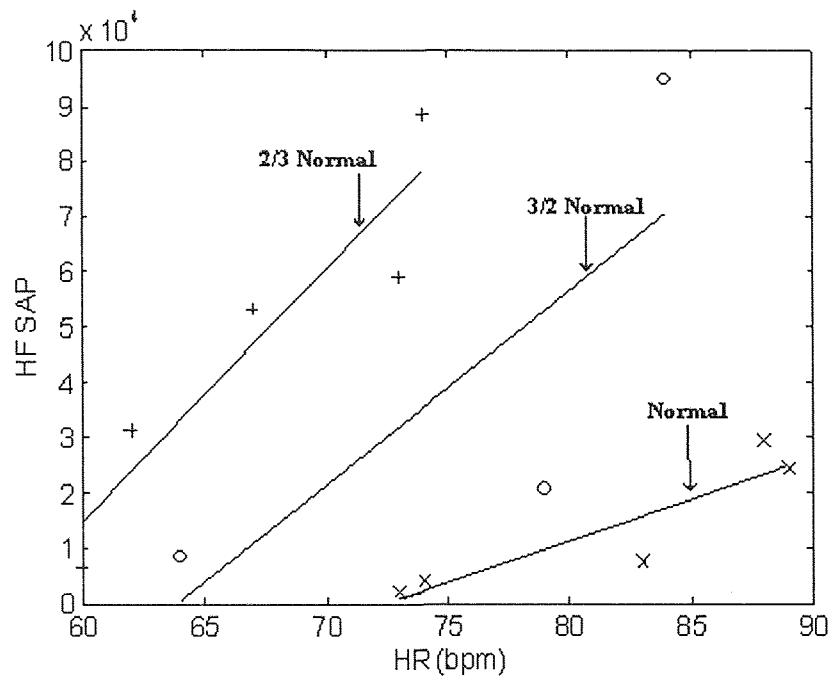


Figure 4.6 Plot of HF SAP vs. HR for Subject 3

4.3.2 Measurement of Sympathetic Activity

As mentioned in the first chapter, it is commonly accepted in present research that the LF peak of the SAP spectrum (LF SAP) is an indicator of purely sympathetic activity. The

next part of this research deals with comparing LF SAP with parameters known to be associated with sympathetic responses to determine if LF SAP is a reliable marker of sympathetic activity.

Since the heart is enervated by both parasympathetic and sympathetic nerves, the interaction of these two systems produce changes in heart rate. For the study presented in this subsection, the HF peak of the IBI spectrum (vagal tone) is used as an indicator of parasympathetic activity and LF SAP (in absolute units) is assumed to indicate purely sympathetic activity. By observing the amount of influence each of these peaks has on heart rate, the relative amounts of influence of the parasympathetic and sympathetic nervous systems on the heart can be inferred. These influences are measured by observing the correlations between HR and vagal tone and between HR and LF SAP. These correlations are shown in tables 4.6 and 4.7. The relationships between these correlations are explained in the discussion that follows.

Table 4.6 Correlations Between HR and LF SAP in Absolute Units

Subject	Respiration Rate		
	2/3 Normal	Normal	3/2 Normal
1	-0.5534	-0.7093	0.6906
2	0.9183	-0.6008	-0.6753
3	0.8026	-0.9722	0.4629
4	0.7432	0.1840	0.9939
5	0.1890	0.5232	

Table 4.7 Correlations Between HR and Vagal Tone

Subject	Respiration Rate		
	2/3 Normal	Normal	3/2 Normal
1	0.2251	-0.8936	-0.8508
2	0.4012	-0.0728	-0.7420
3	-0.4121	-0.9272	-0.9570
4	-0.4271	-0.9185	-0.9405
5	-0.9492	-0.9726	

By observing how corresponding pairs of correlations behave, observations may be made regarding the relative amounts of sympathetic and parasympathetic activity on the heart. Table 4.8 shows the all the possible combinations of correlations that can occur. This table is based on the following assumptions: that purely parasympathetic influence on the heart would result in a strong negative correlation between HR and vagal tone and purely sympathetic influence on the heart results in a strong positive correlation between HR and LF SAP. These assumptions are made due to the fact that sympathetic influence speeds up heart rate and parasympathetic influence slows down heart rate. Also, it is assumed that LF SAP indicates sympathetic activity on the SA node of the heart, although it is a result of sympathetic influence of the vascular system since it is derived from the blood pressure signal.

Table 4.8 Possible Combinations of Correlations

Possibility	HR vs. Vagal Tone	HR vs. LF SAP
1	strong -	strong -
2	strong -	none
3	strong -	strong +
4	none	strong -
5	none	none
6	none	strong +
7	strong +	strong -
8	strong +	none
9	strong +	strong +

Possibility 1 indicates a very strong parasympathetic influence on the heart. This is concluded because HR and vagal tone are expected to be negatively correlated and HR and LF SAP are expected to be positively correlated. Since HR and LF SAP are negatively correlated in this case, it can be concluded that the parasympathetic outflow is so large in magnitude that the parasympathetic nervous system is controlling the heart rate and overrides the sympathetic influence present. Possibility 2 also indicates a strong

parasympathetic influence on heart rate but not as strong as in possibility 1. This is concluded because the expected relationship between HR and vagal tone still exists but the sympathetic nervous system is not affecting HR. Possibility 3 suggests that both divisions of the autonomic nervous system are active, and the strength of the correlations must be considered to determine which is dominant in the role of controlling heart rate. Possibility 4 is physiologically impossible because as shown in possibility 1, a negative correlation between LF SAP and HR is not possible unless there is strong parasympathetic influence on the heart. Possibility 5 suggests that there is not any autonomic influence on heart rate because it shows that there is not any correlation between HR and LF SAP and between HR and vagal tone. Strong sympathetic influence is suggested by the conditions of possibility 6 because HR and LF SAP are positively correlated as expected and there is not any opposing parasympathetic influence. Possibilities 7 and 8 are physiologically impossible because HR and vagal tone can not be positively correlated without strongly opposing sympathetic influence which is indicated by a positive correlation between HR and LF SAP. Finally, possibility 9 indicates a very strong sympathetic response since the parasympathetic influence is overridden by sympathetic influence which is made apparent by the correlation between HR and vagal tone being opposite in magnitude to what is expected.

In order to apply these classifications to the correlations presented in tables 4.6 and 4.7, the correlation values designated 'strong' and 'none' must first be defined. For this study it is chosen that a correlation magnitude of 0.6 be used to distinguish whether or not two variables are correlated.

Next the correlations from tables 4.6 and 4.7 are sorted into the corresponding possibility numbers previously discussed and shown in table 4.8. These results are shown in table 4.9.

Table 4.9 Classification of Pairs of Correlation Coefficients

Subject	Respiration Rate		
	2/3 Normal	Normal	3/2 Normal
1	5	1	3
2	6	4	1
3	6	1	2
4	6	2	3
5	2	2	

From this table, it is seen that all the possibilities that appear were shown to have physiological explanations with the exception of subject 2 at normal respiration rate and subject 1 at 2/3 normal respiration rate. For example, at 2/3 normal respiration rate, possibility 6 appears three times. Possibility 6 was reasoned to indicate strong sympathetic activity and is consistent with the expected results because at 2/3 normal respiration rate, some discomfort is felt, which would elicit a sympathetic response. In the case of the normal respiration rate, possibilities 1 and 2 each appear twice which indicates parasympathetic activity which is expected due to the fact that the subjects are performing at their natural respiration rate and are more comfortable. Since possibility 5 corresponds to low correlations between both HR and vagal tone and between HR and LF SAP, autonomic influence on the heart can not be inferred in this case using this technique.

As previously discussed, possibility 3 was assumed to show both parasympathetic and sympathetic activity because both correlations are greater than 0.6 in magnitude and have the expected signs: positive for HR vs. LF SAP and negative for HR vs. vagal tone. In the case of subject 1 at 2/3 normal respiration rate, the correlation of HR with LF SAP is greater in magnitude and therefore it is conjectured that there is a stronger sympathetic

influence on the heart. Subject 4 at 3/2 normal respiration rate shows a stronger correlation between HR and vagal tone than HR and LF SAP. In this case, it is conjectured that there is a stronger parasympathetic influence on the heart.

Next, the same technique was applied using the LF peak area of the BP spectrum (LF BP) in absolute units instead of LF SAP to determine if the results are similar. The correlations between HR and LF BP in table 4.10. The correlations between HR and vagal tone are shown in table 4.7. These pairs of correlations were then classified using the same method as before. The results are shown in table 4.11.

Table 4.10 Correlations Between HR and LF BP in Absolute Units

Subject	Respiration Rate		
	2/3 Normal	Normal	3/2 Normal
1	-0.4172	-0.8863	0.6064
2	0.6817	0.7770	-0.6870
3	0.6395	-0.9700	0.4370
4	0.4965	0.2250	-0.9993
5	-0.5971	0.2837	

Table 4.11 Classification of Pairs of Correlation Coefficients

Subject	Respiration Rate		
	2/3 Normal	Normal	3/2 Normal
1	5	1	3
2	6	4	1
3	6	1	2
4	5	2	3
5	2	2	

As expected the results are similar when using LF BP instead LF SAP. The only difference between tables 4.9 and 4.11 is that possibility 5 instead of 6 appears in the case of subject 4 at 2/3 normal respiration rate. This is due to the fact that the correlation between HR and LF SAP for this case is 0.7432 while the corresponding correlation between HR and LF BP is 0.4965. This reduced correlation causes this case to change from possibility 6 to possibility 5. As shown in section 3.2.4, the spectral content of the

BP and SAP spectra under current methods are very similar which explains the fact that the results of using LF BP instead of LF SAP in this experiment has little effect on the results.

Next, the same experiment was performed using LF SAP in normalized units as a measure of sympathetic activity and the normalized HF peak of the IBI spectrum as a measure of vagal tone. The purpose of this is to determine the effects of normalizing spectral components on comparing measures of parasympathetic and sympathetic activity. The correlations between HR and LF SAP in normalized units are shown in table 4.12 and the correlations between HR and vagal tone in normalized units are shown in table 4.13.

Table 4.12 Correlations Between HR and LF SAP in Normalized Units

Subject	Respiration Rate		
	2/3 Normal	Normal	3/2 Normal
1	-0.3050	-0.9053	-0.6836
2	-0.9497	0.5622	-0.9748
3	-0.8260	-0.9881	-0.9083
4	-0.1438	-0.0934	-0.9351
5	-0.9162	-0.3585	

Table 4.13 Correlations Between HR and Vagal Tone in Normalized Units

Subject	Respiration Rate		
	2/3 Normal	Normal	3/2 Normal
1	0.1927	-0.1275	-0.8469
2	0.3230	-0.6234	0.9846
3	-0.9202	-0.1629	-0.3093
4	-0.4973	-0.6882	-0.8154
5	0.7814	-0.4528	

Again, corresponding pairs of correlations were classified into the possibilities shown in table 4.8 using the a correlation magnitude of greater than 0.6 to describe a correlation of ‘strong.’ These results are shown in table 4.14. From this table, it can be seen that the results are extremely different from those obtained using absolute units. Many of the possibilities that appear in this table were shown to be without physiological

explanation. Only one of the values in this table is the same as when this experiment is performed using absolute units.

Table 4.14 Classification of Pairs of Correlation Coefficients

Subject	Respiration Rate		
	2/3 Normal	Normal	3/2 Normal
1	5	4	1
2	4	2	7
3	1	4	4
4	5	2	1
5	7	5	

The reason the results are very different when using normalized units is explained by observing the equations used in normalizing the spectral areas. These equations are as follows:

$$\text{LF (n.u.)} = \frac{\text{LF}}{\text{LF} + \text{HF}} * 100 \quad (4.1)$$

$$\text{HF (n.u.)} = \frac{\text{HF}}{\text{LF} + \text{HF}} * 100 \quad (4.2)$$

Since vagal tone in normalized units is computed from equation 4.2, it can be seen that the LF area of the IBI spectrum appears in the denominator. Since the LF peak of the IBI spectrum was shown to indicate a mixture of parasympathetic and sympathetic activity, the measure of vagal tone obtained from this equation depends upon the amount of sympathetic activity that is present in the LF peak of the IBI spectrum. As discussed in section 1.5, methods that determine the proportions of parasympathetic and sympathetic activity in the LF peak of the IBI spectrum do not currently exist. Therefore, in this situation, the normalized the HF area of the IBI spectrum is a poor measure of vagal tone.

This effect is also seen from normalizing the LF SAP using equation 4.1. From this equation, it is seen that the normalized LF area is affected by the presence of the HF

area of the SAP spectrum in the denominator. An example of the results of this are seen from the correlation coefficients (from tables 4.6 and 4.12) for subject 1 at 2/3 normal respiration rate. The correlation between HR and LF SAP in absolute units is 0.9183 and the correlation between HR and LF SAP in normalized units is -0.9497. This difference is explained by observing the data for this subject at this respiration rate which is shown in table 4.15.

Table 4.15 Data for Subject 2 at 2/3 Normal Respiration Rate

Tidal Volume	HR	LF SAP (absolute)	HF SAP (absolute)
0.42	51	17690	5951
0.66	55	30903	19272
0.99	57	27786	43471
1.16	60	31654	59610
1.35	63	37820	91094

By examining this table, it is seen that while LF SAP and HR are directly proportional, so are HF SAP and HR, which was shown in section 4.3.1. Since HF SAP appears in the denominator of the equation used to normalize LF SAP, and increases as HR increases, the normalized LF area is reduced in value as HR increases. This causes the correlation to change from strong positive to strong negative when normalizing LF SAP.

The only exception to this effect is seen in the case of subject 2 at normal respiration rate. When normalizing LF SAP, the correlation with HR is changed from -0.6008 to 0.5622. This is due to the fact that in this case, the correlation between HR and HF SAP is -0.8342 (from table 4.5). This strong negative correlation indicates that as HR increases, HF SAP decreases. Since HF SAP decreases and appears in the denominator of the normalization equation, the normalized LF SAP increases as HR increases.

4.4 Conclusions

In the studies presented in this chapter it was attempted to verify the origin of the various peaks in the SAP spectrum by seeking relationships between the LF and HF peak areas of the SAP spectrum with various cardiac and respiratory parameters.

First, it was verified that the HF peak of the SAP spectrum is strongly correlated with tidal volume. This is expected because the volume of inhaled air directly affects the pressure in the thoracic cavity which affects the blood pressure. The HF peak of the BP spectrum also showed this relationship to tidal volume.

Evaluation of the LF peak in the SAP spectrum was shown to provide an indicator of sympathetic activity when used in conjunction with measures of the strength of relationships between HR and vagal tone. By current methods however, the information held in this LF peak may be distorted due to the interpolation method chosen to preprocess the data. Since current methods of SAP analysis include HRV components in the SAP spectrum, and the LF peak in the IBI spectrum indicates a mixture of parasympathetic and sympathetic activity, some parasympathetic activity is included in the LF peak of the SAP spectrum.

It was shown that normalizing spectral areas can drastically change the results of correlation coefficient calculations. This is due to the fact that in normalizing areas causes other physiological variables to be taken into account. It is therefore concluded that careful consideration be used when choosing whether or not to normalize spectral areas.

It can also be concluded that the relationships between the physiological parameters examined in this experiment are more apparent when the data is grouped by respiration rate. This was demonstrated by the fact that the correlation coefficients

observed were all considerably higher for individual rate than when all the rates were grouped together.

CHAPTER 5

CONCLUSIONS

5.1 Introduction

In this chapter, a summary of the results of the work accomplished in this thesis, as well as suggestions for future studies are presented. Included in these results are the conclusions drawn from the experiments involving interpolation, normalized units, blood pressure analysis algorithms, and rate and volume controlled respiration data.

5.2 Summary of Results

In the first part of this study, different methods of interpolation were evaluated by performing interpolation on both simulated and real IBI and SAP data. The different methods evaluated were tachogram, step interpolation, and cubic spline interpolation. It was found that various interpolation methods introduce different degrees of low pass filtering to spectra derived from the interpolated signal. It was also found that this low pass filter effect was proportional to both the mean IBI duration and the product of mean HR and respiration rate.

Another factor considered in this study is that some interpolation methods, when performed on SAP data, result in the inclusion of HRV components in the spectra. Three different interpolation methods were applied to SAP data and the resulting spectra compared. It was shown that the cubic spline and step interpolation methods both resulted in spectra that include HRV components because the spectra were similar in

content. It was concluded that the tachogram method is the best because HRV content is lost because the time intervals between systolic peaks are not retained.

Next, the effect on normalizing spectral areas on the day to day reproducibility of data was investigated. Power spectral analysis of HRV was performed on EKG data acquired on two separate days for ten subjects and the LF and HF areas of the spectra were computed in both absolute and normalized units. The percent difference from day 1 to day 2 was then computed for each subject for each of the 4 parameters calculated. Since the overall mean percent differences were lower for the normalized areas, it was concluded that normalizing spectral areas aids in the day to day reproducibility of data.

It was also concluded that when choosing whether or not to normalize spectral areas several factors must be considered. While normalized units aid in the reproducibility of day to day results and in comparing spectra derived using different interpolation techniques, normalized results can change drastically due to other physiological parameters.

Next, a set of algorithms were presented to derive BP and SAP spectra from raw blood pressure signals. It was decided to use step interpolation of the SAP because current HRV in our laboratory uses backward step interpolation. It was chosen to keep the SAP and HRV methods the same because the spectra are compared to each other and although both are distorted by the interpolation, they are presumably distorted by the same amount.

It was also found in this study that step interpolation of the SAP results in a spectrum that is similar in LF and HF peak content to the spectrum of the raw blood pressure signal. This was shown by calculating the correlation coefficients between the

corresponding peaks in both spectra. It was concluded that this occurred because the blood pressure signal contains both heart rate and systolic pressure information and step interpolating the SAP results in a signal containing these same two parameters.

Finally, the blood pressure analysis algorithms were applied to data collected from subjects performing a rate and volume controlled respiration study. Along with SAP and BP spectra, various respiratory and HRV parameters were also computed. The purpose of this analysis was to increase understanding of the use of spectral analysis of blood pressure and heart rate as a window to the autonomic nervous system.

The first task accomplished in this study was the verification of the role of respiration on the HF peak of the SAP spectrum. It was found that tidal volume was strongly correlated with the HF peak area of the SAP spectrum which was expected because the volume of inhaled air influences the pressure in the thoracic cavity which affects blood pressure.

It was also found that a strong relationship exists between the HF peak area of the SAP spectrum and heart rate. This was expected because the HF peak area of the SAP spectrum is strongly related to tidal volume. Not only were high correlations found, but 3 subjects showed the same pattern when the data was plotted. It was found that the degree at which volume affects heart rate is determined by the rate of respiration.

Finally, it was shown that the LF peak in the SAP spectrum in absolute units provides an indicator of sympathetic activity when used in conjunction with measures of the strength of relationships between HR and vagal tone in absolute units. The methods developed provide a means of explaining the interaction of the parasympathetic and sympathetic influence on heart rate.

5.3 Future Work

In order to shed more light upon the interpolation issues, the Lomb periodogram should be implemented and used to perform experiments similar to those performed in this research. Since the Lomb periodogram eliminates the need for interpolation, it may provide a more reliable estimate of spectral analysis than do current methods which require interpolation. A benefit to using the Lomb methods is that reliable measures of power spectra are still available even if there are missing data. A downfall to using the Lomb method is that on SAP data, the spacing between systolic peaks and therefore the HRV contribution to the SAP spectrum will be present.

Further studies of interpolation techniques are needed to determine better ways to interpolate heart rate and systolic blood pressure data. The backward step interpolation algorithm used in this research has been proven to result in spectral distortions dependent upon the characteristics of the data. Step interpolation of systolic blood pressure not only includes this same distortion, but also includes heart rate information, which results in difficulty in interpretation of the resulting spectral areas.

A rigorous statistical analysis should be performed on the results of the analysis of the experimental data presented in this thesis. Correlation coefficients and plots are helpful in determining the strength of some relationships between physiological parameters, but more complex interactions such as those that occur between physiological parameters require more complicated statistical procedures.

APPENDIX A

HEART RATE VARIABILITY ANALYSIS STEPS

This section outlines the procedure for performing heart variability analysis in S-Plus. As an example, a data file named k051194a.dat that consists of six channels sampled at 200 Hz. and is two minutes long will be used.

- 1.) First the file is unpacked from the DOS prompt using the following command:

unpack k051194a.dat,k051194a.asc,0-148480/b/das16
(where 148480 is the total number of samples.)

- 2.) Now the data matrix is scanned into S-Plus as follows:

k051194a_matrix(scan("k051194a.asc",skip=1,sep=",",),ncol=6,byrow=T)

- 3.) The first and last three points of the file are then cut off:

k051194a.c_k051194a[3:24744,]

- 4.) The file is then analyzed as follows:

k051194a.l_pslws(k051194a.c)

- 5.) The analyzed file is then plotted to check the accuracy of the R wave detection:

stdgraf(k051194a.l,sr=20)

- 6.) If there is a low outlier, then the erroneous detection is eliminated by:

k051194a.d_dqrs(k051194a.c[,6],k051194a.l\$pk)

- 7.) The elimination is then checked using:

plot(diff(k051194a.d))

- 8.) If there is a high outlier, then the following commands are used:

- a.) If changes were made using dqrs:

k051194a.m_mqrs(k051194a.c[,6],k051194a.d,pout(diff(k051194a.d)))

- b.) If no changes were made using dqrs:

k051194a.m_mqrs(k051194a.c[,6],k051194a.l\$pk,pout(diff(k051194a.l\$pk)))

- 9.) The changes are then written to the finished (.fin) file as follows:

- a.) If no changes were made using either dqrs or mqrs:

k051194a.fin_k051194a.l

- b.) If changes were made using dqrs or both dqrs and mqrs:

k051194a.fin_fwork(k051194a.c,k051194a.m)

c.) If changes were made using dqrs alone:

k051194a.fin_fwork(k051194a.c,k051194a.d)

10.) If changes were made, the finished file is then checked to make sure the changes are correct:

stdgraf(k051194a.fin,sr=20)

11.) If the plots are correct, then the areas under the peaks are found as follows:

a.) Low frequency area (0.05 to 0.15 Hz.):

spect1(k051194a.fin\$isp,low.freq=0.05,high.freq=0.15,srate=200)

b.) High frequency area (0.15 to 0.4 Hz.):

spect1(k051194a.fin\$isp,low.freq=0.15,high.freq=0.4,srate=200)

Note: These limits for the frequency bands may vary depending upon the respiration rate, although they are the ones used the most frequently.

APPENDIX B

HEART RATE VARIABILITY ANALYSIS PROGRAMS

Pslws

```
function(x)
{
  jks <- x[, 2]
  aa <- grep(T, diff(jks) > 1000)
  ljs <- lsbp(x, aa)
  ljs
}
```

Grep

```
function(pattern, text)
.Internal(grep(pattern, text), "dos_grep")
```

Lsbp

```
function(x, x.pk, nt = 8192, ns = 6, decimate = 10, tooruff = 0.8, f = 0.1, ld = 10,
sd
  = 10)
{
  mruff <- max(abs(ruff(diff(x.pk))))
  if(mruff >= tooruff)
    print(paste("ibi's may be too ruff", tooruff, sep = ""))
  x.ecg <- x[, 2]
  x.iu <- iibi(diff(x.pk))
  x.i <- x.iu[seq(1, len(x.iu), decimate)]
  x.sq <- sqdt(x.i, f = f, ld, sd)
  x.isp <- spect(x.i, nt = nt, ns = ns)
  x.rpd <- x[seq(1, len(x[, 1]), 10), 1]
  x.rlw <- lowess(1:len(x.rpd), x.rpd, f = 0.3, iter = 2, delta = ceiling((length(
    x.rpd) * 0.3)/8))$y
  x.rsp <- spect(x.rpd - x.rlw, nt = nt, ns = ns)
  z <- list(pk = x.pk, ibi = x.i, ibiu = x.iu, sq = x.sq, rpd = x.rpd, rlw = x.rlw,
    isp = x.isp, rsp = x.rsp, ecg = x.ecg, )
  z
}
```

Sqdt

```

function(x, f, ldelta, sdelta)
{
  ltr <- lowess(1:length(x), x, f = f, iter = 2, delta = ldelta)$y
  xs <- (1:length(x))[c(F, diff(x) != 0)]
  xs <- (xs)[seq(1, length(xs), sdelta)]
  ys <- sqwv(xs, ltr)
  ys
}

```

Spect

```

function(z, nt = length(z), taper = 0.2, ns = 20)
{
  if(any(is.na(z)))
    stop("NA's not allowed")
  if(taper < 0 | taper > 1)
    stop("taper must be between 0 & 1")
  if(nt < length(z))
    z <- z[1:nt]
  z <- z - mean(z)
  z <- spec.taper(z, taper)
  print(paste("Windowing length per side is ", nt * taper, sep = ""))
  #z <- .Fortran("spcos",
#   x = as.double(z),
#   y = as.double(z),
#   as.integer(length(z)),
#   as.double(taper))$y
  if(nt > length(z))
    z <- c(z, rep(0, nt - length(z)))
  z <- (Mod(fft(z))^2/(2 * pi * nt))[1:(nt %/% 2 + 1)]
  if(ns > 0) {
    z <- spec.smo(z, span = 7) #z <- .Fortran("trsmooth",
#   x = as.double(z),
#   as.integer(length(z)),
#   as.integer(ns))$x
    z <- rev(z)
    z <- spec.smo(z, span = 7) #z <- .Fortran("trsmooth",
#   x = as.double(z),
#   as.integer(length(z)),
#   as.integer(ns))$x
    z <- rev(z)
  }
  z
}

```

Stdgraf

```

function(x, title = " ", wait = T, sr = 20, sr2 = sr * 10)
{
  #z <- attributes(x)
  #if(length(z$names) < 7)
  #   stop("Wrong structure -- check attributes")
  nt <- (length(x$isp) - 1) * 2
  par(mfrow = c(3, 1), mar = c(6.1, 6.1, 4.1, 3.1))
  if(missing(sr)) {
    plot(diff(x$pk), xlab = "Beat Number", ylab = "IBI", main =
          paste(title, "Interbeat Intervals"))
    plot(x$ibi, type = "l", xlab = "Time", ylab = "IIBI", main =
          paste(title, " - IIBI", sep = ""))
    lines(x$sq)
    plot(x$rpd, type = "l", xlab = "Time", ylab = "Resp", main =
          paste(title, " - Resp", sep = ""))
    lines(x$rlw)
    if(wait)
      scan()
    par(mfrow = c(1, 1), mar = c(6.1, 6.1, 4.1, 4.5))
    plot(x$isp[1:500], type = "l", xlab = "Frequency Number",
          ylab = "Power", main = title)
    par(new = T)
    plot(x$rsr[1:500], type = "l", lty = 3, axes = F, xlab = "", ylab = "")
    axis(4)
    mtext("Resp Power - - ", side = 4, line = 3)
  }
  else {
    par(mfrow = c(3, 1), mar = c(6.1, 6.1, 4.1, 3.1))
    plot(diff(x$pk)/sr2, xlab = "Beat Number", ylab = "IBI", main =
          paste(title, " - IBI", sep = ""))
    plot(x$ibi/sr2, type = "l", xlab = "Time", ylab = "IIBI", main =
          paste(title, " - IIBI", sep = ""))
    lines(x$sq/sr2)
    plot(x$rpd, type = "l", xlab = "Time", ylab = "Resp", main =
          paste(title, " - Resp", sep = ""))
    lines(x$rlw)
    if(wait)
      scan()
    xf <- ((1:500) - 1)/nt * sr
    par(mfrow = c(1, 1), mar = c(6.1, 6.1, 4.1, 4.5))
    plot(xf, x$isp[1:500], type = "l", xlab = "Frequency", ylab = "Power",
          main = title)
    par(new = T)
    plot(xf, x$rsr[1:500], type = "l", lty = 3, axes = F, xlab = "",

```

```

        ylab = "")
    axis(4)
    mtext("Resp Power - - ", side = 4, line = 3)
  }
}

```

Mqrs

```

function(x, qx, xout)
{
  if(length(xout$high) == 0) {
    qfx <- list(qx = qx, ibi = diff(qx))
    return(qfx)
    stop()
  }
  print("bracket missing peaks using mouse", quote = F)
  cx <- vector("numeric", 0)
  print(xout$high)
  for(i in xout$high[1:length(xout$high)]) {
    i1 <- i - 2
    i2 <- i + 2
    if(i1 < 1)
      i1 <- 1
    if(i2 > length(qx))
      i2 <- length(qx)
    plot(qx[i1]:qx[i2], x[qx[i1]:qx[i2]], type = "l")
    abline(v = qx[(i1):(i2)])
    bx <- locator()$x
    if(length(bx) > 0) {
      if(length(bx) > 2) {
        bx <- unique(bx)
      }
      if(length(bx) %% 2 > 0) {
        bx <- bx[1:(length(bx) - (length(bx) %% 2))]
      }
      for(j in seq(1, length(bx), 2)) {
        bb <- floor(bx[j])
        be <- ceiling(bx[j] + 1)
        tx <- order(x[bb:be])[length(bb:be)] + bb
        abline(v = tx, lty = 2)
        cx <- c(cx, tx)
      }
    }
  }
  print(cx)
  for(i in 1:length(cx)) {

```

```

        qxu <- qx[qx < cx[i]]
        qxo <- qx[qx > cx[i]]
        qx <- c(qxu, cx[i], qxo)
        print(length(qx))
    }
    #qfx <- list(qx = qx, ibi=diff(qx))
    qfx <- qx
    qfx
}

```

Dqrs

```

function(x, qx)
{
    px <- vector("numeric", 0)
    plot(diff(qx))
    print("identify outliers using mouse", quote = F)
    fx <- identify(diff(qx), plot = F)
    if(length(fx) == 0) {
        qfx <- list(qx = qx, fx = fx, cx = vector("numeric", 0), ibi = diff(qx))
        return(qfx)
        stop
    }
    fx <- unique(fx)
    cx <- vector("numeric", 0)
    print("identify bad peaks using mouse", quote = F)
    for(i in fx[1:length(fx)]) {
        i1 <- i - 2
        i2 <- i + 2
        if(i1 < 1)
            i1 <- 1
        if(i2 > length(qx))
            i2 <- length(qx)
        plot(qx[i1]:qx[i2], x[qx[i1]:qx[i2]], type = "b", pch = "-")
        abline(v = qx[(i1):(i2)])
        zx <- identify(qx[i1]:qx[i2], x[qx[i1]:qx[i2]], plot = F)
        if(length(zx) > 0)
            cx <- c(cx, zx + qx[i1] - 1)
    }
    if(length(cx) == 0) {
        qfx <- list(qx = qx, fx = fx, cx = vector("numeric", 0), ibi = diff(qx))
        return(qfx)
        stop
    }
    for(i in cx) {
        qx <- qx[qx != i]
    }
}

```

```

    }
    #qfx <- list(qx = qx, fx=fx, cx=cx, ibi = diff(qx))
    qfx <- qx
    qfx
  }

```

Fwork

```

function(x, x.pk, nt = 8192, ns = 6, decimate = 10, tooruff = 0.8, f = 0.1,
        ld = 10, sd = 10)
{
  mruff <- max(abs(ruff(diff(x.pk))))
  if(mruff >= tooruff)
    print(paste("ibi's may be too ruff ", tooruff, sep = ""))
  x.i <- iibi(diff(x.pk))
  x.i <- x.i[seq(1, len(x.i), decimate)]
  x.sq <- sqdt(x.i, f = f, ld, sd)
  x.isp <- spect(x.i, nt = nt, ns = ns)
  x.rpd <- x[seq(1, len(x[, 1]), 10), 1]
  x.rlw <- lowess(1:len(x.rpd), x.rpd, f = 0.3, iter = 2, delta = ceiling((length(
    x.rpd) * 0.3)/8))$y
  x.rsp <- spect(x.rpd - x.rlw, nt = nt, ns = ns)
  z <- list(pk = x.pk, ibi = x.i, sq = x.sq, rpd = x.rpd, rlw = x.rlw, isp = x.isp,
    rsp = x.rsp)
  z
}

```

Spect1

```

function(x, low.freq = 0.15, high.freq = 0.4, srate = 200)
{
  isp <- x
  low.no <- round((2 * length(isp) * low.freq * 10)/srate)
  high.no <- round((2 * length(isp) * high.freq * 10)/srate)
  isp.new <- isp[low.no:(high.no - 1)]
  isp.dif <- diff(isp[low.no:high.no])
  area.tmp <- sum(isp.new + isp.dif/2) * (srate/(2 * length(isp) * 10))
  return(area.tmp)
}

```


APPENDIX C

DATA USED IN NORMALIZED UNITS EXPERIMENT

Table C.1 Data Used in Normalized Units Experiment

Subject	LF (absolute)		LF (normalized)		HF (absolute)		HF (normalized)	
	Day 1	Day 2	Day 1	Day 2	Day 1	Day 2	Day 1	Day 2
1	12.6337	6.2583	50.1957	25.1846	12.5352	18.5914	49.8043	74.8154
2	2.2482	2.4465	18.5811	15.6105	9.8512	13.2256	81.4189	84.3895
3	10.3702	13.5509	35.6395	30.9627	18.7273	30.2143	64.3605	69.0373
4	8.7934	9.5450	58.4543	65.7636	6.2498	4.9691	41.5457	34.2364
5	17.7742	19.2989	41.0756	36.9631	25.4977	32.9124	58.9244	63.0369
6	14.0390	36.8345	49.8111	25.8465	14.1455	105.6778	50.1889	74.1535
7	17.6716	5.9812	10.1228	10.6360	156.9010	50.2541	89.8772	89.3640
8	29.3026	27.0500	25.3011	30.8955	86.5127	60.5032	74.6989	69.1045
9	2.9858	2.9855	9.9149	11.1782	27.1284	23.7227	90.0851	88.8218
10	6.9908	13.0446	31.0932	54.3165	15.4926	10.9713	68.9068	45.6835

APPENDIX D

BLOOD PRESSURE VARIABILITY ANALYSIS STEPS

This sections outlines the procedure for performing blood pressure variability analysis in Matlab given a blood pressure in ascii form. The ascii blood pressure wave may be obtained by either unpacking the entire file, loading it into Matlab, then isolating the blood pressure, or writing it from the scanned file in S-Plus to an ascii file that can be loaded into Matlab. As an example, analysis of a blood pressure wave in ascii form, saved as filename k0511bpa.asc is shown.

- 1.) The ascii blood pressure data is first loaded into Matlab as follows:

load k0511bpa.asc

- 2.) The systolic peaks are then detected:

[bp,prsp]=getsap(k0511bpa,20,70)

- 3.) The accuracy of the peak detection is then checked using:

compare(prsp,bp)

- 4.) False detections are eliminated by typing:

prsp=undetected(prsp,bp)

then clicking the cursor on both sides of the false detection.

- 5.) Manual detections are created by typing:

prsp=mdetect(prsp,bp)

then clicking the cursor on both sides of a missed detection.

- 6.) The systolic arterial pressure spectrum is calculated and plotted using:

sapspec(prsp,0.05,0.15,0.4)

- 7.) The blood pressure spectrum is calculated and plotted using:

bpspec(bp,0.05,0.15,0.4)

Note: Since the last two commands also calculate the low and high frequency areas in the spectra, the limits given in the commands may vary depending upon the respiration rate.

APPENDIX E

BLOOD PRESSURE ANALYSIS PROGRAMS

Getsap.m

```
function [bp,prsp]=getsap(bp,thr,hr)

% This program detects the systolic peaks given
% a blood pressure signal.
%
% Compare is then automatically run to check
% detection accuracy.
%
% Syntax: [bp,prsp]=getsap(bp,thr,hr)
% (Where usual values are: thr=20 hr=70)

bp=bp*500/2048;          % Convert into mm Hg.

disp('Detecting systolic peaks...')

prsp=presap(bp,thr,hr);  % Detect systolic peaks

disp('Check detections now...')

compare(prsp,bp)
```

Presap.m

```
function prsp=presap(bp,thr,hr)

% This function takes the blood pressure waveform and returns
% the pre-interpolated systolic arterial blood pressure signal.
%
% Pre-interpolated refers to the interpolated signal but with
% a string of zeros until the first systolic peak was detected.
%
% Syntax: prsp=presap(bp,thr,hr)

j=1;
winsize=12000/hr;
wincomp=-winsize;
bpdiff=diff(bp);

bpmax=max(bp(1:400));    % Height of first peak
```

```

prsp=zeros(1,length(bpdiff));           % Preallocate preibp vector

if bpdiff(1) < 0                         % Set flag:
    flag = 0;                           % Initially falling
else
    flag = 1;                           % Initially rising
end

prsp(1) = 0;

for i=2:1:length(bpdiff)
    if bpdiff(i) >= 0                   % Rising bp wave
        flag = 1;
        prsp(i) = prsp(i-1);           % or

    elseif flag == 0                   % Continuing to fall
        flag = 0;
        prsp(i) = prsp(i-1);           % or

    else                               % Fall after rise
        flag=0;                        % indicates peak.
        if bp(i) > bpmax-thr
            if i-wincomp >= winsize-60
                prsp(i)=bp(i);
                bpmax=bp(i);
                wincomp=i;
            else
                prsp(i)=prsp(i-1);
            end
        else
            prsp(i)=prsp(i-1);
        end
    end
end
end

```

Compare.m

```
function compare(prsp,bp)
```

```

% This function plots the prsp signal on top of the blood
% pressure signal for purposes of viewing the accuracy of
% the detection algorithm.
%
% It plots 1000 points at a time so to see the next 1000
% points, hit the return key. To exit, hit Ctrl-C.
%

```

```
% Syntax: compare(prsp,bp)

lenbp=length(bp);
lenprsp=length(prsp);
i=0;

while lenbp > i+1000
    plot(bp(i+1:i+1000),'b')
    hold on
    plot(prsp(i+1:i+1000),'r')
    hold off
    pause
    i=i+1000;
end
plot(bp(i+1:lenbp),'b')
hold on
plot(prsp(i+1:lenprsp),'r')
hold off
break
```

Undetect.m

```
function prsp=undetect(prsp,bp)

% This program uses the mouse to remove unwanted detections.
% Simply click the mouse on both sides of an incorrect detection.
%
% Syntax: >> prsp=undetect(prsp,bp)

disp('Click on both sides of an incorrect detection.')
disp('(Left to right only)')
disp('Press return when done')

lenbp=length(bp);
lenprsp=length(prsp);
i=0;

while lenbp > i+1000
    plot(bp(i+1:i+1000),'b')
    hold on
    plot(prsp(i+1:i+1000),'r')
    hold off
    [x,y]=ginput;
    x=round(x);
    x=sort(x);
    if size(x) ~= 0
```

```

        n=i.*ones(size(x));
        x=n+x;
        prsp=undet(x,bp,prsp);
        plot(bp(i+1:i+1000),'b')
        hold on
        plot(prsp(i+1:i+1000),'r')
        hold off
        pause
    end
    i=i+1000;
end

plot(bp(i+1:lenbp),'b')
hold on
plot(prsp(i+1:lenprsp),'r')
hold off
[x,y]=ginput;
x=round(x);
x=sort(x);
    if size(x) ~= 0
        n=i.*ones(size(x));
        x=n+x;
        prsp=undet(x,bp,prsp);
        plot(bp(i+1:lenbp),'b')
        hold on
        plot(prsp(i+1:lenprsp),'r')
        hold off
        pause
    end
end

```

Undet.m

```

function prsp=undet(x,bp,prsp)

xpos=1;

for j=1:1:length(x)/2
    for n=x(xpos+1):1:length(prsp)-1
        if prsp(n) == prsp(n+1)
            ending = 1;
        else
            ending = 0;
            break
        end
    end
end
if ending == 0

```

```

        z=0;
        while prsp(x(xpos+1)) == prsp(z+x(xpos+1))
            z=z+1;
        end
        last=z+x(xpos+1)-1;
        for j=x(xpos):1:last
            prsp(j) = prsp(x(xpos)-1);
        end
    else
        for k=x(xpos):1:length(prsp)
            prsp(k) = prsp(x(xpos)-1);
        end
    end
    xpos=xpos+2;
end

```

Mdetect.m

```
function prsp=mdetect(prsp,bp)
```

```

% This program uses the mouse to create a manual
% detection. Simply click the mouse on both sides
% of a peak where a detection should be.
%
% Syntax: >> prsp=mdetect(bp,prsp)

```

```

disp('Click on both sides of a peak that requires a detection.')
disp('Press return when done')

```

```

lenbp=length(bp);
lenprsp=length(prsp);
i=0;

```

```

while lenbp > i+1000
    plot(bp(i+1:i+1000),'b')
    hold on
    plot(prsp(i+1:i+1000),'r')
    hold off
    [x,y]=ginput;
    x=round(x);
    x=sort(x);
    if size(x) ~= 0
        n=i.*ones(size(x));
        x=n+x;
    end
    i=i+1000;
end

```

```

        prsp=mdet(x,bp,prsp);
        plot(bp(i+1:i+1000),'b')
        hold on
        plot(prsp(i+1:i+1000),'r')
        hold off
        pause
    end
    i=i+1000;
end

plot(bp(i+1:lenbp),'b')
hold on
plot(prsp(i+1:lenprsp),'r')
hold off
[x,y]=ginput;
x=round(x);
x=sort(x);
    if size(x) ~= 0
        n=i.*ones(size(x));
        x=n+x;
        prsp=mdet(x,bp,prsp);
        plot(bp(i+1:lenbp),'b')
        hold on
        plot(prsp(i+1:lenprsp),'r')
        hold off
        pause
    end
end

```

Mdet.m

```

function prsp=mdet(x,bp,prsp)

xpos=1;

for i=1:1:length(x)/2
    for j=x(xpos+1):1:length(prsp)-1
        if prsp(j) == prsp(j+1)
            ending = 1;
        else
            ending = 0;
            break
        end
    end
    seg=bp(x(xpos):x(xpos+1));
    bpmax=max(seg);
    locmax=find(seg==max(seg))+x(xpos)-1;

```



```

    if length(locmax) ~= 1
        locmax = locmax(length(locmax));
    end
    if ending == 0
        z=0;
        while prsp(x(xpos+1)) == prsp(z+x(xpos+1))
            z=z+1;
        end
        last=z+x(xpos+1)-1;
        for k=x(xpos):1:locmax-1
            prsp(k) = prsp(x(xpos)-1);
        end
        for l=locmax:1:last
            prsp(l) = bpmax;
        end
    else
        for m=locmax:1:length(prsp)
            prsp(m) = bpmax;
        end
    end
    xpos=xpos+2;
end

```

Sapspec.m

```
function sapspec(prsp,lower,middle,high)
```

```

% This function calculates and plots the power spectrum
% of the systolic arterial pressure using an 8192 point
% fft and a hanning window.

```

```
%
```

```

% Since the first input argument is the prsp vector, the
% leading zeros are first removed in this program.

```

```
%
```

```
% Syntax: sapspec(prsp,lower,middle,high)
```

```
i=1;
```

```
while prsp(i) == 0
```

```
    i=i+1;
```

```
% Count zeros in
```

```
% beginning of prsp
```

```
end
```

```
nzero=i-1;
```

```
lenisap=length(prsp) - nzero;
```

```
% Length of isap
```

```
isap=zeros(1,lenisap);
```

```
% Preallocate isap
```

```
for j=1:1:lenisap
```

```
% Create isap
```

```

        isap(j)=prsp(nzero+j);
end

meansap=mnsap(isap);                % Find mean SAP

disap=decimate(isap,10);            % Decimate isap
[p11,f11]=rspect(disap,8192,0,hanning(length(disap)),20);
LF=area(lower,middle,p11);
HF=area(middle,high,p11);
LFnu=100*LF/(LF+HF);
HFnu=100*HF/(LF+HF);
ratio=LF/HF;
plot(f11(22:246),p11(22:246),'r')
grid
title('Forward Step Interpolation')
xlabel('Frequency (Hz.)')
ylabel('mm. Hg.2 / Hz.')

gtext(sprintf('LF (abs.) = %g',LF))
gtext(sprintf('HF (abs.) = %g',HF))
gtext(sprintf('LF (n.u.) = %f',LFnu))
gtext(sprintf('HF (n.u.) = %f',HFnu))
gtext(sprintf('Ratio (LF/HF) = %f',ratio))
gtext(sprintf('Mean SAP = %f',meansap))

```

Mnsap.m

```

function [meanSAP,sap]=mnsap(isap)

% This function finds the mean systolic arterial pressure
% from the peak detected waveform (isap).

sap(1)=isap(1);

j=2;

for i=2:1:length(isap)
    if isap(i) ~= isap(i-1)
        sap(j)=isap(i);
        j=j+1;
    end
end
meanSAP=mean(sap);

```

Rspect.m

```

function[pxx,freq_vector]=rspect(x,nfft,noverlap>window,fs)

x=x(:);

n=max(size(x));
nwind=length(window);
clear k
k=fix((n-noverlap)/(nwind-noverlap));
index=1:nwind;
KMU = k*norm(window)^2;
h=bar(0,' Finding spectrum.....');
pxx = zeros(nfft,1);
pxx2 = zeros(nfft,1);

for i = 1:k

    xw=window.*x(index);
    index=index+(nwind - noverlap);
    xy=abs(fft(xw,nfft)).^2;
    pxx=pxx+xy;
    pxx2=pxx2+abs(xy).^2;
    bar(i/k);
end

if ~any(any(imag(x)~=0)),
    if rem(nfft,2),
        select = [1:(nfft+1)/2];
    else
        select = [1:nfft/2+1]; % Normal case (evenFFT,real data)
    end
else
    select = 1:nfft;
end

pxx=pxx(select);
pxx2=pxx2(select);
pxx=pxx/KMU;
pxx=pxx(1:500);

freq_vector = (select-1)*fs/nfft;
freq_vector=freq_vector(1:500);

```

Area.m

```

function power=area(lower,upper,pii)

% This program calculates the area under the PSD curve
% given the upper and lower limits in Hz.
%
% This program assumes Fs=20 Hz.

if lower==0.05
    indexlo=22;
elseif lower==0.1
    indexlo=42;
elseif lower==0.15
    indexlo=63;
else
    error('Invalid Limits')
end

if upper==0.15
    indexhi=62;
elseif upper==0.1
    indexhi=41;
elseif upper==0.4
    indexhi=164;
elseif upper==0.5
    indexhi=205;
elseif upper==0.6
    indexhi=246;
elseif upper==0.8
    indexhi=328;
else
    error('Invalid Limits')
end

points=indexhi-indexlo;
power=0;

for i=0:1:points
    power=power+pii(indexlo+i);
end

```

Bpspec.m

```

function bpspec(bp,lower,middle,high)

% This function calculates and plots the power spectrum
% of the blood pressure using an 8192 point fft and a
% hanning window.
%
% Syntax: bpspec(bp,lower,middle,high)

dbp=decimate(bp,10);
[pri,fri]=rspect(dbp,8192,0,hanning(length(dbp)),20);
LF=area(lower,middle,pri);
HF=area(middle,high,pri);
LFnu=100*LF/(LF+HF);
HFnu=100*HF/(LF+HF);
ratio=LF/HF;
plot(fri(22:246),pri(22:246),'r')
grid
title('Blood Pressure Power Spectral Density')
xlabel('Frequency (Hz.)')
ylabel('mm. Hg.2 / Hz.')

gtext(sprintf('LF (abs.) = %g',LF))
gtext(sprintf('HF (abs.) = %g',HF))
gtext(sprintf('LF (n.u.) = %f',LFnu))
gtext(sprintf('HF (n.u.) = %f',HFnu))
gtext(sprintf('Ratio (LF/HF) = %f',ratio))

```

APPENDIX F

RESULTS OF DATA ANALYSIS

Table F.1 Results for Subject 1

File	Tgt. RR	Tgt. Vol.	Comfort	Act. RR	Act. Vol.	H.R.
b051994c	16	0.4	2	17.5	0.49	55
b051994d	16	0.7	4	17.5	0.7	57
b051994e	16	1	4	17.25	0.98	67
b051994f	16	1.2	3	17.25	1.19	69
b051994g	16	1.4	3	17.25	1.36	73
b052094e	24	0.4	3	25	0.44	62
b052094f	24	0.7	4	25.5	0.73	71
b052094g	24	1	3	25.75	0.99	80
b052094h	24	1.2	3	25.2	1.19	82
b052094i	24	1.4	2	26.5	1.33	77
b052094k	11	0.4	4	12	0.364	68
b052094l	11	0.7	4	11.75	0.7	59
b052094m	11	1	4	12	0.96	62
b052094n	11	1.2	3	12	1.15	63
b052094o	11	1.4	3	12.5	1.3	69

File	Mean SAP	IBI Spectrum				Ratio
		LF (abs)	HF (abs)	LF (n.u.)	HF (n.u.)	
b051994c	156.14	19.1648	71.6008	21.1146	78.8854	0.2677
b051994d	155.96	9.8843	39.8755	19.8640	80.1360	0.2479
b051994e	147.18	9.5421	22.7693	29.5317	70.4683	0.4191
b051994f	135.36	5.3738	13.6195	28.2931	71.7069	0.3946
b051994g	133.69	3.2838	17.1135	16.0992	83.9008	0.1919
b052094e	121.13	10.0364	16.6562	37.5999	62.4001	0.6026
b052094f	125.86	5.8965	5.9521	49.7654	50.2346	0.9907
b052094g	123.15	4.1632	1.3285	75.8089	24.1911	3.1338
b052094h	111.51	10.2405	4.4211	69.8457	30.1543	2.3163
b052094i	70.99	8.3483	9.4240	46.9737	53.0263	0.8859
b052094k	113.06	16.0981	130.8026	10.9585	89.0415	0.1231
b052094l	118.58	9.7856	55.7812	14.9246	85.0754	0.1754
b052094m	116.74	10.6984	43.0030	19.9220	80.0780	0.2488
b052094n	116.63	8.7926	86.7034	9.2073	90.7927	0.1014
b052094o	114.69	5.7515	30.0690	16.0564	83.9436	0.1913

Table F.1 (continued) Results for Subject 1

File	SAP Spectrum				
	LF (abs.)	HF (abs.)	LF (n.u.)	HF (n.u.)	Ratio
b051994c	10681.6	4965.3	68.2666	31.7334	2.1512
b051994d	19521.6	7507.7	72.2238	27.7762	2.6002
b051994e	10582.9	9872.6	51.7362	48.2638	1.0719
b051994f	5020.5	16137.4	23.7287	76.2713	0.3111
b051994g	7013.9	15023.0	31.8279	68.1721	0.4669
b052094e	3769.3	4533.9	45.3960	54.6040	0.8314
b052094f	8695.0	10214.4	45.9825	54.0175	0.8513
b052094g	9687.4	29306.6	24.8433	75.1567	0.3306
b052094h	24328.4	40364.3	37.6061	62.3939	0.6027
b052094i	6315.0	9326.7	40.3727	59.6273	0.6771
b052094k	7546.2	23793.3	24.0789	75.9211	0.3172
b052094l	18504.2	51723.7	26.3488	73.6512	0.3578
b052094m	10487.8	59895.2	14.9010	85.0990	0.1751
b052094n	15197.4	99233.5	13.2809	86.7191	0.1531
b052094o	14659.3	100333.0	12.7481	87.2519	0.1461

File	BP Spectrum				
	LF (abs.)	HF (abs.)	LF (n.u.)	HF (n.u.)	Ratio
b051994c	12829.5	5863.2	68.6337	31.3663	2.1881
b051994d	9320.8	2065.2	81.8619	18.1381	4.5133
b051994e	7354.4	8018.3	47.8407	52.1593	0.9172
b051994f	3849.0	9457.5	28.9258	71.0742	0.4070
b051994g	5702.0	12179.0	31.8887	68.1113	0.4682
b052094e	6259.0	6633.8	48.5464	51.4536	0.9435
b052094f	8404.1	10200.6	45.1719	54.8281	0.8239
b052094g	9939.3	33871.3	22.6869	77.3131	0.2934
b052094h	17561.2	69108.6	20.2622	79.7378	0.2541
b052094i	5091.0	10511.2	32.6299	67.3701	0.4843
b052094k	4589.5	7024.9	39.5159	60.4841	0.6533
b052094l	11551.0	14464.5	44.4005	55.5995	0.7986
b052094m	4971.3	22422.2	18.1477	81.8523	0.2217
b052094n	11821.0	33274.4	26.2133	73.7867	0.3553
b052094o	9031.5	47480.0	15.9817	84.0183	0.1902

Table F.2 Results for Subject 2

File	Tgt. RR	Tgt. Vol.	Comfort	Act. RR	Act. Vol.	H.R.
d040794g	19	0.4	4	19	0.431	60
d040794f	19	0.7	3	19.25	0.732	59
d040794e	19	1	3	19.25	1.02	56
d040794d	19	1.2	2	19.75	1.16	53
d040794c	19	1.4	2	19.5	1.43	50
d041294e	13	0.4	3	14.25	0.421	51
d041294f	13	0.7	4	14.5	0.66	55
d041294g	13	1	4	13.75	0.99	57
d041294h	13	1.2	3	13.75	1.16	60
d041294i	13	1.4	2	14	1.35	63
d041294k	28	0.4	2	29.25	0.432	59
d041294l	28	0.7	3	27.75	0.798	62
d041294m	28	1	2	29	1.01	66
d041294n	28	1.2	1	27	1.48	75

File	Mean SAP	IBI Spectrum				
		LF (abs)	HF (abs)	LF (n.u.)	HF (n.u.)	Ratio
d040794g	133.55	12.1322	16.7385	42.0225	57.9775	0.7248
d040794f	123.74	4.5187	21.8931	17.1086	82.8914	0.2064
d040794e	121.44	3.0142	22.0722	12.0153	87.9847	0.1366
d040794d	113.88	2.277	14.9981	13.1808	86.8192	0.1518
d040794c	120.75	3.8179	21.7858	14.9115	85.0885	0.1752
d041294e	105.18	11.2168	13.938	44.5911	55.4089	0.8048
d041294f	124.86	12.8961	35.2457	26.7877	73.2123	0.3659
d041294g	125.59	16.6933	42.3986	28.2497	71.7503	0.3937
d041294h	125.17	14.5171	37.0299	28.1628	71.8372	0.3920
d041294i	139.78	15.523	26.0901	37.3032	62.6968	0.5950
d041294k	144.97	10.5221	5.4195	66.0040	33.9960	1.9415
d041294l	148.07	15.3998	9.1187	62.8089	37.1911	1.6888
d041294m	145.61	3.7973	4.3605	46.5481	53.4519	0.8708
d041294n	130.66	0.8709	2.0257	30.0663	69.9337	0.4299

Table F.2 (continued) Results for Subject 2

File	SAP Spectrum				
	LF (abs.)	HF (abs.)	LF (n.u.)	HF (n.u.)	Ratio
d040794g	9815.4	4135.0	70.3594	29.6406	2.3738
d040794f	14903.4	8103.7	64.7774	35.2226	1.8391
d040794e	4829.5	24310.8	16.5732	83.4268	0.1987
d040794d	10506.8	50630.4	17.1856	82.8144	0.2075
d040794c	27772.0	33547.1	45.2909	54.7091	0.8279
d041294e	17690.4	5951.3	74.8270	25.1730	2.9725
d041294f	30903.2	19272.4	61.5901	38.4099	1.6035
d041294g	27786.0	43471.3	38.9939	61.0061	0.6392
d041294h	31654.4	59610.7	34.6840	65.3160	0.5310
d041294i	37820.0	91094.6	29.3373	70.6627	0.4152
d041294k	79185.1	14106.7	84.8789	15.1211	5.6133
d041294l	28064.8	15830.2	63.9362	36.0638	1.7729
d041294m	33139.2	26800.4	55.2877	44.7123	1.2365
d041294n	25069.1	55856.8	30.9778	69.0222	0.4488

File	BP Spectrum				
	LF (abs.)	HF (abs.)	LF (n.u.)	HF (n.u.)	Ratio
d040794g	17533.2	5491.7	76.1487	23.8513	3.1926
d040794f	20286.5	8472.1	70.5407	29.4593	2.3945
d040794e	5710.5	39010.1	12.7693	87.2307	0.1464
d040794d	5204.6	37823.5	12.0959	87.9041	0.1376
d040794c	7732.0	44202.7	14.8880	85.1120	0.1749
d041294e	17646.2	2824.4	86.2025	13.7975	6.2477
d041294f	24559.3	11422.2	68.2554	31.7446	2.1501
d041294g	25864.2	35443.6	42.1875	57.8125	0.7297
d041294h	34863.1	66422.3	34.4207	65.5793	0.5249
d041294i	25505.2	69988.6	26.7087	73.2913	0.3644
d041294k	61331.6	13248.2	82.2362	17.7638	4.6294
d041294l	22351.2	23796.5	48.4340	51.5660	0.9393
d041294m	19927.3	48973.9	28.9216	71.0784	0.4069
d041294n	17905.0	78052.6	18.6593	81.3407	0.2294

Table F.3 Results for Subject 3

File	Tgt. RR	Tgt. Vol.	Comfort	Act. RR	Act. Vol.	H.R.
I040794c	16	0.4	4	17.5	0.42	74
I040794d	16	0.7	3	17.75	0.744	73
I040794f	16	1.2	2	17.5	1.25	88
I040794g	16	1.4	1	17.5	1.36	89
I042594e	24	0.4	3	25.75	0.488	64
I042594f	24	0.7	3	24.25	0.839	79
I042594g	24	1	2	25.5	0.995	84
I042594k	11	0.4	4	12.25	0.398	60
I042594l	11	0.7	3	11.75	0.64	62
I042594m	11	1	2	11.5	1.02	67
I042594n	11	1.2	2	11.75	1.2	73
I042594o	11	1.4	1	12	1.3	74

File	Mean SAP	IBI Spectrum				
		LF (abs)	HF (abs)	LF (n.u.)	HF (n.u.)	Ratio
I040794c	122.84	5.2701	8.9131	37.1573	62.8427	0.5913
I040794d	118.68	5.3507	6.1938	46.3485	53.6515	0.8639
I040794f	113.35	0.8602	1.6312	34.5268	65.4732	0.5273
I040794g	106.86	2.3315	2.0509	53.2014	46.7986	1.1368
I042594e	131.3	1.8484	4.3314	29.9104	70.0896	0.4267
I042594f	124.31	0.6383	2.7159	19.0299	80.9701	0.2350
I042594g	116.58	0.8008	1.0236	43.8939	56.1061	0.7823
I042594k	116.05	1.2418	8.8513	12.3035	87.6965	0.1403
I042594l	121.39	6.6372	39.4054	14.4153	85.5847	0.1684
I042594m	121.46	7.4512	20.4964	26.6613	73.3387	0.3635
I042594n	117.79	4.6399	9.5980	32.5884	67.4116	0.4834
I042594o	113.87	4.6072	12.4614	26.9923	73.0077	0.3697

Table F.3 (continued) Results for Subject 3

File	SAP Spectrum				
	LF (abs.)	HF (abs.)	LF (n.u.)	HF (n.u.)	Ratio
I040794c	26422.7	3976.5	86.9191	13.0809	6.6447
I040794d	26743.0	2090.0	92.7513	7.2487	12.7956
I040794f	13576.7	29365.1	31.6165	68.3835	0.4623
I040794g	6896.2	24361.2	22.0626	77.9374	0.2831
I042594e	6879.6	8688.9	44.1892	55.8108	0.7918
I042594f	8991.7	20448.2	30.5425	69.4575	0.4397
I042594g	7322.6	94802.6	7.1702	92.8298	0.0772
I042594k	6244.1	6614.5	48.5597	51.4403	0.9440
I042594l	11934.5	31324.0	27.5888	72.4112	0.3810
I042594m	11670.3	53122.5	18.0117	81.9883	0.2197
I042594n	15272.3	58805.3	20.6166	79.3834	0.2597
I042594o	12925.5	88576.1	12.7343	87.2657	0.1459

File	BP Spectrum				
	LF (abs.)	HF (abs.)	LF (n.u.)	HF (n.u.)	Ratio
I040794c	19867.0	1470.7	93.1075	6.8925	13.5085
I040794d	16208.0	5773.0	73.7364	26.2636	2.8076
I040794f	5784.5	11161.7	34.1345	65.8655	0.5182
I040794g	4527.0	21104.0	17.6622	82.3378	0.2145
I042594e	2706.6	3635.3	42.6781	57.3219	0.7445
I042594f	3507.5	9558.1	26.8453	73.1547	0.3670
I042594g	2852.0	36158.2	7.3109	92.6891	0.0789
I042594k	3406.7	789.5	81.1854	18.8146	4.3150
I042594l	7051.7	8574.7	45.1268	54.8732	0.8224
I042594m	6142.3	19649.9	23.8146	76.1854	0.3126
I042594n	8268.0	22446.8	26.9186	73.0814	0.3683
I042594o	6372.6	31455.5	16.8462	83.1538	0.2026

Table F.4 Results for Subject 4

File	Tgt. RR	Tgt. Vol.	Comfort	Act. RR	Act. Vol.	H.R.
s040894f	18	0.4	4	18	0.451	63
s040894c	18	0.7	4	18	0.731	69
s040894d	18	1	4	18.5	1.02	77
s040894g	18	1.2	2	17	0.98	73
s040894e	18	1.4	2	15.5	1.19	77
s051594e	11	0.4	4	14.5	0.335	63
s051594f	11	0.7	4	12	0.725	65
s051594g	11	1	4	11.75	1.05	69
s051594h	11	1.2	4	12	1.15	71
s051594i	11	1.4	4	12	1.33	74
s051594k	25	0.4	3	26.25	0.48	67
s051594l	25	0.7	3	26.25	0.764	77
s051594m	25	1	2	25	0.857	83

File	Mean SAP	IBI Spectrum				
		LF (abs)	HF (abs)	LF (n.u.)	HF (n.u.)	Ratio
s040894f	104.17	5.8409	24.4322	19.2940	80.7060	0.2391
s040894c	106.98	7.5605	18.5630	28.9414	71.0586	0.4073
s040894d	100.88	7.0748	6.9727	50.3634	49.6366	1.0146
s040894g	122.71	14.0537	3.6731	79.2794	20.7206	3.8261
s040894e	110.68	4.6521	4.1492	52.8570	47.1430	1.1212
s051594e	124.07	8.2538	38.1632	17.7818	82.2182	0.2163
s051594f	118.79	12.8047	52.7604	19.5297	80.4703	0.2427
s051594g	118.14	12.8966	56.9268	18.4703	81.5297	0.2265
s051594h	116.73	8.5449	49.1420	14.8125	85.1875	0.1739
s051594i	116.3	7.5798	19.5717	27.9167	72.0833	0.3873
s051594k	122.44	7.1214	10.9007	39.5148	60.4852	0.6533
s051594l	118.95	3.9627	1.2415	76.1443	23.8557	3.1919
s051594m	129.63	1.7602	0.8601	67.1755	32.8245	2.0465

Table F.4 (continued) Results for Subject 4

File	SAP Spectrum				
	LF (abs.)	HF (abs.)	LF (n.u.)	HF (n.u.)	Ratio
s040894f	2460.9	20286.9	10.8181	89.1819	0.1213
s040894c	5015.0	32853.9	13.2431	86.7569	0.1526
s040894d	6464.4	73626.9	8.0712	91.9288	0.0878
s040894g	35970.5	62656.0	36.4714	63.5286	0.5741
s040894e	3988.4	110963.0	3.4696	96.5304	0.0359
s051594e	8074.8	55667.3	12.6679	87.3321	0.1451
s051594f	19082.3	100635.0	15.9395	84.0605	0.1896
s051594g	13783.8	128953.0	9.6568	90.3432	0.1069
s051594h	14976.1	225377.0	6.2309	93.7691	0.0664
s051594i	44731.7	234146.0	16.0399	83.9601	0.1910
s051594k	6313.8	21143.5	22.9950	77.0050	0.2986
s051594l	13328.9	145238.0	8.4059	91.5941	0.0918
s051594m	15988.7	181430.0	8.0989	91.9011	0.0881

File	BP Spectrum				
	LF (abs.)	HF (abs.)	LF (n.u.)	HF (n.u.)	Ratio
s040894f	2079.0	6001.0	25.7302	74.2698	0.3464
s040894c	5606.2	13358.2	29.5617	70.4383	0.4197
s040894d	8060.4	70026.9	10.3223	89.6777	0.1151
s040894g	37891.7	49754.8	43.2324	56.7676	0.7616
s040894e	4916.2	101206.2	4.6326	95.3674	0.0486
s051594e	8690.1	14538.3	37.4115	62.5885	0.5977
s051594f	17194.0	32858.2	34.3521	65.6479	0.5233
s051594g	8531.0	63827.5	11.7899	88.2101	0.1337
s051594h	8535.6	94990.8	8.2449	91.7551	0.0899
s051594i	26567.4	106255.0	20.0022	79.9978	0.2500
s051594k	12641.4	18194.5	40.9957	59.0043	0.6948
s051594l	7582.9	139021.3	5.1724	94.8276	0.0545
s051594m	4956.9	215903.6	2.2444	97.7556	0.0230

Table F.5 Results for Subject 5

File	Tgt. RR	Tgt. Vol.	Comfort	Act. RR	Act. Vol.	H.R.
x040694c	17	0.4	2	17.5	0.48	73
x040694d	17	0.7	4	16.75	0.725	78
x040694e	17	1	4	17	1.04	86
x040694f	17	1.2	3	17.25	1.18	88
x040694g	17	1.4	2	17.5	1.33	89
x041394d	25	0.4	4	24.75	0.46	69
x041394f	25	0.7	3	24.75	0.8	80
x041394k	12	0.4	4	14.25	0.45	66
x041394l	12	0.7	4	13.5	0.713	71
x041394m	12	1	4	13.5	0.98	75
x041394n	12	1.2	3	13.5	1.18	77
x041394o	12	1.4	2	13.25	1.4	80

File	Mean SAP	IBI Spectrum				
		LF (abs)	HF (abs)	LF (n.u.)	HF (n.u.)	Ratio
x040694c	112.46	2.3973	9.1291	20.7983	79.2017	0.2626
x040694d	114.58	0.3371	8.9049	3.6475	96.3525	0.0379
x040694e	111.01	0.8191	5.4456	13.0748	86.9252	0.1504
x040694f	105.66	1.5170	4.6543	24.5815	75.4185	0.3259
x040694g	102.44	1.5570	3.9044	28.5092	71.4908	0.3988
x041394d	106.57	0.8575	10.5613	7.5095	92.4905	0.0812
x041394f	100.64	2.4489	2.9564	45.3055	54.6945	0.8283
x041394k	112.85	6.5145	28.2269	18.7514	81.2486	0.2308
x041394l	95.24	1.4805	25.5661	5.4739	94.5261	0.0579
x041394m	94.67	1.9811	20.6092	8.7697	91.2303	0.0961
x041394n	102.12	1.0163	22.4886	4.3238	95.6762	0.0452
x041394o	103.22	1.1232	17.5791	6.0057	93.9943	0.0639

Table F.5 (continued) Results for Subject 5

File	SAP Spectrum				
	LF (abs.)	HF (abs.)	LF (n.u.)	HF (n.u.)	Ratio
x040694c	4240.4	9515.7	30.8255	69.1745	0.4456
x040694d	2316.3	36343.4	5.9914	94.0086	0.0637
x040694e	6600.1	85592.5	7.1591	92.8409	0.0771
x040694f	12461.2	33501.7	27.1114	72.8886	0.3720
x040694g	3975.3	51360.4	7.1840	92.8160	0.0774
x041394d	9919.4	37329.7	20.9939	79.0061	0.2657
x041394f	22515.3	115904.0	16.2660	83.7340	0.1943
x041394k	10319.6	28211.1	26.7828	73.2172	0.3658
x041394l	8280.7	81999.8	9.1722	90.8278	0.1010
x041394m	9942.4	90053.6	9.9428	90.0572	0.1104
x041394n	13180.7	223348.0	5.5726	94.4274	0.0590
x041394o	9220.6	287368.0	3.1089	96.8911	0.0321

File	BP Spectrum				
	LF (abs.)	HF (abs.)	LF (n.u.)	HF (n.u.)	Ratio
x040694c	3731.9	3996.5	48.2881	51.7119	0.9338
x040694d	2446.0	12188.7	16.7137	83.2863	0.2007
x040694e	6761.9	41051.4	14.1423	85.8577	0.1647
x040694f	6036.8	19698.8	23.4570	76.5430	0.3065
x040694g	1965.6	24672.0	7.3790	92.6210	0.0797
x041394d	7505.5	18961.7	28.3577	71.6423	0.3958
x041394f	11797.5	62457.6	15.8878	84.1122	0.1889
x041394k	8392.9	6773.3	55.3395	44.6605	1.2391
x041394l	9452.6	31008.6	23.3621	76.6379	0.3048
x041394m	8765.6	44048.0	16.5972	83.4028	0.1990
x041394n	8745.2	63864.7	12.0441	87.9559	0.1369
x041394o	4045.9	100943.2	3.8536	96.1464	0.0401

REFERENCES

- [1] A. J. Vander, J. H. Sherman, and D. S. Luciano, *Human Physiology: The Mechanisms of Body Function*, Sixth Edition, New York: McGraw Hill Publishing Company, 1994, pp. 194-198, 221-222, 410-500.
- [2] A. C. Guyton, *Textbook of Medical Physiology*, Seventh Edition, Philadelphia: W. B. Saunders Company, 1986, pp. 150-181, 218-256.
- [3] M. V. Kamath, E. L. Fallen, "Power Spectral Analysis of Heart Rate Variability: A Noninvasive Signature of Cardiac Autonomic Function." *Critical Reviews in Biomedical Engineering*, Vol. 21, pp. 245-311, 1993.
- [4] M. Leifer, "Influences of Cardiac and Respiratory Parameters on Heart Rate Variability." *MS Thesis, New Jersey Institute of Technology*, October 1994.
- [5] A. Milliani, M. Pagani, F. Lombardi, S. Cerutti, "Cardiovascular Neural Regulation Explored in the Frequency Domain." *Circ. Res. Adv. Ser.*, Vol.84, pp. 482-492, 1991.
- [6] M. Pagani, F. Lombardi, S. Guzzetti, O. Rimoldi, R. Furlan, P. Pizzinelli, G. Sandrone, G. Malfatto, S. Dell'Orto, E. Piccaluga, M. Turiet, G. Baselli, S. Cerutti, A. Milliani, "Power Spectral Analysis of Heart Rate and Arterial Pressure Variabilities as a Marker of Sympathovagal Interaction in Man and Conscious Dog." *Circ. Res.*, Vol. 59, pp. 178-193, 1986.
- [7] J. Elghozi, D. Laude, A. Girard, "Effects of Respiration on Blood Pressure and Heart Rate Variability in Humans." Vol. 18, *Clinical and Experimental Pharmacology and Physiology*, pp. 735-742, 1991.
- [8] K. Inoue, S. Miyake, M. Kumashiro, H. Ogata, T. Ueta, T. Akatsu, "Power Spectral Analysis of Blood Pressure Variability in Traumatic Quadriplegic Humans." *Am. J. Physiol.*, 260 (*Heart Circ. Physiol.* 29), pp. H842-H847, 1991.
- [9] A. Millani, M. Pagani, F. Lombardi, "Physiology and Clinical Implications of Variability of Cardiovascular Parameters with Focus on Heart Rate and Blood Pressure." *Am. J. Physiol.*, Vol. 73, pp. 3C-9C, 1994.
- [10] S. Guzzetti, C. Cogliati, C. Broggi, C. Carozzi, D. Caldiroli, F. Lombardi, A. Milliani, "Influences of Neural Mechanisms on Heart Period and Arterial Pressure Variabilities in Quadriplegic Patients." *Am. J. Physiol.*, 256 (*Heart Circ. Physiol.* 35), pp. H1112-H1120, 1994.
- [11] J. Haaksma, J. Brouwer, W. A. Dijk, L. J. M. Mulder, H. J. G. M. Crijns, K. I. Lie, "Heart Rate Dependent Changes in Spectral Analysis." *Comput. Cardiol.* pp. 45-48, 1994.

- [12] S. Shin, W. N. Tapp, S. S. Reisman, and B. H. Natelson, "Assessment of Autonomic Regulation by the Method of Complex Demodulation." *IEEE Trans. Biomed. Eng.*, Vol. 36, pp. 274-283, 1983.
- [13] F. Grüneis, A. W. Frey, M. Dambacher, M. Adt, "Modification of Respiratory Sinus Arrhythmia by Mean Heart Rate." *Comput. Cardiol.* pp. 49-52, 1994.
- [14] A. W. Frey, C. Hagenmiller, J. Baumert, F. Grueneis, M. Dambacher, K. Theisen, M. Adt, "The Respiratory Sinus Arrhythmia as a Function of Breathing Frequency Revisited." *Comput. Cardiol.* pp. 41-44, 1994.
- [15] B. W. Hyndman, C. Zeelenberg, "Spectral Analysis of Heart Rate Variability Revisited: Comparison of the Methods." *Comput. Cardiol.* pp. 719-722, 1993.
- [16] W. H. Press, S. A. Teukolsky, W. T. Vetterling, B. P. Flannery, *Numerical Recipes in C: The Art of Scientific Computing*, Second Edition, New York, Cambridge University Press, 1992, pp. 575-584.
- [17] G. B. Moody, "Spectral Analysis of Heart Rate Without Resampling." *Comput. Cardiol.* pp. 715-718, 1993.